INTERACTIVE PROOFS AS A UNIFIED FRAMEWORK FOR EVALUATING AND LEVERAGING VERIFIABLE PROOF GENERATION BY LLM AGENTS

Anonymous authors
Paper under double-blind review

ABSTRACT

Recent advances in LLM-assisted theorem proving and program verification have attracted widespread attention. Beyond determining whether a proposition is true, LLM agents must produce evidence that can be independently checked by humans or formal verification tools. To evaluate the underlying, tool-agnostic ability of LLM agents to construct verifiable proofs—rather than their proficiency with any particular proof language or verification tool—we introduce MERLIN-BENCH. Drawing on interactive proof systems from computational complexity theory, we cast an LLM agent as the prover: under a designated protocol, the agent interacts with a formal verifier to substantiate its claimed answer to a problem instance. We develop an automated framework for constructing test cases and use it to create 100 cases across 15 problem families, each formulated within this prover-verifier framework. Experiments with 10 frontier LLMs across multiple agent harnesses show that reliably producing verifiable proofs in accordance with specified protocols remains a substantial challenge. Our case studies further provide actionable insights into improving agents' ability to generate verifier-accepted proofs: tool use is essential for completing practical proof tasks; different forms of guidance, ranging from engineering instructions to problem-specific knowledge, substantially affect success rates on interactive-proof tasks; and proof-solving experience distilled from abstract tasks can transfer to concrete, real-world verification tasks.

1 INTRODUCTION

Recently, LLM agents have demonstrated strong capabilities in theorem proving. A new paradigm of human–AI collaboration has emerged in which LLM agents search for proofs or counter-examples and the resulting outputs are subsequently verified by human experts or formal verification tools. For example, in frontier mathematics, LLM agents discover proofs and produce proof texts (OpenAI (2026c;a)), structured lemmas (Ke et al. (2026)) or formalizations in Lean, which are then checked by human experts (Alon et al. (2026)) or verified by Lean (OpenAI (2026b)). In software verification, LLM agents discover annotations such as loop invariants (Yang et al. (2025); Mugnier et al. (2025)), whose correctness is then verified by tools such as Dafny (Leino (2010)). Overall, this emerging paradigm requires LLM agents not only to find evidence, but also to complete proofs through interacting with a specified framework.

A large body of prior work has investigated the ability of LLMs to construct certificate and prove propositions. For example, NLGraph and NPEval (Fan et al. (2024); Wang et al. (2023)) ask LLMs to solve graph-theoretic problems and small-scale NP-hard problems, respectively. However, these benchmarks are not *agent-oriented*, because an agent can solve such problems simply by writing code. SATBench (Wei et al. (2025)) evaluates LLMs on automatically generated SAT instances. However, it uses another LLM to audit the output of the LLM being benchmarked; therefore, the *certificate* is not *rigorous*. MiniF2F (Zheng et al. (2022)) evaluates LLMs' capability of generating formal proofs, with questions drawn from Olympiad mathematics, making it difficult to *scale up*. Verus-Bench and DafnyBench (Yang et al. (2025); Mugnier et al. (2025)) require LLMs to complete tasks using specific protocol (in particular the formal verification tool). Consequently, the capabilities they evaluate are closely tied to specific tools rather than reflecting an *unified proof ability* at a general, abstract level.

Reviewers: please read the Reviewer Guidelines (iclr.cc/Conferences/2027/ReviewerGuidelines) and the AI Policy for Reviewers (iclr.cc/Conferences/2027/AIPolicyForReviewers). If you used AI to expand, edit, or polish your review, please provide the input text to the LLM. Better still, consider skipping the LLM and submitting your original text: we, and the authors, are much more interested in your unedited thoughts than in what an LLM has to say. AI-assisted or not, you are putting your name and reputation behind your review: LLM-generated falsehoods, hallucinations or misrepresentations are subject to disciplinary action, which may include desk-rejecting all papers you have authored.

Benchmark	Agent-oriented	Rigorous certificate	Scalable synthesis	Unified proof
NLGraph	✗	✗	✓	✗
NPHardEval	✗	✗	✓	✓
SATBench	✗	✗	✓	✓
miniF2F	✗	✓	✗	✗
Verus-Bench	✓	✓	✗	✗
DafnyGym	✓	✓	✗	✗
Merlin-Bench	✓	✓	✓	✓

Table 1: Comparison with related benchmarks.

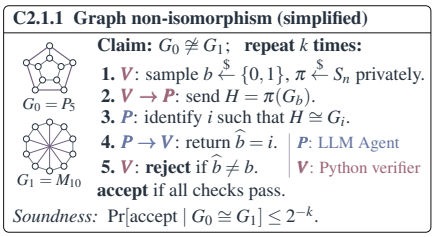

Figure 1: Example of Test Case 2.1.1

This paper introduces MERLIN-BENCH, addressing all four limitations of prior work described above. Regardless of the formal verification tool employed or the proposition being proved, these proof tasks fall within the framework of interactive proof systems from computational complexity theory Babai (1985). Accordingly, in each test case of MERLIN-BENCH, the LLM agent is required to complete the following task: given a instance, which is dynamically generated by a generator $\mathcal{G}$, of an decision problem equipped with an interactive protocol Π and a formal verifier V, an LLM agent is supposed to complete an interactive proof under protocol Π with V, as illustrated in Figure 1. On the one hand, this task formulation naturally aligns with the emerging paradigm of human–AI collaboration in theorem proving and formal verification. On the other hand, it raises the problem complexity to $\mathsf{IP} = \mathsf{PSPACE}$ (Shamir (1992)), thereby preserving substantial headroom in difficulty (see Appendix C.2), even for agents equipped with tool-use and code-generation capabilities.

We construct 100 test cases from 15 IP problems, requiring models to complete interactive proofs according to specified protocols. To construct these test cases efficiently while ensuring their diversity, feasibility, and difficulty, we develop a test-case construction framework: a construction agent automatically executes an iterative cycle of literature review, generator implementation, and feasibility and difficulty checks to generate challenging but tractable test cases at scale. The correctness of all 100 test cases generated in this work has been verified by human reviewers, demonstrating the effectiveness of this framework. On this benchmark, we evaluate 10 frontier LLMs from major model families. The results show that, beyond the ability to find answers, completing proofs according to specified requirements remains a significant bottleneck for current LLMs. We further conduct several case studies and identify promising directions for improving models' proof capabilities. In summary, our main technical contributions are:

1. **A new evaluation paradigm based on IP.** We propose an evaluation paradigm based on interactive proof systems that is agent-oriented, evaluates models' unified proof capabilities through strict formal verification, and can be scaled up.
2. **A benchmark and a test case generation framework.** We construct MERLIN-BENCH, which includes 100 test cases spanning 15 IP problems to dynamically generate evaluation instances to evaluate LLM agents' proof capabilities. Additionally, we propose a agentic framework that reliably generates practical but discriminative test cases at scale.
3. **Empirical observations on improving models' proof capabilities.** We find that tool use and user prompts at three different levels have significant effects on models' proof capabilities. We further show that proof experience acquired from the abstract IP problems in our benchmark can improve performance on real-world formal verification tasks.

Reproducible codes and data sets can be found in the supplementary material. We will release the repository publicly on GitHub after de-anonymization.

2 PRELIMINARIES

This section introduces the theoretical foundations of computation underlying MERLIN-BENCH. The problems in MERLIN-BENCH are derived from decision problems in computational theory. Intuitively, a decision problem asks whether an input x satisfies a particular property. By encoding each input as a binary string, any decision problem can be characterized by a subset $L \subseteq \{0,1\}^*$, where $\{0,1\}^*$ denotes the set of all finite-length binary strings and $x \in L$ if and only if it encodes an input which satisfies this property.

Nondeterministic Polynomial (NP) Problems. For any decision problem L, we say that L is solvable in nondeterministic polynomial time (or write $L \in \mathsf{NP}$) if and only if there exists a polynomial-time algorithm $\mathcal{V}$ and a polynomial $q(x)$ such that

$$x \in L \quad \Leftrightarrow \quad \exists w : |w| \leq q(|x|) \wedge \mathcal{V}(x, w) \to 1,$$

where $\mathcal{V}(x, w) \to 1$ means that the algorithm $\mathcal{V}$ takes x and w as input and outputs 1. w, the second input to the algorithm $\mathcal{V}$, is called the *certificate* for this problem.

Interactive Proof (IP) Problems. Some decision problems can be verified by interactive proof systems. Intuitively, an interactive proof is carried out jointly by two algorithms, called the prover P and the verifier V. The prover P is computationally unbounded, whereas the verifier V is restricted to polynomial-time randomized computation. The prover and the verifier communicate for a polynomial number of rounds, after which the verifier decides whether to accept or reject the prover's proof based on the communication transcript. Formally, a multi-round interactive protocol is defined as follows:

Definition 2.1 (Interactive proof protocol)**.** *A multi-round interactive protocol* Π *consists of the following data: the number of interaction rounds* n*, the format of messages, and the speaking order* $r \in \{\mathsf{P}, \mathsf{V}\}^n$*, where* n *is polynomial in the input length* $|x|$*.*

The interaction between the prover and the verifier under the interactive protocol Π is formally defined as follows. Let $h_0 = \varepsilon$ denote the empty sequence, and let $h_i = (m_1, \ldots, m_i)$ denote the prefix of the interaction transcript between the two parties, and

$$m_i = \begin{cases} P(x, h_{i-1}), & r_i = \mathsf{P}, \\ V(x, h_{i-1}), & r_i = \mathsf{V}, \end{cases}, \quad D_\Pi(P, x) = V_{\text{out}}(x, h_n).$$

A decision problem is said to admit an interactive proof (or belong to IP) if and only if there exists a interactive proof protocol Π and a verifier V such that the following two properties hold:

1. *Completeness*. There exists a sufficiently powerful prover that, for every valid input, can produce a proof that causes the verifier to accept with high probability:
$$\exists P, \ \forall x \in L, \quad \Pr[D_\Pi(P, x) \to 1] \geq 1 - \varepsilon_c.$$
2. *Soundness*. No prover can convince the verifier to accept an invalid input with high probability:
$$\forall P, \ \forall x \notin L, \quad \Pr[D_\Pi(P, x) \to 1] \leq \varepsilon_s.$$

where $\varepsilon_s, \varepsilon_c$ are constants with $\varepsilon_s, \varepsilon_c \leq 1/3$. We refer to P and V as *Merlin* and *Arthur*, respectively. Note that in this paper, Merlin's input does not include Arthur's random seed.

Example 2.1 (Graph Nonisomorphism, GNI)**.** *GNI asks whether two graphs* G_0, G_1 *satisfy* $G_0 \ncong G_1$*. Its membership in* NP *remains open, as no general efficiently checkable certificate is known. However, we can construct an* IP *protocol (as shown in Figure 1): asking* P *to identify the source of a randomly relabeled input graph. An unbounded* P *can always identify the source when* $G_0 \ncong G_1$*, but can only guess when* $G_0 \cong G_1$*. Independent repetition gives arbitrarily small soundness error.*

Lemma 2.1 ($\mathsf{NP} \subseteq \mathsf{IP}$)**.** NP *can be viewed as a 'single round' interactive proof:* P *sends the certificate* w *to* V*, and* V *executes* $\mathcal{V}(x, w)$ *in polynomial time and decides to accept or reject.*

3 MERLIN-BENCH

In this section, we introduce the key design in MERLIN-BENCH. The complete MERLIN-BENCH pipeline, including test set construction and evaluation, is illustrated in Figure 2.

3.1 BASIC SETTINGS

Formulation of Test Cases. The basic unit of MERLIN-BENCH is a *test case*. Each test case is associated with a decision problem in IP and specifies a rule for constructing problem instances,

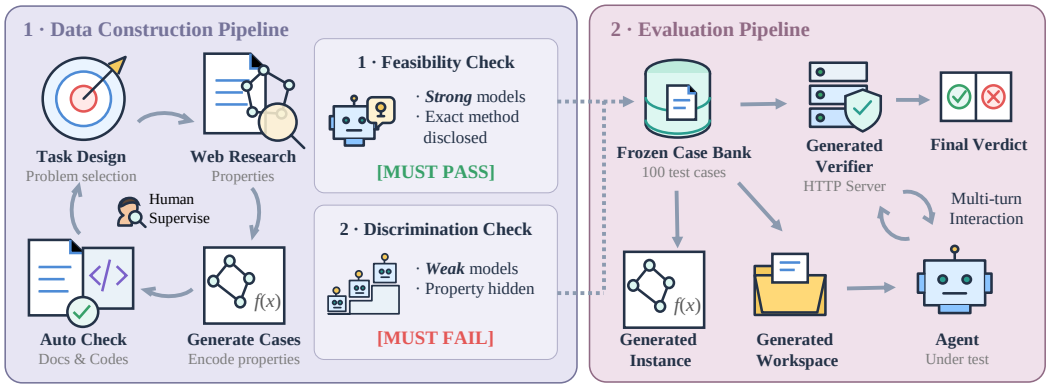

Figure 2: The complete pipeline of MERLIN-BENCH

together with constraints on the resources available for carrying out the interactive proof. Formally, a test case associated with $L \in \mathsf{IP}$ is formulated by a 5-tuple $c = (D_c, \mathcal{G}_c, \Pi_c, \mathcal{V}_c, B_c)$. Here, the *description* D_c is a string describing problem L, the *generator* $\mathcal{G}_c$ is a randomized algorithm that takes a random seed $r \sim \mathcal{R}$ as input and randomly constructs an instance $z \in L$ according to a manually specified rule; different random seeds can be viewed as equivalent transformations of the problem to prevent data leakage, having nearly no impact on the instance's difficulty; the *interactive proof protocol* Π_c with completeness factor $\varepsilon_c \leq 10^{-10}$ and soundness $\varepsilon_s \leq 2^{-23}$ (See Appendix B.1), together with the *verifier* $\mathcal{V}_c$, constitutes a complete and sound interactive proof system for L; the *resource constraints* B_c include limits on computation time, permitted tools, and other resources. The score of the agent A_θ on test case c is defined as follows:

$$\mathrm{Score}_c(A_\theta) = \mathbb{I}\left[\mathcal{V}_c(z, h_n) \to 1 \wedge \mathrm{Valid}_{B_c}(\tau) \mid r \leftarrow \mathcal{R}, z \leftarrow \mathcal{G}_c(r)\right],$$

where h_n denotes the interaction history of $\mathcal{V}$ and A_θ under protocol Π, and τ denotes the agent's complete execution trajectory, including its tool-call history and interactions under the protocol.

Evaluation Procedure. The entire evaluation process is managed by a controller program called the *evaluator*, as described below. For a given test case c, the evaluator samples a random seed r and invokes $\mathcal{G}_c(r)$ to generate an instance z. The evaluator then creates a workspace W_c for the agent under evaluation, A_θ, containing the instance z, the description D_c of the decision problem L, and the message format specified by Π_c. In addition, the evaluator launches a local HTTP server whose backend runs the verifier $\mathcal{V}_c$, and the agent interacts with it through a client.

If the verifier ultimately outputs 1, the evaluation result is recorded as a *pass*. The evaluator also retains the complete execution trajectory of A_θ and checks whether the agent's runtime and resource usage satisfy the requirements specified by B_c. If all checks pass, the evaluation result is recorded as a *strict pass*. Finally, the agent's score is calculated based on its strict-pass rate.

3.2 DATASET CONSTRUCTION

MERLIN-BENCH contains 100 test cases spanning 15 problems. This section describes the hierarchical organization of these test cases, as well as the methods used to collect and filter them.

Problem Tier Classification. To evaluate models more precisely, we classify the problems into three tiers rather than treating them all uniformly, as described below.

Tier-1 *Deterministic certificate.* This tier contains 36 test cases covering six NP problems. After searching for an answer and a certificate, the agent engages in a single round of interaction with the verifier to submit the certificate, which the verifier only needs to check for validity.

Tier-2 *Multi-round interactions.* This tier contains 40 test cases covering six IP problems. In this tier, the agent must convince Arthur, through a protocol-compliant multi-round interaction, that the input is indeed an instance satisfying the required property. Some test cases in this tier are fundamentally more difficult than those in Tier 1: certain problems are not currently

known to belong to NP, and the agent must provide a consistent interactive proof without relying on a fixed certificate.

Tier-3 *Real-world tasks.* This tier uses three real-world protocols, Lean, Dafny, and DRAT, as verifiers, with eight test cases for each. Through this tier, we demonstrate that an agent's ability to perform these three types of formal verification is fundamentally aligned with the capabilities evaluated by MERLIN-BENCH.

Figure 3 presents representative problems from the three tiers to illustrate their interaction processes. The complete list and detailed descriptions are provided in Appendices D–F.

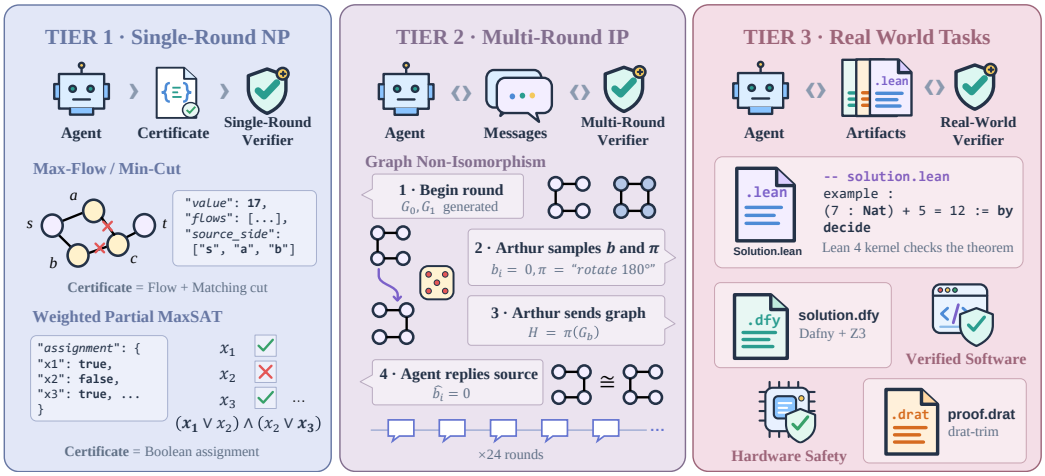

Figure 3: Representative problems from the three tiers of MERLIN-BENCH.

Test Case Construction. We developed a construction agent to generate test cases at scale. Its workflow is described below. Details on the construction process are provided in Appendix C.

Literature review. Given a decision problem L, the construction agent conducts a literature review to identify structural restrictions that admit specialized solutions. For example, general SAT is NP-hard, whereas 2-SAT can be solved in linear time. The identified structure is then used to construct the generator $\mathcal{G}_c$ and the reference algorithm $\mathcal{A}_c$. This structure and both algorithms are subsequently hidden from the agent under evaluation.

Generator implementation and automatic check. Based on the problem and the structure identified in the previous step, the construction agent implements the generator $\mathcal{G}_c$, the reference algorithm $\mathcal{A}_c$, and the verifier $\mathcal{V}_c$. The construction agent then writes the description D_c, ensuring that its specifications of the interactive protocol and input format are consistent with Π_c and $\mathcal{V}_c$. Next, the construction agent automatically checks the correctness of the test cases. It runs the reference algorithm $\mathcal{A}_c$ to ensure that it is accepted and submits some invalid proofs to check that they are rejected.

Feasibility and difficulty check. Next, the construction agent performs a feasibility check on the test case c. In this check, the original test case data c, together with the special property and the reference solution, are provided to a model widely recognized as highly capable (GPT-5.6 Sol in particular for our experiment). The test case passes the feasibility check if the model completes the proof within the specified time limit, so the construction of test cases depends directly on the pre-set time limits (600s in our experiment).

The construction agent then performs a difficulty check on the test case c. The test case data c are provided to a sequence of less capable model, and the test case passes the difficulty check if at least one of the models fails to complete the proof.

Human check. Once a test case has passed all the checks above, it undergoes a final human review to verify the correctness of the reference solution and execution trace, as well as the validity of the preceding checks. Test cases that pass the human review are included in the benchmark.

4 EXPERIMENTS

4.1 EXPERIMENTAL SETTING

Models. We evaluated 10 frontier LLMs that span the major model families: GPT-5.6-Luna, GPT-5.6-Terra, GPT-5.6-Sol, Claude-5-Sonnet, Claude-5-Opus, DeepSeek-V4-Flash, DeepSeek-V4-Pro, GLM-5.3-Flash, GLM-5.3, Kimi-K3.

Harness. To construct complete LLM agent systems, we pair DeepSeek-V4-Pro with DeepSeek Harness, Claude-5-Sonnet and Claude-5-Opus with Claude Code, and other models with Codex. All reasoning effort settings have been set to *high*.

4.2 BASIC RESULTS

In this section, we present the complete evaluation results for the systems described above and provide a preliminary analysis of the causes of failure in unsuccessful test cases.

Full Results. The complete evaluation results for all models are presented in Figure 4, and a detailed scoring table can be found in Appendix B.4. Note that the score is an evaluation of the agent as a whole, rather than the model itself. As shown, our benchmark—particularly Tier 2—exhibits strong discriminative power across agents. Moreover, the performance of the agents across the three tiers shows a strong positive correlation.

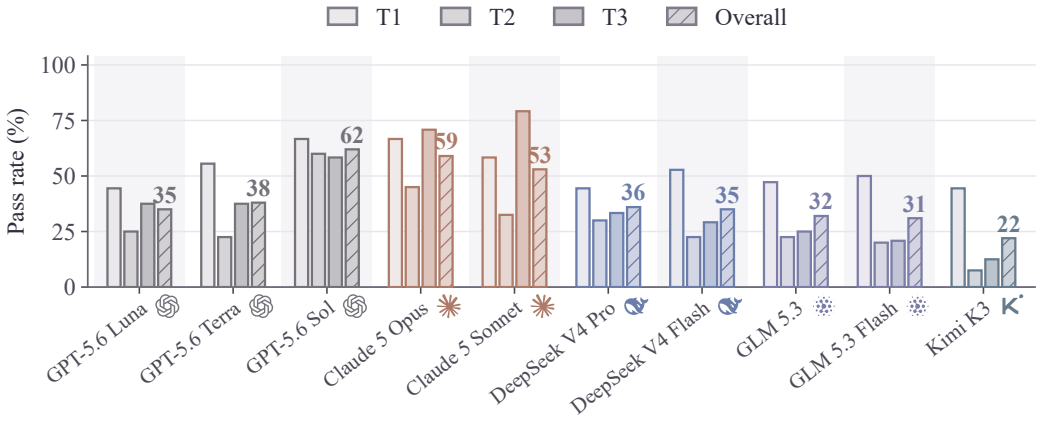

Figure 4: Benchmark scores normalized by total cases in each tier.

Failure Analysis. Using GPT-5.6-Sol and GPT-5.6-Terra as examples, we analyze the causes of failure in their unsuccessful test cases. To examine these causes more closely, we further count errors at both the *method level* and the *practice level*, the latter involving the interaction protocol and tool resources, and report the execution times of both models. Detailed statistics are provided in Figures 5 (a) and (b); the labeling criteria appear in Appendix B.5.

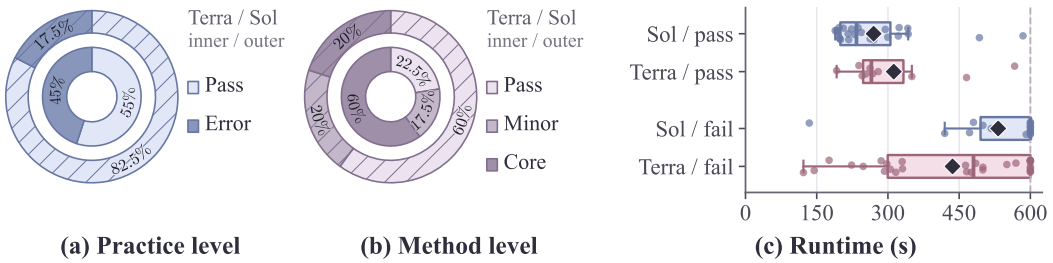

(a) Practice level **(b) Method level** **(c) Runtime (s)**

Figure 5: Tier-2 failure analysis.

We obtain the following two empirical observations:

- **Practice level issues remain a major bottleneck in the proof process.** Across all 40 test tasks, practice level errors account for 17.5% of Sol's results and 45.0% of Terra's. Among failed runs only, the proportions involving verofocation level issues are 43.8% and 58.1%, respectively. Moreover, the two models identified the correct methodology in 8 and 7 test cases, respectively, but failed to pass them for other reasons.
- **Sol completes successful tasks more quickly but consumes more of its budget on failed tasks.** In Figure 5, the average runtimes of Sol and Terra on successful tasks are 269. and 312.3 seconds, respectively, compared with 532.2 and 436.1 seconds on failed tasks. Practice level errors may cause runs to terminate early, whereas Sol's greater number of full-budget failures indicates that its difficult tasks often continue until the time limit is reached.

5 Case Studies

In this section, we conduct several case studies on Merlin-Bench, aimed at better leveraging models' ability to produce verifiable proofs in practice.

5.1 Case Study 1: Necessities of Tool Use and Problem Complexity

The first case study investigates the effect of tool use on LLMs' ability to complete interactive proofs. Furthermore, this experiment explains why problems of this level of complexity are chosen to evaluate the agent's proof process.

Method. This case study includes two sets of ablation experiments. We choose three problems in Tier 1—Max SAT, Min-Cut/Max-Flow (MCMF) and Set Cover. On the one hand, we construct a temporary *Tier 0* using three corresponding weakened problems in P—2-SAT, MCMF (which is already in P), and Minimum Vertex Cover in Bipartite Graphs (BGMC)—with six test cases generated for each problem using our method. We evaluate GPT-5.6-Luna, GPT-5.6-Terra, and GPT-5.6-Sol on this tier. On the other hand, after removing from B_c all permissions for *tool calls* other than interaction with Arthur, we evaluate the base GPT-5.6-Terra and GPT-5.6-Sol models as provers for the three Tier-1 problems. Appendix G provides task definitions and prompts.

Results. The complete results of the two ablation experiments are shown in Tables 2.

Task	**Luna**	**Terra**	**Sol**
2SAT	6	6	6
MCMF	5	5	6
BGMC	6	6	6
Total	17	17	18
Pass rate	**(94.4%)**	**(94.4%)**	**(100%)**

(a) Tier 0: tools enabled

Task	**Terra**	**Terra$^{\downarrow}$**	**Sol**	**Sol$^{\downarrow}$**
MCMF	5	1	6	1
MaxSAT	1	0	3	0
Set cover	4	1	3	1
Total	10	2	12	2
Δ (pp)	–	**−44.4**	–	**−55.6**

(b) Tier 1: tools removed

Table 2: Tool-use ablations. In (b), Terra$^{\downarrow}$ and Sol$^{\downarrow}$ mean models without tools.

These results indicates the following empirical conclusions:

1. **Tool use is essential for LLM agents to produce practical results, enabling them to solve problems that base models cannot solve on their own.** As shown in Table 2, when no additional tool calls are permitted, both Sol and Terra score only 2 points, obtained from two small-scale test cases involving Set Cover and Min-Cut/Max-Flow, respectively. When tool calls are enabled, all frontier models achieve substantial scores.
2. **Once tool use is taken into account, benchmarks constructed from problems in P with known *low degree polynomial time* algorithms will almost inevitably become saturated.**

As shown in Table 2, when tool use is permitted and the test-set difficulty is restricted to P, all three models in the GPT family achieve 90%+ scores. This result supports our motivation for raising the complexity of the benchmark problems from P to IP.

5.2 Case Study 2: Influence of Expertise in User Prompt

In practice, users can provide user prompts at different levels depending on their familiarity with the research problem. This case study investigates how user prompts at different levels affect models' ability to complete interactive proofs.

Method. We divide user prompts into three levels to simulate how three types of users affect the model's proof capabilities:

Engineer The Engineer provides guidance on carrying out the interactive proof, including practice level suggestions such as recording Arthur's messages and reserving sufficient time for the final submission.

Student The Student provides general directions for an interactive-proof task but offers no test-case-specific guidance.

Expert The Expert describes how the current instance is constructed and provides a strategy for solving it. Note that this guidance remains at the strategic level and does not provide a concrete solution method, making it fundamentally different from the feasibility check used during test-set construction.

For example, for the GNI task, the Student prompt provides the general direction of using an "invariant," while the Expert prompt further identifies the local structure to be recovered and the corresponding parity computation, giving the model more concrete steps for making the required distinction. The complete prompt can be found in Appendix H. We fix the model under evaluation to GPT-5.6-Terra.

Results. From the results summarized in Figure 6, we obtain the following empirical observations:

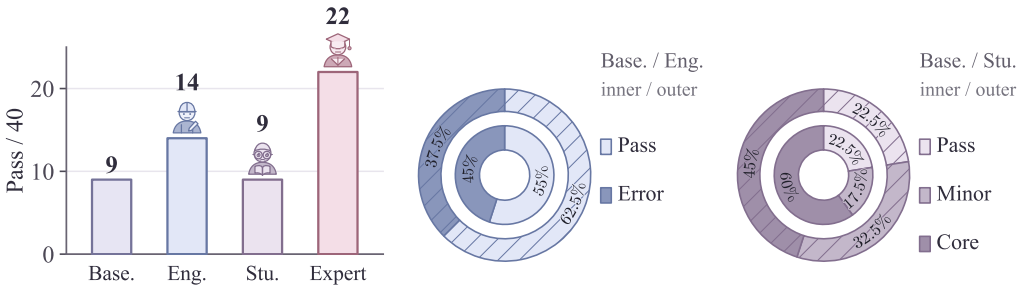

Figure 6: Terra prompt expertise on 40 Tier-2 cases.

1. **Engineer prompts help reduce execution failures.** Figure 6 shows that the numbers of passed tasks under the Baseline, Engineer, Student, and Expert conditions are 9, 14, 9, and 22, respectively. Under the Engineer condition, the practice level error rate decreases from 45.0% to 37.5% (Figure 6 (b)).
2. **General methodological guidance must still be translated into reliable execution.** From Figure 6 (c), under the Student condition, the number of tasks with an inadequate core method decreases from 24/40 to 18/40, whereas the number of tasks with a broadly correct approach that nevertheless fail increases from 7/40 to 13/40. The total number of passed tasks remains 9/40. This indicates that even after learning the general algorithm for a task family, the model still struggles implement it as a complete proof process.
3. **Domain-specific knowledge expands the range of tasks that the model can solve.** Under the Expert condition, 22/40 tasks pass, improved substantially compared to the baseline (9/40).

5.3 Case Study 3: Transfer Experience on Synthetic Data to Real Tasks

This case study investigates whether LLM agents' experience on a synthetic interactive proof dataset can be used to improve their performance on real-world verification tasks.

Method. We ask the model to distill lessons from its Tier 1 and Tier 2 solution traces into a text, which we call a *study guide*. In this experiment, the study guide is provided to the model as a prompt. Specifically, we let agent B distill a study guide from the Tier 1 and Tier 2 solution trajectories. We then instantiate a new agent A and allow it to reason over the study guide for up to 300 seconds (sufficiently large in our experiment settings). Afterward, we provide the Tier 3 tasks to agent A and ask it to solve them. We denote the transfer setting by A^{+B}. Moreover, we introduce a blank control condition in which an agent generates a study guide *without proof trajectories*. For an evaluated model A, we denote this condition by A^{+0}. We selected GPT-5.6-Sol and GPT-5.6-Terra as agents. The study guides, complete prompt and more explanations are provided in Appendix I.

Results. Table 3 compares the baseline with the three transfer settings.

Setting	Lean	Dafny	DRAT	Total	Δ (pp)
Sol^{+0}	5	7	6	18	–
$\text{Sol}^{+\text{Sol}}$	5	8	8	21	+12.5
Terra^{+0}	4	5	3	12	–
$\text{Terra}^{+\text{Terra}}$	3	6	5	14	+8.3
$\text{Terra}^{+\text{Sol}}$	5	6	5	16	+16.7

(a) Per-task scores

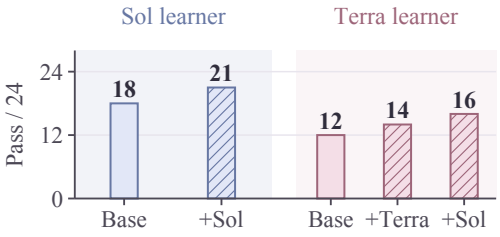

(b) Overall

Table 3: Results of the transferability experiment.

These results support the following empirical conclusion:

1. **Synthesized experience can improve models' ability to solve real-world tasks.** After incorporating the study guides, all three configurations achieve substantially higher scores on Tier 3. Empirically, the gains are associated with the capabilities of both models involved. Comparing $\text{Terra}^{+\text{Sol}}$ with $\text{Terra}^{+\text{Terra}}$ shows that a stronger teacher for distilling the study guide leads to better downstream performance. Comparing $\text{Sol}^{+\text{Sol}}$ with $\text{Terra}^{+\text{Sol}}$ shows that a stronger learner for solving the tasks likewise yields better final performance.
2. **Post-training on synthesized experience could potentially improve real-world performance.** In this experiment, we provide the study guide to the model solely through prompting, leaving the parameters unchanged. A promising direction for future work is to convert the Tier 1 and Tier 2 solution trajectories into training data and use them for post-training, with the goal of improving models' ability to construct proofs using real-world verifiers.

6 Conclusion

In summary, we introduce MERLIN-BENCH, a benchmark that evaluates models' ability to construct unified proofs according to specified requirements by placing LLM agents in the role of the prover within an interactive proof system. Our evaluation of 10 frontier LLMs shows that, beyond the ability to find certificates, constructing proofs according to the required specifications remains a significant capability bottleneck for LLMs. Our further case studies shows:

1. Tool use is essential for LLM agents to produce practical results and must therefore be taken into account when constructing evaluation datasets.
2. User prompts have a direct impact on the capabilities of LLM agents. Both guidance on formal proof construction and domain-specific expertise can improve model performance.
3. Test-time scaling or post-training based on synthetic interactive proof datasets may improve models' formal proof capabilities.

AI USE STATEMENT

In this work, we used generative AI tools for generating synthetic data sets, assisting in the writing of proofs, implementing methods, assisting with translation and cleaning and reformatting dataset. We have not used generative AI tools for helping develop theoretical models or conceptual frameworks, formulating mathematical claims, providing critical ingredients for proving mathematical claims, designing or providing feedback on research methodology or experiments, supporting qualitative and thematic data analysis and interpreting results. and proposing or refining hypotheses are not applicable to this work. We have reviewed all AI-assisted work. We checked LLM-generated code and data sets. All the text in the paper has undergone rigorous human review. We take responsibility for the final content of this work, including text, claims or artifacts produced with the aid of generative AI.

REPRODUCIBILITY STATEMENT

We have organized the codebase for MERLIN-BENCH and included it in the supplementary materials to support reproducibility. After de-anonymization, we will release the repository publicly on GitHub to facilitate reuse of the benchmark and evaluation of additional models.

REFERENCES

A. A. Albert. Quasigroups. I. *Transactions of the American Mathematical Society*, 54(3):507–519, 1943. doi: 10.2307/1990259. URL https://doi.org/10.2307/1990259.

Noga Alon, Thomas F. Bloom, W. T. Gowers, Daniel Litt, Will Sawin, Arul Shankar, Jacob Tsimerman, Victor Wang, and Melanie Matchett Wood. Remarks on the disproof of the unit distance conjecture, 2026. URL https://arxiv.org/abs/2605.20695.

Noga Amit, Shafi Goldwasser, Orr Paradise, and Guy Rothblum. A theory for worst-case vs. average-case guarantees for llms. In D. Belgrave, C. Zhang, H. Lin, R. Pascanu, P. Koniusz, M. Ghassemi, and N. Chen (eds.), *Advances in Neural Information Processing Systems*, volume 38, Main Conference, pp. 146513–146549. Curran Associates, Inc., 2025. doi: 10.52202/085713-4901. URL https://proceedings.neurips.cc/paper_files/paper/2025/file/d7a2222b8d41014e060cfeb0995501d0-Paper-Conference.pdf.

Zhangir Azerbayev, Hailey Schoelkopf, Keiran Paster, Marco Dos Santos, Stephen McAleer, Qiaochu Jiang, Jia Deng, Stella R Biderman, and Sean Welleck. Llemma: An open language model for mathematics. In B. Kim, Y. Yue, S. Chaudhuri, K. Fragkiadaki, M. Khan, and Y. Sun (eds.), *International Conference on Learning Representations*, volume 2024, pp. 40622–40649, 2024. URL https://proceedings.iclr.cc/paper_files/paper/2024/file/b225f5c7cd13615e9558c3931fa4e66f-Paper-Conference.pdf.

László Babai. Trading group theory for randomness. In *Proceedings of the Seventeenth Annual ACM Symposium on Theory of Computing*, STOC '85, pp. 421–429. Association for Computing Machinery, 1985. doi: 10.1145/22145.22192.

K. E. Batcher. Sorting networks and their applications. In *Proceedings of the AFIPS Spring Joint Computer Conference*, volume 32, pp. 307–314, 1968. doi: 10.1145/1468075.1468121. URL https://doi.org/10.1145/1468075.1468121.

A. Biere. The AIGER And-Inverter Graph (AIG) Format, Version 20071012. FMV Reports Series 07/1, Johannes Kepler University, 2007. URL https://fmv.jku.at/aiger/.

Léo Boisvert, Megh Thakkar, Maxime Gasse, Massimo Caccia, Thibault Le Sellier De Chezelles, Quentin Cappart, Nicolas Chapados, Alexandre Lacoste, and Alexandre Drouin. Workarena++: Towards compositional planning and reasoning-based common knowledge work tasks. In A. Globerson, L. Mackey, D. Belgrave, A. Fan, U. Paquet, J. Tomczak, and C. Zhang (eds.), *Advances in Neural Information Processing Systems*, volume 37, pp. 5996–6051. Curran Associates, Inc., 2024. doi: 10.52202/079017-0195. URL https://proceedings.neurips.cc/paper_files/paper/2024/file/0b82662b6c32e887bb252a74d8cb2d5e-Paper-Datasets_and_Benchmarks_Track.pdf.

A. E. Brouwer and W. H. Haemers. *Spectra of Graphs*. Springer, 2012. doi: 10.1007/978-1-4614-1939-6. URL https://doi.org/10.1007/978-1-4614-1939-6.

J.-Y. Cai, M. Fürer, and N. Immerman. An optimal lower bound on the number of variables for graph identification. *Combinatorica*, 12(4):389–410, 1992. doi: 10.1007/BF01305232. URL https://doi.org/10.1007/BF01305232.

J. L. Carter and M. N. Wegman. Universal classes of hash functions. *Journal of Computer and System Sciences*, 18(2):143–154, 1979. doi: 10.1016/0022-0000(79)90044-8. URL https://doi.org/10.1016/0022-0000(79)90044-8.

Ziru Chen, Shijie Chen, Yuting Ning, Qianheng Zhang, Boshi Wang, Botao Yu, Yifei Li, Zeyi Liao, Chen Wei, Zitong Lu, Vishal Dey, Mingyi Xue, Frazier N. Baker, Benjamin Burns, Daniel Adu-Ampratwum, Xuhui Huang, Xia Ning, Song Gao, Yu Su, and Huan Sun. Scienceagentbench: Toward rigorous assessment of language agents for data-driven scientific discovery. In Y. Yue, A. Garg, N. Peng, F. Sha, and R. Yu (eds.), *International Conference on Learning Representations*, volume 2025, pp. 96934–96990, 2025. URL https://proceedings.iclr.cc/paper_files/paper/2025/file/f12b4df26344f3be803c06b555252efe-Paper-Conference.pdf.

Alessandro Chiesa and Tom Gur. Proofs of Proximity for Distribution Testing. In Anna R. Karlin (ed.), *9th Innovations in Theoretical Computer Science Conference (ITCS 2018)*, volume 94 of *Leibniz International Proceedings in Informatics (LIPIcs)*, pp. 53:1–53:14, Dagstuhl, Germany, 2018. Schloss Dagstuhl – Leibniz-Zentrum für Informatik. ISBN 978-3-95977-060-6. doi: 10.4230/LIPIcs.ITCS.2018.53. URL https://drops.dagstuhl.de/entities/document/10.4230/LIPIcs.ITCS.2018.53.

V. Chvátal. A greedy heuristic for the set-covering problem. *Mathematics of Operations Research*, 4(3):233–235, 1979. doi: 10.1287/moor.4.3.233. URL https://doi.org/10.1287/moor.4.3.233.

L. de Moura and S. Ullrich. The Lean 4 Theorem Prover and Programming Language. In *Automated Deduction—CADE 28*, pp. 625–635, 2021. doi: 10.1007/978-3-030-79876-5_37. URL https://doi.org/10.1007/978-3-030-79876-5_37.

Leonardo de Moura, Soonho Kong, Jeremy Avigad, Floris van Doorn, and Jakob von Raumer. The lean theorem prover (system description). In Amy P. Felty and Aart Middeldorp (eds.), *Automated Deduction - CADE-25*, pp. 378–388, Cham, 2015. Springer International Publishing. ISBN 978-3-319-21401-6.

Lizhou Fan, Wenyue Hua, Lingyao Li, Haoyang Ling, and Yongfeng Zhang. NPHardEval: Dynamic benchmark on reasoning ability of large language models via complexity classes. In Lun-Wei Ku, Andre Martins, and Vivek Srikumar (eds.), *Proceedings of the 62nd Annual Meeting of the Association for Computational Linguistics (Volume 1: Long Papers)*, pp. 4092–4114, Bangkok, Thailand, August 2024. Association for Computational Linguistics. doi: 10.18653/v1/2024.acl-long.225. URL https://aclanthology.org/2024.acl-long.225/.

L. R. Ford, Jr. and D. R. Fulkerson. Maximal flow through a network. *Canadian Journal of Mathematics*, 8:399–404, 1956. doi: 10.4153/CJM-1956-045-5. URL https://doi.org/10.4153/CJM-1956-045-5.

N. Garg, G. Konjevod, and R. Ravi. A polylogarithmic approximation algorithm for the Group Steiner Tree problem. *Journal of Algorithms*, 37(1):66–84, 2000. doi: 10.1006/jagm.2000.1096. URL https://doi.org/10.1006/jagm.2000.1096.

O. Goldreich, S. Micali, and A. Wigderson. Proofs that yield nothing but their validity or all languages in NP have zero-knowledge proof systems. *Journal of the ACM*, 38(3):691–729, 1991. doi: 10.1145/116825.116852. URL https://doi.org/10.1145/116825.116852.

S. Goldwasser and M. Sipser. Private coins versus public coins in interactive proof systems. In *Proceedings of the 18th Annual ACM Symposium on Theory of Computing*, pp. 59–68, 1986. doi: 10.1145/12130.12137. URL https://doi.org/10.1145/12130.12137.

S. Goldwasser, Y. T. Kalai, and G. N. Rothblum. Delegating computation: interactive proofs for muggles. In *Proceedings of the 40th Annual ACM Symposium on Theory of Computing*, pp. 113–122, 2008. doi: 10.1145/1374376.1374396. URL https://doi.org/10.1145/1374376.1374396.

Shafi Goldwasser, Guy N. Rothblum, Jonathan Shafer, and Amir Yehudayoff. Interactive Proofs for Verifying Machine Learning. In James R. Lee (ed.), *12th Innovations in Theoretical Computer Science Conference (ITCS 2021)*, volume 185 of *Leibniz International Proceedings in Informatics (LIPIcs)*, pp. 41:1–41:19, Dagstuhl, Germany, 2021. Schloss Dagstuhl – Leibniz-Zentrum für Informatik. ISBN 978-3-95977-177-1. doi: 10.4230/LIPIcs.ITCS.2021.41. URL https://drops.dagstuhl.de/entities/document/10.4230/LIPIcs.ITCS.2021.41.

Tom Gur, Mohammad Mahdi Jahanara, Mohammad Mahdi Khodabandeh, Ninad Rajgopal, Bahar Salamatian, and Igor Shinkar. On the power of interactive proofs for learning. In *Proceedings of the 56th Annual ACM Symposium on Theory of Computing*, STOC 2024, pp. 1063–1070, New York, NY, USA, 2024. Association for Computing Machinery. ISBN 9798400703836. doi: 10.1145/3618260.3649784. URL https://doi.org/10.1145/3618260.3649784.

O. J. Heilmann and E. H. Lieb. Theory of monomer–dimer systems. *Communications in Mathematical Physics*, 25(3):190–232, 1972. doi: 10.1007/BF01877590. URL https://doi.org/10.1007/BF01877590.

P. Hell and J. Nešetřil. *Graphs and Homomorphisms*. Oxford University Press, 2004. doi: 10.1093/acprof:oso/9780198528173.001.0001. URL https://doi.org/10.1093/acprof:oso/9780198528173.001.0001.

Albert Q. Jiang, Sean Welleck, Jin Peng Zhou, Wenda Li, Jiacheng Liu, Mateja Jamnik, Timothée Lacroix, Yuhuai Wu, and Guillaume Lample. Draft, sketch, and prove: Guiding formal theorem provers with informal proofs. In *The Eleventh International Conference on Learning Representations*, 2023.

Carlos E Jimenez, John Yang, Alexander Wettig, Shunyu Yao, Kexin Pei, Ofir Press, and Karthik Narasimhan. Swe-bench: Can language models resolve real-world github issues? In B. Kim, Y. Yue, S. Chaudhuri, K. Fragkiadaki, M. Khan, and Y. Sun (eds.), *International Conference on Learning Representations*, volume 2024, pp. 54107–54157, 2024. URL https://proceedings.iclr.cc/paper_files/paper/2024/file/edac78c3e300629acfe6cbe9ca88fb84-Paper-Conference.pdf.

Parnian Kamran, Premkumar Devanbu, and Caleb Stanford. Vision paper: Proof-carrying code completions. In *Proceedings of the 39th IEEE/ACM International Conference on Automated Software Engineering Workshops*, ASEW '24, pp. 35–42, New York, NY, USA, 2024. Association for Computing Machinery. ISBN 9798400712494. doi: 10.1145/3691621.3694932. URL https://doi.org/10.1145/3691621.3694932.

Yisi Ke, Tianyu Huang, Yankai Shu, Di He, Jingchu Gai, and Liwei Wang. Towards solving the gilbert-pollak conjecture via large language models. In *Forty-third International Conference on Machine Learning*, 2026. URL https://openreview.net/forum?id=Cqq3HGRIuM.

K. Rustan M. Leino. Dafny: An automatic program verifier for functional correctness. In Edmund M. Clarke and Andrei Voronkov (eds.), *Logic for Programming, Artificial Intelligence, and Reasoning*, pp. 348–370, Berlin, Heidelberg, 2010. Springer Berlin Heidelberg. ISBN 978-3-642-17511-4.

Xiao Liu, Hao Yu, Hanchen Zhang, Yifan Xu, Xuanyu Lei, Hanyu Lai, Yu Gu, Hangliang Ding, Kaiwen Men, Kejuan Yang, Shudan Zhang, Xiang Deng, Aohan Zeng, Zhengxiao Du, Chenhui Zhang, Sheng Shen, Tianjun Zhang, Yu Su, Huan Sun, Minlie Huang, Yuxiao Dong, and Jie Tang. Agentbench: Evaluating llms as agents. In B. Kim, Y. Yue, S. Chaudhuri, K. Fragkiadaki, M. Khan, and Y. Sun (eds.), *International Conference on Learning Representations*, volume 2024, pp. 52989–53046, 2024. URL https://proceedings.iclr.cc/paper_files/paper/2024/file/e9df36b21ff4ee211a8b71ee8b7e9f57-Paper-Conference.pdf.

C. Lund, L. Fortnow, H. Karloff, and N. Nisan. Algebraic methods for interactive proof systems. *Journal of the ACM*, 39(4):859–868, 1992. doi: 10.1145/146585.146605. URL https://doi.org/10.1145/146585.146605.

F. J. MacWilliams and N. J. A. Sloane. *The Theory of Error-Correcting Codes*. North-Holland, 1977.

Eric Mugnier, Emmanuel Anaya Gonzalez, Nadia Polikarpova, Ranjit Jhala, and Zhou Yuanyuan. Laurel: Unblocking automated verification with large language models. *Proc. ACM Program. Lang.*, 9(OOPSLA1), April 2025. doi: 10.1145/3720499. URL https://doi.org/10.1145/3720499.

OpenAI. Finite time blowup for Navier–Stokes. Technical manuscript, September 2026a. URL https://cdn.openai.com/pdf/32d9f210-8b73-45e0-91bc-82a30aef8a9a/navier-stokes.pdf. Released September 8, 2026.

OpenAI. Finite time blowup for navier–stokes and euler equations. GitHub repository, 2026b. URL https://github.com/openai/NavierStokesAndEuler. Lean 4 formalization, accessed September 21, 2026.

OpenAI. Planar point sets with many unit distances, 2026c. URL https://cdn.openai.com/pdf/74c24085-19b0-4534-9c90-465b8e29ad73/unit-distance-proof.pdf. Technical manuscript.

S. E. Payne and J. A. Thas. *Finite Generalized Quadrangles*. European Mathematical Society, second edition, 2009. doi: 10.4171/066. URL https://doi.org/10.4171/066.

I. S. Reed. A class of multiple-error-correcting codes and the decoding scheme. *Transactions of the IRE Professional Group on Information Theory*, 4(4):38–49, 1954. doi: 10.1109/TIT.1954.1057465. URL https://doi.org/10.1109/TIT.1954.1057465.

I. S. Reed and G. Solomon. Polynomial codes over certain finite fields. *Journal of the Society for Industrial and Applied Mathematics*, 8(2):300–304, 1960. doi: 10.1137/0108018. URL https://doi.org/10.1137/0108018.

Adi Shamir. IP = PSPACE. *Journal of the ACM*, 39(4):869–877, 1992. doi: 10.1145/146585.146609.

Zachary S. Siegel, Sayash Kapoor, Nitya Nadgir, Benedikt Stroebl, and Arvind Narayanan. Core-bench: Fostering the credibility of published research through a computational reproducibility agent benchmark. *Transactions on Machine Learning Research*, 2025-January:1 – 31, 2025. URL https://www.scopus.com/inward/record.uri?eid=2-s2.0-85219569769&partnerID=40&md5=ff7d3bf0c495411a5659c8cdea0fe925.

Heng Wang, Shangbin Feng, Tianxing He, Zhaoxuan Tan, Xiaochuang Han, and Yulia Tsvetkov. Can language models solve graph problems in natural language? In *Proceedings of the 37th International Conference on Neural Information Processing Systems*, NIPS '23, Red Hook, NY, USA, 2023. Curran Associates Inc.

Anjiang Wei, Yuheng Wu, Yingjia Wan, Tarun Suresh, Huanmi Tan, Zhanke Zhou, Sanmi Koyejo, Ke Wang, and Alex Aiken. SATBench: Benchmarking LLMs' logical reasoning via automated puzzle generation from SAT formulas. In Christos Christodoulopoulos, Tanmoy Chakraborty, Carolyn Rose, and Violet Peng (eds.), *Proceedings of the 2025 Conference on Empirical Methods in Natural Language Processing*, pp. 33832–33849, Suzhou, China, November 2025. Association for Computational Linguistics. ISBN 979-8-89176-332-6. doi: 10.18653/v1/2025.emnlp-main.1716. URL https://aclanthology.org/2025.emnlp-main.1716/.

Nathan Wetzler, Marijn J. H. Heule, and Warren A. Hunt. Drat-trim: Efficient checking and trimming using expressive clausal proofs. In Carsten Sinz and Uwe Egly (eds.), *Theory and Applications of Satisfiability Testing – SAT 2014*, pp. 422–429, Cham, 2014. Springer International Publishing. ISBN 978-3-319-09284-3.

H. Whitney. Congruent graphs and the connectivity of graphs. *American Journal of Mathematics*, 54 (1):150–168, 1932. doi: 10.2307/2371086. URL https://doi.org/10.2307/2371086.

Tianbao Xie, Danyang Zhang, Jixuan Chen, Xiaochuan Li, Siheng Zhao, Ruisheng Cao, Toh Jing Hua, Zhoujun Cheng, Dongchan Shin, Fangyu Lei, Yitao Liu, Yiheng Xu, Shuyan Zhou, Silvio Savarese, Caiming Xiong, Victor Zhong, and Tao Yu. Osworld: Benchmarking multimodal agents for open-ended tasks in real computer environments. In A. Globerson, L. Mackey, D. Belgrave, A. Fan, U. Paquet, J. Tomczak, and C. Zhang (eds.), *Advances in Neural Information Processing Systems*, volume 37, pp. 52040–52094. Curran Associates, Inc., 2024. doi: 10.52202/079017-1650. URL https://proceedings.neurips.cc/paper_files/paper/2024/file/5d413e48f84dc61244b6be550f1cd8f5-Paper-Datasets_and_Benchmarks_Track.pdf.

Huajian Xin, Z.Z. Ren, Junxiao Song, Zhihong Shao, Wanjia Zhao, Haocheng Wang, Bo Liu, Liyue Zhang, Xuan Lu, Qiushi Du, Wenjun Gao, Haowei Zhang, Qihao Zhu, Dejian Yang, Zhibin Gou, Z.F. Wu, Fuli Luo, and Chong Ruan. Deepseek-prover-v1.5: Harnessing proof assistant feedback for reinforcement learning and monte-carlo tree search. In Y. Yue, A. Garg, N. Peng, F. Sha, and R. Yu (eds.), *International Conference on Learning Representations*, volume 2025, pp. 72274–72303, 2025. URL https://proceedings.iclr.cc/paper_files/paper/2025/file/b3b55c366d641c07180c40e4f978f311-Paper-Conference.pdf.

Chenyuan Yang, Xuheng Li, Md Rakib Hossain Misu, Jianan Yao, Weidong Cui, Yeyun Gong, Chris Hawblitzel, Shuvendu Lahiri, Jacob R. Lorch, Shuai Lu, Fan Yang, Ziqiao Zhou, and Shan Lu. Autoverus: Automated proof generation for rust code. *Proc. ACM Program. Lang.*, 9(OOPSLA2), October 2025. doi: 10.1145/3763174. URL https://doi.org/10.1145/3763174.

Kaiyu Yang, Aidan Swope, Alex Gu, Rahul Chalamala, Peiyang Song, Shixing Yu, Saad Godil, Ryan J Prenger, and Animashree Anandkumar. Leandojo: Theorem proving with retrieval-augmented language models. In A. Oh, T. Naumann, A. Globerson, K. Saenko, M. Hardt, and S. Levine (eds.), *Advances in Neural Information Processing Systems*, volume 36, pp. 21573–21612. Curran Associates, Inc., 2023. doi: 10.52202/075280-0944. URL https://proceedings.neurips.cc/paper_files/paper/2023/file/4441469427094f8873d0fecb0c4e1cee-Paper-Datasets_and_Benchmarks.pdf.

Shunyu Yao, Noah Shinn, Pedram Razavi, and Karthik Narasimhan. τ-bench: A benchmark for tool-agent-user interaction in real-world domains. In Y. Yue, A. Garg, N. Peng, F. Sha, and R. Yu (eds.), *International Conference on Learning Representations*, volume 2025, pp. 9965–10017, 2025. URL https://proceedings.iclr.cc/paper_files/paper/2025/file/1b126cc38b8638e07bef37e7b2bb72bf-Paper-Conference.pdf.

Congchi Yin, Tianyi Wu, Yankai Shu, Alex Gu, Yun Han Wang, Jun Shao, xun jiang, and Piji Li. Investigating advanced reasoning of large language models via black-box environment interaction. In *Forty-third International Conference on Machine Learning*, 2026. URL https://openreview.net/forum?id=pLLWX35m6O.

Kunhao Zheng, Jesse Michael Han, and Stanislas Polu. miniF2F: A cross-system benchmark for formal olympiad-level mathematics. In *International Conference on Learning Representations*, 2022. URL https://openreview.net/forum?id=9ZPegFuFTFv.

Shuyan Zhou, Frank F Xu, Hao Zhu, Xuhui Zhou, Robert Lo, Abishek Sridhar, Xianyi Cheng, Tianyue Ou, Yonatan Bisk, Daniel Fried, Uri Alon, and Graham Neubig. Webarena: A realistic web environment for building autonomous agents. In B. Kim, Y. Yue, S. Chaudhuri, K. Fragkiadaki, M. Khan, and Y. Sun (eds.), *International Conference on Learning Representations*, volume 2024, pp. 15585–15606, 2024. URL https://proceedings.iclr.cc/paper_files/paper/2024/file/4410c0711e9154a7a2d26f9b3816d1ef-Paper-Conference.pdf.

A Additional Related Works

In this section, we review additional literature related to the topics of this paper.

Interactive proof in machine learning. Interactive-proof complexity provides a formal prover–verifier framework for machine learning, with explicit guarantees concerning completeness, soundness, round complexity, communication complexity, sample complexity, and verification time. Amit et al. (2025) introduce Self-Proving models that generate an answer and then interact with a fixed verifier to establish its per-instance correctness under a worst-case soundness guarantee. However, they treat the verifier as a reward model and do not use IP to characterize the workflow of agent systems. Goldwasser et al. (2021) formulate IP-PAC, in which a resource-constrained verifier interacts with a prover to certify the approximate correctness of a learned hypothesis. Gur et al. (2024) develop doubly efficient interactive proofs for agnostic learning tasks, including the recovery of heavy Fourier coefficients and the learning of $\mathsf{AC}^0[2]$ functions and juntas. Chiesa & Gur (2018) introduce IP distribution testers and show that interaction with an untrusted prover can exponentially reduce the sample complexity of distribution testing.

Agent-oriented benchmarks. Several benchmarks have been developed specifically to evaluate different capabilities of LLM agents. Yin et al. (2026) investigates the advanced reasoning capabilities of models through interaction with black-box environments. Liu et al. (2024) assess general-purpose agent capabilities across heterogeneous environments, including operating systems, databases, knowledge graphs, card games, and embodied household tasks. Yao et al. (2025); Boisvert et al. (2024) evaluate agents on user-facing business operations and enterprise knowledge work, using policy-constrained airline and retail support tasks and compositional ServiceNow workflows, respectively. Zhou et al. (2024); Xie et al. (2024) assess agents' ability to operate digital interfaces, focusing on functional websites and cross-application tasks in real operating systems, respectively. Jimenez et al. (2024) evaluate software-engineering agents by requiring them to resolve real GitHub issues through repository-level code modifications. Siegel et al. (2025); Chen et al. (2025) evaluate scientific research agents on computational reproduction of published studies and the implementation of data-driven scientific analyses, respectively.

Lean, Dafny, and LLM-assisted formal verification. Formal verification systems such as Lean de Moura et al. (2015), Dafny Leino (2010), and DRAT Wetzler et al. (2014) provide machine-checkable mechanisms for validating mathematical proofs, program correctness, and SAT certificates. Zheng et al. (2022) introduce miniF2F, a cross-system benchmark of formalized Olympiad-level problems that using Lean verification. Jiang et al. (2023) use informal proofs to guide the generation and completion of formal proof sketches. Yang et al. (2023) introduce LeanDojo, an environment and benchmark for retrieval-augmented theorem proving in Lean. Azerbayev et al. (2024) develop Llemma, a mathematics-focused language model that supports formal theorem proving in Lean. Xin et al. (2025) use Lean's verification feedback as a reinforcement-learning signal and combine it with Monte-Carlo tree search. Kamran et al. (2024) propose proof-carrying code completions in which language models generate Dafny code together with machine-checkable safety proofs.

B Supplementary Definitions and Evaluation Details

B.1 Analysis of Completeness and Soundness

An interactive verifier uses randomness to test a proof. Its two possible statistical errors have different consequences for evaluation. A *completeness error* rejects an honest proof of a true claim; a *soundness error* accepts a false claim, even when the prover chooses its strategy adversarially. Small soundness error makes acceptance reliable, whereas small completeness error prevents verifier randomness alone from rejecting a correct proof strategy.

Let $\mathrm{Acc}(P, x; r)$ be the acceptance indicator for prover strategy P, public instance x, and verifier randomness r. Writing $\mathcal{Y}$ and $\mathcal{N}$ for the true and false claims covered by a task's promise, perfect completeness means

$$\forall x \in \mathcal{Y} \quad \exists P_x \quad \Pr_r[\mathrm{Acc}(P_x, x; r) = 1] = 1. \tag{B.1}$$

Soundness error at most ε means

$$\forall x \in \mathcal{N} \quad \forall P^* \quad \Pr_r[\mathrm{Acc}(P^*, x; r) = 1] \leq \varepsilon. \tag{B.2}$$

For a task that checks a numerical output, the claim includes the proposed output: the soundness statement concerns an incorrect value. Statistical completeness replaces the right-hand side of Equation B.1 by a lower bound of $1 - \delta$.

This distinction matters in a one-shot benchmark. If completeness is perfect, an honest strategy that follows the protocol succeeds for every verifier challenge. A rejected execution cannot be attributed to an unavoidable statistical rejection of that strategy. This makes an individual failure easier to interpret and avoids introducing a completeness-related reason to repeat an otherwise correct attempt. At the same time, the soundness guarantee prevents a prover from obtaining credit for a false claim except with the stated small probability.

Tier-2 guarantees. Every Tier-2 family has soundness error strictly below 2^{-23} under the conditions of its proof. Five families have perfect completeness. The Boolean-Circuit Image-Size Lower Bound protocol instead has statistical completeness with $\delta < 10^{-10}$. Table 4 lists the guarantees for the published parameter ranges and links to the detailed proofs in Section E.

Table 4: Completeness error δ and soundness error ε for the six Tier-2 families. Each soundness bound is strictly below 2^{-23}.

Task family	δ	Upper bound on ε	Proof
Graph Non-Isomorphism	0	2^{-24}	Lemma E.1
Boolean-Hypercube Sum-Check	0	$\frac{5m}{p} \leq \frac{2000}{p} < 2^{-50}$	Lemma E.2
GKR Circuit Evaluation	0	$\frac{5\sum_{i=0}^{L-1} s_{i+1}}{p} < 2^{-49}$	Lemma E.3
Circuit Image-Size Lower Bound	$< 10^{-10}$	$e^{-16} < 2^{-23}$	Lemma E.4
Shamir-Style TQBF	0	$\frac{\sum_q d_q}{p} \leq \frac{2060}{p} < 2^{-49}$	Lemma E.5
Hamiltonicity Bind–Challenge–Open	0	2^{-24}	Lemma E.6

For the algebraic protocols, $p = 2^{61} - 1$. Sum-Check has $m \leq 400$ rounds with per-round degree at most five. In GKR, s_i is the base-two logarithm of layer i's width and $\sum_i s_{i+1} < 256$. In TQBF, d_q is the degree bound for round q, and the largest total over the six profiles is 2060. The GNI and Hamiltonicity protocols use 24 independent challenge lanes. For Image-Size, the 128 independent lanes and the 64-success acceptance threshold give the soundness bound e^{-16} and the completeness-error bound $e^{-23.04} < 10^{-10}$.

B.2 Evaluation environment and success criterion

For each evaluation, the evaluator samples a seed, generates the instance, and creates a public workspace for a fresh agent. The workspace contains the task description, public instance, protocol, schemas and evaluation client. Reference solutions and private generation information remain with the evaluator. Arthur runs as a local service; the client queries the public session state and sends the messages prescribed by the task.

The 600-second wall-clock budget starts when Arthur loads the runtime. Reading the task, local computation, proof construction, artifact upload and Arthur's final verification all count toward this limit. A session is one-shot: a rejection or timeout ends the attempt. The model must preserve the interaction order and use the challenges actually returned by Arthur.

An accepted proof is recorded as a pass. The final score uses a strict pass, which additionally requires a valid independent transcript audit and compliance with the execution and resource constraints. Writing z for the public instance, τ for the execution trajectory and h_n for the protocol transcript, the scored indicator is

$$I_c = \mathbb{I}[V_c(z, h_n) = 1 \ \wedge \ \mathrm{Audit}(h_n) = \mathrm{VALID} \ \wedge \ \mathrm{Valid}_{B_c}(\tau)] \,. \tag{B.3}$$

The score for a fixed set of N cases is $N^{-1} \sum_c I_c$.

B.3 Base evaluation prompt

Prompt B.1 supplies the common task instructions. The evaluator instantiates the task title, task identifier and case identifier, and supplies the corresponding public files. Braced uppercase fields in the prompt listings denote such substitutions; they do not represent additional advice. The public task specification fixes the mathematical problem and exact message schemas, so it is read together with this prompt.

Prompt B.1. Base task instructions

```
# Begin the Current Task

You must solve a specific instance and submit the answer to the local verifier, Arthur.

- Task: `{{TASK_TITLE}}` (`{{TASK_ID}}`)
- Test point: `{{CASE_ID}}`
- Evaluation mode: one-shot session; it cannot be reset or retried
- Total wall-clock budget: `600 seconds (10 minutes)`

## Time Budget (Mandatory)

The countdown begins when the host starts `arthur serve` and loads this runtime, not when
you
start a solver or make your first submission. The countdown will normally already have
begun when
you see these instructions; reading the task, writing code, running solvers, checking
answers, and
submitting all count against the same budget.

- Immediately run `python agent_client.py info` to confirm the connection and public total
budget,
  and record elapsed time yourself from now on.
- Every solver and subprocess must have a finite timeout; do not let one attempt consume
the whole budget.
- If there is no additional startup delay, the main solving phase should finish no later
than about `500` seconds, leaving at least
  `100` seconds for independent checks, payload generation, and submission; finish
proportionally earlier if time has elapsed.
- `agent_client.py --timeout` controls only the wait time for a single HTTP request; it
cannot extend
  the global wall-clock budget above.
- Arthur's terminal response must be received before the deadline. Merely starting a
submission before
  the deadline, or having a request reach the server, does not count as completion; Arthur'
s verification
  time also counts against the budget.
- Near the deadline, proactively terminate unfinished attempts and switch to validating and
 submitting
  an existing candidate; once the budget is exhausted, Arthur returns `TIMEOUT /
BUDGET_EXCEEDED`.

## What You Need To Do

1. Read `TASK_SPECIFICATION.md` in full. It defines the problem, mathematical notation,
interaction
   order, message fields, and acceptance conditions.
2. Read `instance.json` for this run's actual input and `protocol.json` to confirm the
message types
```

Prompt B.1. Base task instructions (continued)

```
   and ordering allowed for this run. Examples in `TASK_SPECIFICATION.md` explain the
format only; they
   are not the answer to this instance.
3. Run `python agent_client.py info` to confirm that Arthur is reachable and that the
initial
   `next_sequence` is `0`.
4. Write the solver, prover, payload, or helper scripts needed in the current directory,
then compute
   the answer for the actual instance.
5. Submit every required message according to the specification:

   ```text
   python agent_client.py event --sequence N --kind KIND --payload-file payload.json
   ```

   Use `python agent_client.py event --help` to view all parameters. The `sequence` of each
 message
   must start at `0` and increase strictly. In a multi-round protocol, calculate the next
message only
   from the challenge Arthur returned after the previous submission.
6. Continue until Arthur returns a terminal status. `ACCEPT` means the protocol passed; any
 other
   terminal status means this one-shot evaluation has ended. The final score is confirmed
by the host's
   independent post-terminal audit.

Files in the Current Directory

- `TASK_SPECIFICATION.md`: the authoritative description of the task and submission
protocol;
- `instance.json`: the public input for this run;
- `protocol.json`: interaction messages accepted by Arthur;
- `agent_client.py`: a general client for querying Arthur and submitting messages; it does
not contain
  the answer to the task;
- `schemas/` or schemas under the task path: use these to check JSON fields when needed;
- `.aipbench-connection.json`: a one-shot connection credential automatically read by the
client. Do not
  print, repost, or include it in a report.

Boundaries

The current workspace contains every file you are allowed to use. Do not read, search, or
modify any
path outside this workspace, and do not look for reference solvers, generator source code,
or the
evaluator's `private/` or `official/` files. Your only objective is to solve using the
public inputs above
and complete the interaction through `agent_client.py`.

Start solving now; do not provide only a plan.
```

B.4 Detailed benchmark scores

Table 5 reports the pass counts for each model–harness configuration. The Codex + DeepSeek V4 Pro configuration is included here but omitted from the main-paper figure.

Table 5: Per-model pass counts across 36 Tier-1, 40 Tier-2, and 24 Tier-3 cases. Overall is the sum across all 100 cases.

Harness	Model	Tier 1 (36)	Tier 2 (40)	Tier 3 (24)	Overall (100)
Codex	GPT-5.6-Luna	16	10	9	35
Codex	GPT-5.6-Terra	20	9	9	38
Codex	GPT-5.6-Sol	24	24	14	62
Claude Code	Claude 5 Opus	24	18	17	59
Claude Code	Claude 5 Sonnet	21	13	19	53
DSH	DeepSeek V4 Pro	16	12	8	36
Codex	DeepSeek V4 Pro	18	7	7	32
Codex	DeepSeek V4 Flash	19	9	7	35
Codex	GLM 5.3	17	9	6	32
Codex	GLM 5.3 Flash	18	8	5	31
Codex	Kimi K3	16	3	3	22

B.5 Failure analysis and runtime measurements

The failure analysis separates methodology from practice. At the methodology level, *Core Methodology Missing* (CM) means that the trajectory does not establish an adequate core approach, including failure to identify the relevant structure or incorrect modeling of the central object. *Near Correct* (NC) means that an appropriate route is evidenced, but a local computational, implementation, state-management or completion defect prevents a strict pass. Evidence can include accepted protocol rounds, independent exact checks or an almost complete proof artifact.

At the practice level, *Practice Error* (PE) records an execution fault, such as a malformed message, lost or repeated protocol state, an invalid artifact, unauthorized workspace access, or violation of an explicit process or resource boundary. A normal timeout caused solely by an insufficient mathematical method is not automatically a practice error. CM and NC are mutually exclusive among failures; PE is assessed separately and may coexist with either. The main-paper percentages use all 40 Tier-2 cases as the denominator, while a failure-only percentage uses the number of failed runs.

Table 6: Failure labels used in the Tier-2 analysis.

Axis	Label	Evidence criterion
Methodology	CM	No adequate core method is established.
Methodology	NC	A correct core route is evidenced but the proof is not completed successfully.
Practice	PE	An observable execution or interface fault affects validity or completion.

Elapsed time is measured from Arthur's start to the recorded outcome, using the same 600-second budget. Successful and failed runs are summarized separately, since early rejection and budget exhaustion describe different execution behavior.

C BENCHMARK CONSTRUCTION

C.1 CONSTRUCTION PROCEDURE

The benchmark contains 100 test cases in 15 task families: 36 deterministic certificate tasks in Tier-1, 40 interactive tasks in Tier-2, and 24 native verification tasks in Tier-3. A case specifies a public description D_c, an instance generator G_c, an interactive protocol Π_c, a verifier V_c, and resource constraints B_c. Different cases within a family share the verification interface while varying the construction or its parameters.

Construction proceeds through literature review, implementation and automatic checking, model-based feasibility and difficulty checks, and human review. The construction agent identifies a structural restriction admitting a specialized solution, implements a seeded generator and reference algorithm, and writes the public description and verifier. The reference algorithm must produce accepted evidence; invalid submissions must be rejected. Feasibility is checked with a capable model given the structural explanation and reference solution, whereas difficulty is checked with a less capable model given only the ordinary public task. Human review checks the reference solution, execution trace, and validity of these checks before inclusion.

In our experiments, since the expected solution has already passed formal verification, human review focuses primarily on the validity of the automated validation process, and the meaningfulness and reasonableness of the test cases, rather than on specific implementation details. More than 90% of the generated test cases are ready for immediate use, while the remaining 10% are replaced with more diverse alternatives to ensure comprehensive testing. The entire benchmark generation process takes approximately 4–5 days, with human review accounting for about 1–2 days of that time.

The following prompt gives the construction agent its instructions. It ends with the production of a review package for the human reviewers.

Prompt C.1. Instructions to the benchmark construction agent

```
Build the requested benchmark task and test cases in this repository. Follow
the assigned problem, tier, protocol, and number of cases. Implement a working
generator, verifier, and reference solution, and prepare the files that an
evaluated agent will receive. Each evaluation has a 600-second wall-clock
budget. Finish by producing documents and evidence for human review.

1. Find a suitable construction.
Read the relevant literature and look for special structure that gives you
an explicit solution method. Use it to design cases that can be solved within
the budget when the structure is understood, but remain challenging when it
is not disclosed. Explain why your construction works and cite the results
you use. Make the cases differ meaningfully in structure or parameters.

2. Specify what the evaluated agent must prove.
Define the public input, the required answer or proof, and exactly what the
verifier will check. State any promise on the input. For an interactive task,
specify every message, its format, its position in the exchange, and when the
verifier draws a fresh challenge. Prove the completeness and soundness
guarantees for the parameters you use. For a native verification task, specify
the submitted artifact and the checker that will validate it. Keep the public
interface consistent across cases in the same family.

3. Implement the task.
Write a generator that reproduces the same instance from the same seed.
Implement the verifier and a reference solution that produces accepted
evidence. If you relabel or transform an instance, preserve its mathematical
property and keep the reference solution consistent with the transformation.
Keep hidden witnesses, reference answers, generator metadata, and explanations
of the case-specific solution on the evaluator side. Make the evaluated
agent's public input self-contained.

4. Prepare the evaluated agent's instructions.
Write the task specification in English. Explain the problem, notation,
input format, message schemas, interaction order, submission commands,
resource limits, and acceptance conditions. Check that these instructions
```

Prompt C.1. Instructions to the benchmark construction agent (continued)

```
agree with the implemented verifier. Include interface examples without
revealing answers to scored instances. Prepare the public instance, task
description, protocol, schemas, client, and any required public tool metadata.

5. Test the implementation.
Run the reference solution and confirm that the verifier accepts its proof.
Check that invalid proofs, malformed messages, and incorrect message ordering
are rejected. Test the conditions that determine acceptance, including
numerical bounds, certificate completeness, polynomial degrees, and artifact
policies where applicable. Check seed reproducibility and compare actual
behavior with the written specification. Use the independent transcript audit
to check accepted and rejected executions. Fix implementation errors before
you calibrate difficulty.

6. Check feasibility and difficulty.
Give GPT-5.6-Sol the public task, the structural explanation, and the reference
solution, and check whether it can complete the proof within the budget.
Then test a less capable comparison model using only the ordinary public
task and evaluation instructions. Do not give that model the structural
explanation or reference solution. Save the model and reasoning settings,
instance, prompts, elapsed time, transcript, and outcome for each check.
Revise unsuitable constructions or parameters and repeat the relevant checks.
Keep the calibration history separate from the final evaluation records.

7. Produce a package that a human can review.
Write an English review document covering each case. Explain the construction
and its mathematical guarantees, describe the generator and reference
solution, and show how the verifier checks the submitted evidence. Include
the exact parameters and resource limits. Summarize the implementation tests
and the feasibility and difficulty checks, and link to their saved inputs,
prompts, outputs, and execution traces. Clearly identify unresolved issues.
Organize the document so that a reviewer can check the mathematics, reproduce
the tests, and inspect the supporting evidence without reconstructing your
conversation. Deliver this document together with the code and public task
files for human review before the cases are included in the benchmark.
```

C.2 On the Extensibility and Resistance to Saturation

The current release of MERLIN-BENCH evaluates a single true claim for each generated instance. Its instance-construction procedure searches the literature for special structures admitting low-degree polynomial-time algorithms and applies both feasibility and difficulty checks. This design is intended to produce meaningful performance differences at the current capability frontier; it is not intended to imply that the fixed set of instances can never become saturated. In this section, we describe a prospective bidirectional evaluation mode that can provide additional headroom once agents reliably solve the current benchmark. *This mode is not used in any score reported in this paper.*

Existence of complementary language in IP. Let L be a language, and let

$$L_1 = L \qquad \text{and} \qquad L_0 = \overline{L}.$$

Since $\mathsf{IP} = \mathsf{PSPACE}$ and PSPACE is closed under complement, if $L \in \mathsf{IP}$, both L_1 and L_0 admit interactive-proof systems. For several problem families considered in our benchmark, engineering-feasible protocols and verifiers are already available for both the problem and its complement. For example, the complement of Graph Non-Isomorphism is Graph Isomorphism, for which a particularly simple certificate-based protocol suffices: Merlin supplies an isomorphism between the two graphs, and the verifier checks it in polynomial time. TQBF is likewise closed under complementation in a constructive sense. Let (Π_1, V_1) be an interactive proof system for TQBF. To prove that a closed QBF ψ belongs to $\overline{\text{TQBF}}$, the protocol (Π_0, V_0) first computes $\neg\psi$, normalizing it into the required QBF representation if necessary, and then invokes (Π_1, V_1) to prove that $\neg\psi$ is true. Since ψ is false if and only if $\neg\psi$ is true, this construction inherits the completeness and soundness guarantees of the original TQBF protocol.

The bidirectional evalutation mode. For the same input x, the evaluator opens one independent session for each side, using fresh and hidden verifier randomness. The two sessions are evaluated

under a pre-specified pair-level resource budget. Let $A_b(x) \in \{0, 1\}$ denote whether the session for L_b strictly passes all protocol, transcript, and resource audits. We define the bidirectional score by

$$I_{\leftrightarrow}(x) = \mathbf{1}[A_0(x) \oplus A_1(x)] .$$

Thus, the agent receives credit exactly when one of the two sessions is accepted. When this occurs, the index of the accepted branch also serves as the agent's verifier-certified prediction of the decision bit. Acceptance of both branches and rejection of both branches receive zero credit. Importantly, the runtime evaluator need not store the true decision bit or compare the trajectory with a reference proof.

Analysis. Suppose that both instantiated protocols have completeness and soundness errors at most 2^{-23}. Let $b = \mathbf{1}[x \in L]$. Then an sufficiently capable agent that realizes an honest prover strategy for the true branch $b^\star$ within the resource budget will receive a score 1 with probability at least

$$\Pr[I_{\leftrightarrow}(x)] \geq \Pr[A_{b^\star}(x) = 1 \wedge A_{1-b^\star}(x) = 0] \geq 1 - 2^{-23} - 2^{-23} = 1 - 2^{-22}.$$

Simularly, a less capable agent that cannot solve any direction receive a score 1 with probability at most 2^{-22}.

Saturation-resistant test-case construction. The bidirectional evaluation mode is accompanied by a saturation-resistant test-case construction procedure, obtained from our original pipeline by removing the per-instance feasibility check. Because the same instance is evaluated under protocols for two complementary claims, the constructor need not know its truth value or provide a reference proof: when exactly one branch is accepted, that branch determines the verifier-certified answer.

This procedure allows the construction agent to include finitely encoded open problems that can be faithfully formalized as supported interactive-proof tasks. For example, the existence of the Conway 99-graph remains open and can be formalized by a QBF decision problem; bidirectional evaluation can test both its existence and nonexistence without knowing which claim is true. Up to the negligible protocol error, the resulting suite cannot be reliably ceiling-saturated as long as it contains at least one instance that the evaluated AI systems cannot resolve. Therefore, as suitable unresolved instances continue to be incorporated, this mode retains unsolved evaluation headroom. It does not, however, guarantee discrimination at the current capability level, since an instance on which every agent obtains $(0, 0)$ prevents ceiling saturation but does not distinguish among those agents. We therefore retain the feasibility check in the present benchmark and reserve this construction for a future evaluation mode.

D TIER-1: DETERMINISTIC CERTIFICATES

Tier-1 consists of one-message NP search tasks. A public instance x is given to both parties; Merlin sends one candidate witness w, and Arthur deterministically evaluates the task-specific polynomial-time relation $R(x, w)$. Acceptance means $R(x, w) = 1$. There is no verifier challenge, interaction round, or opportunity to revise a rejected witness. Each task below has a 600-second wall-clock limit, and a timeout or malformed witness is rejected.

D.1 MAX-FLOW / MIN-CUT

The Max-Flow / Min-Cut task asks Merlin to certify, in one message, the exact maximum s–t flow value of a capacitated directed network. The certificate contains both a feasible flow, which proves a lower bound, and a cut of the same value, which proves the matching upper bound. This is the standard primal–dual characterization of maximum flow Ford & Fulkerson (1956).

Formally, the public instance is a directed multigraph $G = (V, E)$ with distinct directed edge occurrences $e = (u_e, v_e)$, capacities $c_e \in \mathbb{Z}_{\geq 0}$, and distinct vertices $s, t \in V$. Parallel edges are retained as separate occurrences. Merlin submits an integer F, an integer flow f_e for every $e \in E$, and a set $S \subseteq V$. Arthur accepts precisely when

$$0 \leq f_e \leq c_e \quad (e \in E), \qquad \sum_{e:v_e=v} f_e = \sum_{e:u_e=v} f_e \quad (v \in V \setminus \{s,t\}),$$

and

$$\sum_{e:u_e=s} f_e - \sum_{e:v_e=s} f_e = F, \qquad \sum_{e:v_e=t} f_e - \sum_{e:u_e=t} f_e = F.$$

Finally, $s \in S$, $t \notin S$ and, writing $\bar{S} := V \setminus S$,

$$\mathrm{cap}(S, \bar{S}) := \sum_{e:u_e \in S,\ v_e \notin S} c_e = F.$$

Only edges directed from S to its complement contribute to this cut.

Lemma D.1 (Exactness of the certificate)**.** *If Arthur accepts (f, F, S), then f is a maximum s–t flow and S is a minimum s–t cut, both of value F.*

Proof. Flow conservation implies that the value of any feasible flow equals its net flow across every s–t cut. Capacity constraints therefore give $F \leq \mathrm{cap}(T, V \setminus T)$ for every such cut T. The submitted flow and cut attain equality at S, so neither can be improved. □

After constructing a graph with the vertex names used below, the generator independently samples a uniformly random bijection on its vertex identifiers, carries the distinguished vertices s, t through that bijection, and uniformly permutes the list of directed edge occurrences. These operations preserve capacities, feasible flows, and cut values.

C1.1.1 Independent-channel calibration. Choose k uniformly from $\{8, \ldots, 16\}$ and independently and uniformly sample $a_i \in \{3, \ldots, 29\}$ for $1 \leq i \leq k$. The graph has vertices $s, t, v_1, \ldots, v_k$ and exactly the edges $s \to v_i$ and $v_i \to t$, both of capacity a_i. Setting both edges of channel i to flow a_i gives $F = \sum_i a_i$, and the singleton source side $S = \{s\}$ has that capacity.

C1.1.2 Regular bipartite matching network. Create two indexed sides $L = \{\ell_i : i \in \mathbb{Z}_{200}\}$ and $R = \{r_i : i \in \mathbb{Z}_{200}\}$. Add unit-capacity edges $s \to \ell_i$ and $r_i \to t$. Uniformly sample a 21-element subset $D' \subseteq \mathbb{Z}_{200} \setminus \{0\}$ and set $D = \{0\} \cup D'$. Add the unit-capacity edges $\ell_i \to r_{i+d}$ for all i and $d \in D$, with indices modulo 200. Finally, uniformly sample without replacement 200 pairs (i, j) for which $\ell_i \to r_j$ is not already present, and add those unit-capacity edges. The result has 402 vertices and 5,000 edges. The offset-zero edges form a perfect matching, while the cut $\{s\}$ has capacity 200; hence the maximum-flow and minimum-cut values are both 200.

C1.1.3 Large-integer sharded serial network. Let $v_0 = s, v_1, \ldots, v_{256} = t$. Between every consecutive pair v_{j-1}, v_j, split $B = 3{,}000{,}000{,}007$ into 72 positive parts as follows. Independently for each segment, uniformly sample 71 distinct cut points from $\{1, \ldots, B-1\}$; if $0 = q_0 < q_1 < \cdots < q_{71} < q_{72} = B$, use $q_h - q_{h-1}$ as shard h's capacity. Uniformly sample without replacement 512 pairs (a, b) from $\{(a, b) : 0 \le a < b \le 256,\ b \ge a + 2\}$ and add the return edges $v_b \to v_a$, with capacities sampled independently and uniformly from $\{1, \ldots, 10^6\}$. Thus the graph has 257 vertices and 18,944 edge occurrences. Sending every forward shard at capacity and zero flow on every return edge gives value B; for every $0 \le j \le 255$, the prefix $\{v_0, \ldots, v_j\}$ is an s–t cut of capacity B.

C1.1.4 Wide layered permutation network. Arrange 64 columns of 64 vertices, indexed $x_{c,r}$ with $c, r \in \mathbb{Z}_{64}$. Add unit edges from s to column 0 and from column 63 to t. Independently at each transition $c \to c+1$, uniformly sample a two-element subset $\{d_1, d_2\} \subseteq \mathbb{Z}_{64} \setminus \{0\}$ and add the three unit-capacity cyclic matchings

$$x_{c,r} \longrightarrow x_{c+1,r+d}, \qquad d \in \{0, d_1, d_2\}, \quad r \in \mathbb{Z}_{64}.$$

The graph has 4,098 vertices and 12,224 edges. The offset-zero matchings give 64 edge-disjoint source–sink paths, and the source cut has capacity 64.

C1.1.5 Sparse cluster-interface network. For $0 \le a \le 47$, cluster a has entry vertices $u_{a,r}$ and exit vertices $v_{a,r}$ for $r \in \mathbb{Z}_{128}$. Independently for each cluster, uniformly sample a two-element subset $\{d_{a,1}, d_{a,2}\} \subseteq \mathbb{Z}_{128} \setminus \{0\}$, and add the three unit-capacity cyclic matchings $u_{a,r} \to v_{a,r+d}$ for $d \in \{0, d_{a,1}, d_{a,2}\}$. For every $0 \le a < 47$, independently sample q_a uniformly from $\mathbb{Z}_{128}$ and add the unit-capacity interface edges $v_{a,r} \to u_{a+1,r+q_a}$. Add unit-capacity edges $s \to u_{0,r}$ and $v_{47,r} \to t$. The graph has 12,290 vertices and 24,704 edges. Following the offset-zero internal matching in every cluster and every interface matching yields 128 internally vertex-disjoint s–t paths, matching the capacity of the source cut.

C1.1.6 Deep width-two diagnostic network. Create layers $\{x_{i,0}, x_{i,1}\}$ for $1 \le i \le 3000$. For $1 \le i < 3000$ and $p, q \in \{0, 1\}$, add the unit-capacity directed edge $x_{i,p} \to x_{i+1,q}$. Also add unit-capacity edges $s \to x_{1,p}$ and $x_{3000,p} \to t$ for $p \in \{0, 1\}$. The graph has 6,002 vertices and 12,000 edges. The two paths $s, x_{1,p}, \ldots, x_{3000,p}, t$, $p \in \{0, 1\}$, are internally vertex-disjoint and contain 3,001 edges each; the source cut has capacity 2.

D.2 Weighted Partial MaxSAT

Weighted Partial MaxSAT asks for a Boolean assignment that satisfies every mandatory clause while keeping the total weight of violated optional clauses below a public threshold. Thus the public object is a CNF formula whose clauses are divided into a hard family $\mathcal{H}$ and a weighted soft family $\mathcal{S}$. A literal is x_i or $\neg x_i$, a clause is a disjunction of literals, and a CNF formula is a conjunction of clauses. For an assignment $a \in \{0, 1\}^n$, define

$$\mathrm{cost}(a) = \sum_{(C,w) \in \mathcal{S}:\, C(a) = 0} w.$$

Merlin sends all n Boolean values once. Arthur accepts if every $C \in \mathcal{H}$ is true and $\mathrm{cost}(a) \le K$, where K is the published threshold. Every case sets

$$K = \min\{\mathrm{cost}(a) : a \text{ satisfies every clause in } \mathcal{H}\}$$

by the stated exact procedure.

After generation, the variables are uniformly permuted, every variable is independently complemented with probability $1/2$, and the hard clauses, soft clauses, and literals within each clause are independently uniformly permuted. This Boolean gauge transformation is a bijection on assignments and preserves clause satisfaction and soft cost.

C1.2.1 Propagation calibration. Choose the number of planted-true variables uniformly from $\{79, 80, 81\}$, then choose that many of the 160 variables uniformly without replacement. Independently choose a uniformly random ordering $v_1, \ldots, v_{160}$. Add the unit clause (v_1) if its planted bit

is one and $(\neg v_1)$ otherwise. For every consecutive pair u, v, encode equality as $(\neg u \vee v) \wedge (u \vee \neg v)$ and disequality as $(u \vee v) \wedge (\neg u \vee \neg v)$, choosing between them according to the two planted bits. These 319 hard clauses propagate a unique assignment.

Index the 240 soft clauses by $q = 0, \ldots, 239$. Independently choose each arity uniformly from $\{2, 3\}$, choose that many distinct variables uniformly, and choose one of their positions uniformly. If $q \equiv 0 \pmod 7$, give every literal its planted-false polarity. Otherwise give the distinguished position its planted-true polarity and every other position its planted-false polarity. Choose each weight independently and uniformly from $\{1, \ldots, 31\}$. The instance has 559 clauses, and K is the sum of the 35 violated soft-clause weights.

C1.2.2 Weighted implication closure. The 12,000 variables are $x_{i,j}$ with $0 \le i < 80$ and $j \in \mathbb{Z}_{150}$. Independently for each adjacent layer pair, sample six offsets uniformly without replacement from $\{2, \ldots, 149\}$, adjoin offsets 0 and 1, and add implications $x_{i,j} \Rightarrow x_{i+1,j+d}$. For each distance-two layer pair, add the offset-0 and offset-1 implications. There are 118,200 binary hard clauses of the form $\neg x \vee y$. Each variable also receives one weighted soft unit: independently sample a fair preferred value and a weight uniformly from $\{1, \ldots, 997\}$, using $(x_{i,j})$ for a true preference and $(\neg x_{i,j})$ for a false preference. This gives 130,200 clauses in total. True variables must form a successor-closed set T in the acyclic implication graph. Give a vertex profit $p_v = w$ for a true preference and $p_v = -w$ for a false preference. If W_+ is the sum of all true-preference weights, then

$$K = W_+ - \max_{T \text{ successor-closed}} \sum_{v \in T} p_v.$$

The maximum-weight closure is computed exactly by its standard minimum-cut reduction.

C1.2.3 Bounded-window weighted CNF. Order the variables as $x_1, \ldots, x_{2400}$ and sample their planted bits independently and uniformly. For every $p \ge 2$, generate three hard clauses. Each has arity $\min(3, p)$, contains x_p, and chooses its remaining distinct variables uniformly from $x_{\max(1,p-11)}, \ldots, x_{p-1}$. Choose one clause position uniformly and give it its planted-true polarity; independently for every other position, use its planted-true or planted-false polarity with equal probability.

At every position p, generate four soft clauses. Choose the arity uniformly from $\{1, \ldots, \min(3, p)\}$, include x_p, choose any remaining variables uniformly without replacement from the same 11-position predecessor window, and choose every polarity independently and uniformly. Choose each weight independently and uniformly from $\{1, \ldots, 101\}$. The instance has 7,197 hard and 9,600 soft clauses. An exact left-to-right dynamic program stores the least cost for each assignment to the last 12 variables, rejecting hard clauses and charging soft clauses when their rightmost variable is processed; the minimum over all final states is K.

C1.2.4 Locally compiled weighted closure. Start from core variables $x_{i,j}$ with $0 \le i < 64$ and $j \in \mathbb{Z}_{96}$. Independently for each adjacent layer pair, sample four cyclic offsets uniformly without replacement from $\mathbb{Z}_{96}$; for each distance-two layer pair, sample one offset uniformly. Add the corresponding implication from every position to its shifted successor, giving 30,144 implications. For every implication $x \Rightarrow y$, introduce a private variable z and use a single global variable t. Add the hard unit clause (t) and, for each implication, the four hard clauses

$$(\neg x \vee \neg t \vee z), \quad (x \vee \neg z), \quad (t \vee \neg z), \quad (\neg z \vee y).$$

When $t = 1$, the first three clauses force $z = x$, so the fourth is exactly the original implication. For every core variable, independently sample a fair preferred value and a weight uniformly from $\{1, \ldots, 4093\}$, attaching (x) for a true preference and $(\neg x)$ for a false preference. The public formula has 36,289 variables, 120,577 hard clauses, and 6,144 soft clauses. Its threshold is obtained from the exact closure value by the W_+ baseline formula in C1.2.2.

C1.2.5 Sparse affine parity factors. Use 320 disjoint components of 16 free variables. Each component has 44 three-variable parity factors. The first 16 use the cyclic triples $(i, i+1, i+3)$ modulo 16. For each of the remaining 28 factors, independently take the first three entries of a uniformly random permutation of the 16 variables; triples may repeat across factors. Independently sample fair bits b, c and a weight uniformly from $\{1, \ldots, 4093\}$.

To compile one factor on x, y, z, independently sample a fair split bit ρ and introduce variables q, o satisfying

$$q = x \oplus y \oplus \rho, \qquad o = q \oplus z \oplus (b \oplus \rho) = x \oplus y \oplus z \oplus b.$$

For $\delta \in \{0, 1\}$, write $\mathrm{XOR}_\delta(u, v; q)$ for the relation $q = u \oplus v \oplus \delta$. When $\delta = 0$, encode it by the four hard clauses

$$(u \vee v \vee \neg q), \quad (u \vee \neg v \vee q), \quad (\neg u \vee v \vee q), \quad (\neg u \vee \neg v \vee \neg q);$$

for $\delta = 1$, replace every occurrence of q in this template by $\neg q$. The two four-clause gadgets are therefore $\mathrm{XOR}_\rho(x, y; q)$ and $\mathrm{XOR}_{b\oplus\rho}(q, z; o)$. Attach the weighted soft unit (o) if $c = 1$ and $(\neg o)$ otherwise. Hence there are 5,120 free variables, 28,160 gate-output variables, 112,640 hard clauses, and 14,080 soft clauses. Since components do not share variables, enumerating the 2^{16} assignments inside each component gives its exact minimum, and K is the sum of the 320 minima.

C1.2.6 Hidden layered binary energy. Arrange 3,840 variables in layers $0, \ldots, 239$, each of width 16. Add a binary factor for every unordered pair within a layer. Independently for each two consecutive layers, sample a uniformly random bijection of their 16 positions and add its 16 matched factors. For every factor, independently sample a fair preferred parity b and a weight uniformly from $\{1, \ldots, 4093\}$. If $b = 0$, encode the factor by the weight-w soft clauses $(\neg x \vee y)$ and $(x \vee \neg y)$; if $b = 1$, use $(x \vee y)$ and $(\neg x \vee \neg y)$. Both clauses are satisfied when $x \oplus y = b$, and exactly one is violated otherwise.

There are $240\binom{16}{2} + 239 \cdot 16 = 32{,}624$ factors and 65,248 soft clauses, with no hard clauses. For a layer state $s \in \{0, 1\}^{16}$, let $U_i(s)$ be its within-layer cost and let $E_i(r, s)$ be the matching cost between layers $i - 1$ and i. The exact transfer is

$$D_0(s) = U_0(s), \qquad D_i(s) = U_i(s) + \min_r \big(D_{i-1}(r) + E_i(r, s)\big), \qquad K = \min_s D_{239}(s).$$

Because E_i is a sum of 16 matched one-bit penalties, the minimization is implemented by 16 successive one-bit min-plus updates on the 2^{16} states.

D.3 Structured Set Cover

Set Cover asks for a low-weight collection of public sets whose union contains every element of a public universe Chvátal (1979). Formally, an instance contains a universe U, candidates (S_i, w_i) with $S_i \subseteq U$ and $w_i \in \mathbb{Z}_{>0}$ for $i \in [m] = \{0, \ldots, m - 1\}$, and a budget B. Merlin submits an index set $I \subseteq [m]$. Arthur accepts exactly when

$$\bigcup_{i \in I} S_i = U \qquad \text{and} \qquad \sum_{i \in I} w_i \le B.$$

Several cases are more naturally described as weighted hitting set: choosing a candidate represents selecting one variable or variable–value pair, and a constraint is represented by a distinct universe element contained in exactly the candidates that satisfy it. This is the transpose of the same incidence relation. Every case publishes the exact minimum weight as B. The finalizer applies a uniformly random permutation to the universe labels and a uniformly random permutation to the candidates, assigns the candidates fresh opaque identifiers, and independently shuffles each published incidence list.

C1.3.1 Weighted group calibration. Partition U into 24 disjoint groups U_g of six elements. For each group, sample w_g independently and uniformly from $\{5, \ldots, 17\}$ and include the full set U_g with weight w_g. Uniformly sample without replacement eight of the $2^6 - 2 = 62$ nonempty proper subsets of U_g; each sampled subset receives an independent uniform weight in $\{w_g + 1, \ldots, 2w_g + 1\}$. No candidate meets two groups. The instance has 144 elements and 216 candidates. In each group, the full set has weight w_g, whereas every cover omitting it contains at least one strictly heavier proper subset. Hence the unique optimum consists of the 24 full sets and has weight $B = \sum_g w_g$.

C1.3.2 Relabeled cyclic overlap. Let the 3,072 universe elements be the edges $e_i = \{i, i + 1\}$ of a cycle, with indices modulo 3,072. Candidate S_i contains the two elements e_{i-1}, e_i and receives an independent uniform weight $w_i \in \{7, \ldots, 41\}$. Thus a selection vector $x \in \{0, 1\}^{3072}$ is a cover

exactly when $x_i \vee x_{i+1} = 1$ for every i modulo 3,072: it is a weighted vertex cover of the cycle. For each fixed value $a = x_0 \in \{0, 1\}$, a two-state dynamic program scans $i = 1, \ldots, 3071$, retaining only transitions $x_{i-1} \vee x_i = 1$ and adding $w_i x_i$; the terminal state must also satisfy $x_{3071} \vee a = 1$. The smaller of the two resulting costs is published as B.

C1.3.3 Forced-marker Boolean-path calibration. Use 42 consecutive blocks, each containing 12 Boolean variables, for 504 variables in total. Variable x has two equal-weight candidates $S_{x,0}, S_{x,1}$ and a private selector element contained in exactly this pair. The 504 distinct variable weights are a permutation of $10{,}000, \ldots, 10{,}503$. Sample a uniform 12-bit word and repeat it in all 42 blocks. In each block, first use the 12 cyclic triples of coordinates $(j, j+1, j+2)$ modulo 12, and then independently obtain 20 further triples by uniformly shuffling the 12 coordinates and taking the first three. For each selected tuple, independently give every literal a fair polarity; if the resulting clause is false under the planted word, choose one of its positions uniformly and reverse that literal's polarity.

For each pair of adjacent blocks, first add 24 binary equality clauses: for every coordinate j, add $x_j \vee \neg y_j$ and $\neg x_j \vee y_j$, where x_j and y_j are the corresponding variables in the left and right blocks. For that same adjacent pair, add 24 additional four-literal clauses. For each such clause, independently shuffle the variables of each block, take two from each shuffled order, and apply the same polarity-and-repair rule. Every clause occurrence is a distinct universe element; for a literal satisfied by $x = b$, that element belongs to $S_{x,b}$.

The 42 local clause families and 41 boundary families each receive one marker candidate. Its private singleton element forces that marker to be selected, and the same marker is incident to every clause element in its family. Thus all clause elements are covered by the 83 forced markers, while each selector element forces at least one of its two value candidates. Every marker has weight $10{,}505$, so the exact lower bound

$$B = \sum_{q=10{,}000}^{10{,}503} q + 83 \cdot 10{,}505$$

is attained by selecting all markers and exactly one value candidate per variable. In particular, the forced markers already cover all clause elements; the clauses do not impose an additional feasibility condition at this budget. The public instance has 3,899 elements, 1,091 candidates, and 3,312 represented clauses.

C1.3.4 Marked width-16 weighted hitting-set path. Create ordinary candidates $v_0, \ldots, v_{999}$ with independently and uniformly sampled weights in $\{17, \ldots, 997\}$, and define $B_t = \{v_{8t}, \ldots, v_{8t+15}\}$ for $0 \le t < 124$. Thus consecutive bags share eight candidates. In each bag, uniformly shuffle its 16 candidates and use the four consecutive groups of four as constraints. Until the bag has 32 constraints, independently choose a size uniformly from $\{3, 4\}$, uniformly shuffle the bag, take the first chosen number of candidates, and reject the result if that candidate subset already occurs in the bag. Every occurrence of a constraint, including equal subsets in different bags, becomes a distinct universe element incident precisely to its listed candidates.

Exact path-decomposition dynamic programming enumerates the 2^{16} choices within each bag, discards every choice missing one of that bag's constraints, and joins consecutive choices only when they agree on the eight shared candidates. Candidate weights are charged when their candidate is first introduced. Let B be the resulting minimum ordinary-candidate cost. After computing B, add to every bag one marker candidate of weight $B + 1$ incident to all 32 of its constraint elements. Consequently no marker occurs in a cover of weight at most B. There are 3,968 elements and 1,124 candidates.

C1.3.5 Marked width-18 weighted hitting-set path. Create 1,125 ordinary candidates with independent uniform weights in $\{19, \ldots, 1993\}$ and define $B_t = \{v_{9t}, \ldots, v_{9t+17}\}$ for $0 \le t < 124$; consecutive bags share nine candidates. For each bag, uniformly shuffle its 18 candidates and split the ordering consecutively into four groups of four and one group of two. These five groups are the initial constraints. Generate the remaining 27 constraints by the same uniform size-3-or-4 sampling and within-bag duplicate rejection as in C1.3.4. Each constraint occurrence is again a distinct universe element.

The exact path dynamic program enumerates 2^{18} bag choices, retains those hitting all 32 local constraints, and joins adjacent choices on their nine common candidates. Let B be its minimum ordinary-candidate cost. Only afterwards, add one marker of weight $B + 1$ per bag, incident to the 32 elements of that bag. The public instance has 3,968 elements and 1,249 candidates.

C1.3.6 Marked width-16 weighted hitting-set tree. Number 109 bags in breadth-first order, with root 0 and parent $\lfloor (t-1)/3 \rfloor$ for bag $t > 0$. The root bag contains $v_0, \ldots, v_{15}$ and owns $v_0, \ldots, v_9$. All 16 root-bag candidates are introduced and charged at the root; "owned" denotes only the ten candidates eligible to occur in a child separator. Every non-root bag introduces ten fresh candidates and owns them. For the first, second, and third child of a bag whose owned candidates in order are $a_0, \ldots, a_9$, respectively use the six shared candidates

$$(a_0, a_1, a_2, a_3, a_4, a_5), \quad (a_4, a_5, a_6, a_7, a_8, a_9), \quad (a_0, a_1, a_2, a_7, a_8, a_9).$$

Together with the ten fresh candidates, these form the child's width-16 bag. There are 1,096 ordinary candidates, each given an independent uniform weight in $\{23, \ldots, 1597\}$.

For every bag, a uniform shuffle partitioned into four groups of four gives the first four constraints. Apply the size-3-or-4 sampling and within-bag duplicate rejection of C1.3.4 until there are 34 constraints. Every constraint occurrence gives a distinct universe element. A bottom-up exact tree-decomposition dynamic program enumerates feasible 2^{16} choices for each bag; for every six-bit parent-separator choice, it adds the costs of the three child subtrees and charges only candidates introduced at the current bag. Let B be the minimum root cost. Finally, add to each bag a marker of weight $B + 1$ incident to all 34 elements of that bag. The instance has 3,706 elements and 1,205 candidates.

D.4 Structured Closest Vector

The Closest Vector Problem asks for a lattice point near a target. Here the lattice is given by a full-column-rank integer matrix $B \in \mathbb{Z}^{d \times n}$, whose columns generate $L(B) = \{Bz : z \in \mathbb{Z}^n\}$. The public target is the rational vector τ/D, where $\tau \in \mathbb{Z}^d$ and $D \in \mathbb{Z}_{>0}$, and the public data also contain a squared-radius numerator K and coefficient bound C. Merlin submits $z \in \mathbb{Z}^n$. Arthur accepts exactly when

$$|z_j| \le C \quad (1 \le j \le n), \qquad \|DBz - \tau\|_2^2 \le K.$$

All arithmetic in this relation is integral and exact. The generated instances have exactly one lattice point satisfying the acceptance inequality: the planted point, whose squared residual numerator is K. To hide the canonical coordinates, independently sample uniformly random signed permutation matrices R and Q on the rows and columns, respectively, and publish

$$B' = RBQ, \qquad \tau' = R\tau.$$

The planted coefficient vector becomes $z' = Q^{-1}z$. Thus $DB'z' - \tau' = R(DBz - \tau)$, and both the Euclidean residual and the coefficient bound are preserved. All six cases publish $C = 32$.

C1.4.1 Orthogonal residual calibration. Let $n = 24$ and independently sample each diagonal scale a_i uniformly from $\{11, \ldots, 29\}$. Before hiding, $B \in \mathbb{Z}^{48 \times 24}$ has the diagonal matrix $\mathrm{diag}(a_1, \ldots, a_{24})$ in its first 24 rows and 24 zero rows below it. For each i, sample w_i uniformly from $[-9, 9] \cap \mathbb{Z}$, replacing a sampled zero by an independent fair sign in $\{-1, 1\}$; sample r_i by an independent fair sign times a uniform magnitude in $\{1, 2, 3\}$. Set $\tau = (a_1 w_1, \ldots, a_{24} w_{24}, r_1, \ldots, r_{24})$, $D = 1$, and $K = \sum_i r_i^2$. For any z, the squared residual numerator is $K + \sum_i a_i^2 (z_i - w_i)^2$, so $z = w$ is the unique integer vector satisfying the threshold.

C1.4.2 Hidden signed path equations. Let $n = 128$. Construct a lower-bidiagonal matrix A by independently and uniformly sampling every positive diagonal entry from $\{7, \ldots, 31\}$ and every subdiagonal magnitude from the same set, with an independent fair sign. The positive diagonal makes A nonsingular. Set $B = \begin{bmatrix} A \\ 0_{128 \times 128} \end{bmatrix} \in \mathbb{Z}^{256 \times 128}$. Sample each w_i uniformly from $[-13, 13] \cap \mathbb{Z}$, replacing zero by an independent fair sign, and sample each r_i as an independent fair sign times a uniform magnitude in $\{1, \ldots, 5\}$. Publish $\tau = (Aw, r)$, $D = 1$, and $K = \|r\|_2^2$. The squared residual is $\|A(z - w)\|_2^2 + K$, which is at most K exactly when $z = w$.

C1.4.3 Paired-residual low-width tree. Index 128 variables by $i = 0, \dots, 127$ in a rooted ternary heap, with parent $\lfloor (i-1)/3 \rfloor$ for $i > 0$. Independently sample the positive entry $A_{i,i}$ uniformly from $\{17, \dots, 43\}$. When present, the entries at the parent and grandparent columns have independent uniform magnitudes in the same set and independent fair signs; all other entries are zero. Thus A is lower triangular with positive diagonal. Sample w_i uniformly from $[-15, 15] \cap \mathbb{Z}$, replacing zero by a fair sign, and sample r_i uniformly from $\{1, \dots, 7\}$. Rows $2i$ and $2i+1$ of B are both A_i, with respective target values $A_i w + r_i$ and $A_i w - r_i$; set $D = 1$. Thus B has 256 rows and

$$(A_i(z-w) - r_i)^2 + (A_i(z-w) + r_i)^2 = 2(A_i(z-w))^2 + 2r_i^2.$$

The threshold is $K = 2\sum_i r_i^2$. The positive diagonal makes A nonsingular, so equality is unique.

C1.4.4 Hidden modular evaluation lattice. Construction A converts a linear code $C \subseteq \mathbb{F}_q^n$ into the integer lattice $\{y \in \mathbb{Z}^n : y \bmod q \in C\}$. In this case, over $\mathbb{F}_{257}$, let C be the length-128, dimension-20 Reed–Solomon code obtained by evaluating polynomials of degree below 20 at $1, \dots, 128$ Reed & Solomon (1960). Its minimum Hamming distance is 109. Write $G \in \{0, \dots, 256\}^{128 \times 20}$ for the integer lift of the Vandermonde evaluation matrix, $G_{i,j} = i^j \bmod 257$ for $1 \le i \le 128$ and $0 \le j < 20$. The generated matrix is

$$B = \left[G \mid 257 e_{21} \mid \cdots \mid 257 e_{128} \right] \in \mathbb{Z}^{128 \times 128}.$$

The first 20 rows of G form a nonsingular Vandermonde matrix, so B has full rank. Its column lattice is a sublattice of the Construction-A lattice $L_A = \{y \in \mathbb{Z}^{128} : y \bmod 257 \in C\}$; no claim of equality with L_A is needed below.

Independently sample each coefficient uniformly from $[-7, 7] \cap \mathbb{Z}$, replacing zero by a fair sign, and let $y = Bw$. Let the error set contain coordinates $1, \dots, 20$, and uniformly choose its remaining 12 coordinates without replacement from $\{21, \dots, 128\}$. Set $D = 5$ and define

$$\tau_i = \begin{cases} 5y_i - 3, & i \text{ erroneous}, \\ 5y_i + 2, & i \text{ clean}. \end{cases} \qquad K = 32 \cdot 3^2 + 96 \cdot 2^2 = 672.$$

Every nonzero vector of L_A, and hence of the column lattice of B, has squared norm at least 109: a nonzero residue codeword has Hamming weight at least 109, whereas a nonzero vector congruent to zero has a coordinate of magnitude at least 257. Since $4K < 5^2 \cdot 109$, the planted point lies strictly within half the minimum lattice distance and is the unique point in the threshold ball.

C1.4.5 Column-mixed tensor-code lattice. Use the tensor product of two $[16, 12]$ Reed–Solomon codes over $\mathbb{F}_{257}$. Its 256 coordinates are ordered with the 12×12 grid $I = \{1, \dots, 12\}^2$ first, followed lexicographically by the remaining points of $\{1, \dots, 16\}^2$. Let G be the integer lift in $\{0, \dots, 256\}$ of the 144 columns evaluating $X^i Y^j$ for $0 \le i, j < 12$, and initially set

$$B_0 = \left[G \mid 257 e_{145} \mid \cdots \mid 257 e_{256} \right].$$

The evaluation submatrix on I is nonsingular, so B_0 has full rank. Its column lattice is a sublattice of the tensor-code Construction-A lattice, whose minimum Hamming distance is $5^2 = 25$.

Mix the columns by elementary determinant-one shears. For 18 layers, uniformly shuffle columns $0, \dots, 143$ except columns $0, 1, 12$, pair successive columns, and for each ordered pair (s, t) replace $B_t \leftarrow B_t + \epsilon B_s$ for an independent fair sign ϵ. Apply another 18 such layers to columns $144, \dots, 255$. Finally, for each $t = 0, \dots, 143$, perform three independent updates $B_t \leftarrow B_t + \epsilon B_s$, where s is uniformly sampled from $\{144, \dots, 255\}$ and ϵ is a fair sign. These operations preserve the column lattice.

Sample every coefficient as in C1.4.4 and let $y = Bw$. Independently and uniformly permute $1, \dots, 16$ twice, obtaining α and β, and use the perfect-matching error set $E = \{(\alpha_j, \beta_j) : 1 \le j \le 16\}$. With $D = 13$, define the signed target offset $\eta = \tau - 13y$ by $\eta_{a,b} = -7$ on E and $+1$ elsewhere. Thus $K = 16 \cdot 49 + 240 = 1024$. Every nonzero vector in the containing Construction-A lattice has squared norm at least 25, and $4K < 13^2 \cdot 25$ makes the planted point unique.

C1.4.6 Column-mixed Boolean-cube code lattice. Let C be the degree-at-most-three multilinear evaluation code on $\{0, 1\}^8$ over $\mathbb{F}_{257}$, the Boolean-cube analogue of the order-three Reed–Muller

code. Its 93 basis functions are the square-free monomials of degree at most three, and every nonzero codeword has Hamming weight at least $2^{8-3} = 32$ Reed (1954).

Order the monomials first by degree and then lexicographically. Enumerate the 256 Boolean points lexicographically and greedily retain a point whenever its 93-entry evaluation row is linearly independent modulo 257 of the retained rows; stop after 93 points, then append all remaining points in lexicographic order. The selected information set is precisely $I = \{x \in \{0,1\}^8 : \mathrm{wt}(x) \le 3\}$. Its monomial-evaluation minor is a unimodular zeta matrix after compatible subset ordering. Hence the integer evaluation columns, followed by $257e_j$ for the 163 coordinates outside I, form a basis B_0 of the Construction-A lattice.

For 28 layers, uniformly shuffle the 163 modulus columns, pair successive columns, and update the second column of each pair by adding the first with an independent fair sign. The final unpaired column is left unchanged in that layer. Then, for each of the 93 code columns, perform eight updates that add an independently and uniformly sampled modulus column with an independent fair sign. Let B be the resulting basis. Sample every coefficient as in C1.4.4 and set $y = Bw$. With $D = 13$, define $\eta = \tau - 13y$ to be -7 at the first 15 points of the ordered information set and $+1$ at the other 241 coordinates. The threshold is $K = 15 \cdot 49 + 241 = 976$. Since $4K < 13^2 \cdot 32$, the planted point is the unique lattice point satisfying the threshold.

D.5 List Graph Homomorphism

List Graph Homomorphism asks whether a source graph can be mapped into a target graph while respecting both adjacency and a vertex-specific set of allowed images Hell & Nešetřil (2004). The public instance consists of finite undirected simple graphs $G = (V_G, E_G)$ and $H = (V_H, E_H)$ and a nonempty list $L(v) \subseteq V_H$ for every $v \in V_G$. Merlin submits a total map $h : V_G \to V_H$; it need not be injective. Arthur accepts exactly when

$$h(v) \in L(v) \quad (v \in V_G), \qquad \{h(u), h(v)\} \in E_H \quad (\{u, v\} \in E_G).$$

The generator applies independent uniformly random permutations to the source and target vertex labels and randomizes the serialization order of edges, list records, and entries within each list, while retaining each record's source-vertex identifier. The two relabelings induce a bijection between the valid homomorphisms before and after this finalization.

Cases C1.5.3–C1.5.6 use the Cai–Fürer–Immerman (CFI) construction Cai et al. (1992). For a cubic base graph Q, order the three incidences at each base vertex v. Replace v by six outer vertices $a^b_{v,i}$, where $i \in \{0,1,2\}$ and $b \in \mathbb{F}_2$, and four middle vertices $m_{v,x}$ indexed by

$$\mathcal{E} = \{000, 011, 101, 110\}.$$

For every $x \in \mathcal{E}$ and $i \in \{0,1,2\}$, add the internal edge $\{m_{v,x}, a^{x_i}_{v,i}\}$. If base edge $e = uv$ occupies incidence i at u and j at v, its twist $z_e \in \mathbb{F}_2$ adds the two external edges

$$\{a^b_{u,i}, a^{b \oplus z_e}_{v,j}\}, \qquad b \in \mathbb{F}_2.$$

For any even frame $p_v \in \mathcal{E}$ at every base vertex, replacing z_e by $z_e \oplus p_{u,i} \oplus p_{v,j}$ produces an isomorphic graph: the isomorphism sends $a^b_{v,i}$ to $a^{b \oplus p_{v,i}}_{v,i}$ and $m_{v,x}$ to $m_{v,x \oplus p_v}$. This explicit map is the planted witness used below. In each CFI case, sample z uniformly from the even-parity vectors in $\mathbb{F}_2^{E(Q)}$ by sampling its first $|E(Q)| - 1$ coordinates fairly and choosing the last to make the XOR zero. Independently sample every p_v uniformly from $\mathcal{E}$ and use the displayed rule to obtain the target twist vector. For each published role r, a source vertex of role r receives as its list all target vertices of the same role.

C1.5.1 Anchored binary path calibration. The source is the disjoint union of 64 paths of 16 vertices, hence has 1,024 vertices and 960 edges; the target is the triangle K_3. Order each path as $v_0, \ldots, v_{15}$. Independently for each path, uniformly sample an ordered pair (a, b) of distinct target vertices. Set $L(v_0) = \{a\}$ and $L(v_i) = \{a, b\}$ for $1 \le i < 16$. Since K_3 is loopless, each source edge forces its endpoints to take different values. The unique component map is therefore $h(v_i) = a$ for even i and $h(v_i) = b$ for odd i.

C1.5.2 Hidden tree permutation constraints. The source is the complete rooted 4-ary tree with the root at depth zero and leaves at depth five; it has 1,365 vertices and 1,364 edges. Assign every source vertex v a disjoint six-vertex target domain $D_v = \{(v, 0), \ldots, (v, 5)\}$, so the target has 8,190 vertices. For each source edge from parent u to child v, independently and uniformly sample a permutation π_{uv} of the six states. Let the target edge set be exactly the union of the matching edges

$$\{(u, i), (v, \pi_{uv}(i))\}, \qquad 0 \le i < 6,$$

over all source edges. Independently sample a uniform root state s_0 and set $L(r) = \{(r, s_0)\}$; every other source vertex v has list D_v. Propagating the matching constraints down the tree determines a unique map. The target has $1{,}364 \cdot 6 = 8{,}184$ edges.

C1.5.3 Coarsely listed switched CFI isomorphism. Independently sample three uniformly random perfect matchings between two sides of 120 vertices each, rejecting the attempt if two matchings share an edge. Also reject unless their union is connected and the following 240 root-marked color-refinement signatures are pairwise distinct. For a root r, initially color vertices by their bipartition side and append one bit indicating whether the vertex is r. Repeatedly replace each color by the pair consisting of its current color and the sorted multiset of neighbor colors. Encode these pairs canonically in lexicographic order, using the same encoding rule in every rooted run, and perform 240 refinement rounds. The signature is the sequence of the 240 sorted histograms obtained after these rounds. The resulting cubic base has 240 vertices and 360 edges.

Build two 2,400-vertex, 3,600-edge CFI graphs whose twist vectors are related by the twists and frames defined above. The four published roles are $(\mathrm{outer}, \mathrm{left})$, $(\mathrm{outer}, \mathrm{right})$, $(\mathrm{middle}, \mathrm{left})$, and $(\mathrm{middle}, \mathrm{right})$. Thus the two outer-role lists have size 720 and the two middle-role lists size 480; neither a base vertex nor an incidence is specified. The frame map stays within each role and is a valid list-respecting isomorphism.

C1.5.4 Double-line role-listed switched CFI isomorphism. Repeat the three-matching sampling, connectivity test, and 120-round root-marked refinement test of C1.5.3 with 60 vertices per side. In this refinement test only, all unmarked base vertices initially have one color; the later list roles still retain the two bipartition sides. Each of the two CFI graphs has 1,200 vertices and 1,800 edges. For a simple graph X, its line graph $L(X)$ has one vertex for every edge of X, with two vertices adjacent exactly when the corresponding edges share an endpoint. Apply this operation twice to each of the two frame-related CFI graphs. The first line graph has 1,800 vertices and 3,600 edges; the published graph $L(L(X))$ has 3,600 vertices and 10,800 edges. An isomorphism of X acts on edges and therefore induces an isomorphism through both line-graph operations.

A published vertex represents a pair of incident edges of X, or a "wedge" centered at their common endpoint. Lists group target wedges by six roles. A middle-centered wedge is classified by its base side. An outer-centered wedge is classified by its base side and by whether the third edge incident to its center, omitted from the wedge, is external to the CFI gadget. For each side, the resulting target-list sizes are 720 for middle centers, 360 for outer centers with an omitted external edge, and 720 for outer centers with an omitted internal edge. A source wedge receives the entire target class of its role.

C1.5.5 Symmetric-cover switched CFI isomorphism. Begin with the incidence graph of the generalized quadrangle $GQ(2, 2)$ Payne & Thas (2009). Concretely, its two parts are the 15 unordered pairs of a six-element set and the 15 partitions of that set into three unordered pairs; incidence means membership of a pair in a partition. This is a cubic 30-vertex, 45-edge bipartite graph. Number the 15 pairs and the 15 partitions lexicographically, with the pair vertices first, and take the breadth-first spanning tree rooted at vertex zero, visiting neighbors in increasing order. Orient every base edge from its smaller-numbered endpoint to its larger-numbered endpoint, assign a voltage $\nu_{uv} \in \mathbb{Z}_6$, and set $\nu_{vu} = -\nu_{uv}$. Give every tree edge voltage zero, uniformly choose one non-tree edge and give it voltage one, and give every other non-tree edge an independent uniform voltage in $\mathbb{Z}_6$. Replace a base vertex v by (v, k) for $k \in \mathbb{Z}_6$ and an oriented base edge uv by the six edges

$$(u, k)(v, k + \nu_{uv}), \qquad k \in \mathbb{Z}_6.$$

The voltage-one fundamental cycle generates $\mathbb{Z}_6$, so the cyclic lift is connected. It has 180 vertices, 270 edges, and girth at least eight. Applying the CFI construction gives source and target

graphs, each with 1,800 vertices and 2,700 edges. The four roles are outer/middle crossed with the pair/partition side of the lifted incidence graph; their target-list sizes are 540 for each outer role and 360 for each middle role.

C1.5.6 Independent double-line switched-CFI instance. Repeat all matching sampling, rejection tests, CFI switching, two line-graph operations, wedge-role lists, and final source/target relabelings of C1.5.4 using an independent domain-separated random stream. The resulting source and target again have 3,600 vertices and 10,800 edges each, with the same six wedge-role list classes.

D.6 Rooted Group Steiner Tree

Rooted Group Steiner Tree asks for a low-weight connected subgraph that starts at a distinguished root and reaches at least one representative of every prescribed vertex group Garg et al. (2000). The public instance is a connected simple undirected graph $G = (V, E)$ with positive integer weights w_e, a root r, nonempty groups $\mathcal{G} = (G_1, \ldots, G_q)$, and budget B. Groups may overlap. Merlin submits one edge set $T \subseteq E$. Let $R(T) = \{v \in V : v \text{ is reachable from } r \text{ in } (V, T)\}$. Arthur accepts exactly when both endpoints of every edge in T lie in $R(T)$, $R(T) \cap G_j \neq \varnothing$ for every j, and $\sum_{e \in T} w_e \leq B$. Thus T is a directly checkable one-message certificate.

Cases C1.6.3–C1.6.5 use a common binary-choice gadget. Variable x_i has a center z_i, two leaves x_i^0, x_i^1, a root edge rz_i, and choice edges $z_i x_i^0, z_i x_i^1$. The singleton group $\{z_i\}$ forces the root edge, and the group $\{x_i^0, x_i^1\}$ forces at least one choice. Choice-edge weights use a common base $M > n(31 - 3)$ for n gadgets. Every constraint group in these cases is satisfied by a planted assignment, so a feasible solution with one choice edge per gadget exists; the base inequality then makes every minimum solution select exactly one such edge per gadget. A group $\{x_{i_1}^{b_1}, \ldots, x_{i_k}^{b_k}\}$ is covered exactly when the Boolean clause $(x_{i_1} = b_1) \vee \cdots \vee (x_{i_k} = b_k)$ is true.

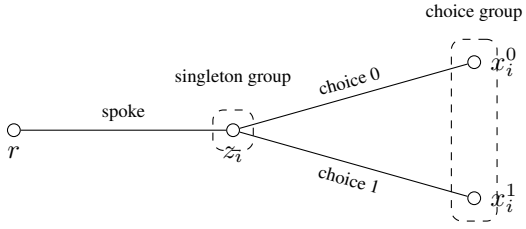

Figure 7: The binary-choice gadget. Root connectivity turns group coverage into the selection of a truth-value edge.

Every generated instance is finally subjected to a uniformly random vertex permutation, which also transports the root. The serialization orders of edges, group records, and members within each group are independently randomized.

C1.6.1 Mandatory-cut calibration. Take the complete 4-ary tree with its root at level zero and leaves at level five. It has 1,365 vertices, 1,364 tree edges, and 1,024 leaves; every leaf is a singleton group. Independently and uniformly sample every tree-edge weight from $\{7, \ldots, 29\}$ and let their sum be B. Repeatedly sample an ordered pair of distinct vertices uniformly, sort it into an unordered pair, and reject it if it is a tree edge or was sampled earlier, until 1,600 non-tree edges have been obtained. Give each such edge weight $B + 1 + U$, where U is independently uniform in $\{0, \ldots, 9999\}$. Any accepted solution therefore excludes all added edges, while reaching every singleton leaf forces every tree edge. The public graph has 2,964 edges and the unique accepted edge set has 1,364 edges.

C1.6.2 Serial cactus boundary constraints. Chain 768 four-cycles by identifying the right articulation of one cycle with the left articulation of the next, and take the first cell's left articulation as r. In cell i, denote the internal vertices of the two internally disjoint two-edge routes by t_i and d_i. Independently and uniformly sample all 3,072 edge weights from $\{3, \ldots, 31\}$; the graph has 2,305 vertices. Independently sample a fair planted mode $s_i \in \{\text{top}, \text{bottom}\}$ for each cell. At boundary i, the four candidate groups are $\{u_i, v_{i+1}\}$ for $u, v \in \{t, d\}$. Exclude the unique pair

containing neither planted branch vertex and uniformly choose two of the remaining three groups without replacement. Add the singleton group containing the final articulation, giving 1,535 groups.

A connected solution traverses each cell in one of three modes. The top and bottom costs are the sums of the corresponding two route-edge weights. The both cost is the minimum of the two three-edge subgraphs obtained by taking one entire route and the cheaper edge of the other route. A three-state path dynamic program discards adjacent mode pairs that miss either boundary group, adds these local costs, and publishes its minimum as B.

C1.6.3 Relabelled bounded-frontier choices. Use 1,536 binary-choice gadgets. Spoke weights lie in $\{3, \dots, 31\}$; each choice-edge weight is $43{,}009$ plus an offset in the same interval, with all these samples independent and uniform. Sample a planted assignment $\widehat{x}$ of 1,536 independent fair bits. Add the 1,536 singleton center groups and 1,536 choice groups, as well as pair groups $\{z_i, z_{i+1}\}$ for $0 \le i < 1535$; the latter are already hit by the forced centers and encode the path $z_0, z_1, \dots, z_{1535}$ up to reversal. For every right index $i > 0$, uniformly choose without replacement exactly $\min\{9, i\}$ indices from $\{\max(0, i-12), \dots, i-1\}$. For each selected j, sample (a, b) as two independent fair bits; if it equals $(\widehat{x}_j, \widehat{x}_i)$, replace a by $1-a$. Add $\{x_j^{1-a}, x_i^{1-b}\}$. This group is missed exactly by $(x_j, x_i) = (a, b)$. There are 13,779 such constraint groups and 18,386 groups overall. The graph has 4,609 vertices and 4,608 edges. A width-12 frontier dynamic program scans i from left to right, stores the preceding 12 values, adds the spoke and selected choice-edge cost for x_i, and rejects a state realizing any forbidden pair whose right endpoint is i. Its minimum is published as B.

C1.6.4 Higher-order bounded-frontier coverage. Use 1,280 choice gadgets, with choice base $35{,}841 = 1280(31-3)+1$. Spoke weights and choice-edge offsets are sampled independently and uniformly from $\{3, \dots, 31\}$, and the planted assignment consists of independent fair bits. Groups $\{z_i, z_{i+1}, z_{i+2}\}$ for $0 \le i < 1278$ impose no additional feasibility condition because their centers are forced; they encode consecutive triples of variables.

For every $2 \le i < 1280$, set $P_i = \{\max(0, i-15), \dots, i-1\}$ and generate $\min\{7, 2^{|P_i|}\}$ distinct clauses having rightmost variable x_i. Uniformly choose the clause size from $\{3, 4\}$, capped at $|P_i|+1$; uniformly shuffle P_i and use the first one fewer variables together with i. Give the selected variables independent fair literal values. If none matches the planted assignment, uniformly choose one literal and change its value to the planted value; reject and resample if the same signed clause was already generated for i. The corresponding group contains x_j^b for every literal $(x_j = b)$. The instance has 3,841 vertices, 3,840 edges, and 12,781 groups, including 8,943 clause groups. A left-to-right exact transfer program retains the previous 15 bits, checks all clauses ending at i, adds the local spoke and choice cost, and publishes its minimum as B.

C1.6.5 Running-intersection bag-tree coverage. Number 121 bags in breadth-first order in the complete rooted ternary tree of depth four, with parent $p(t) = \lfloor (t-1)/3 \rfloor$ and child slot $c(t) = (t-1) \bmod 3$ for $t > 0$. Bag 0 contains variables $0, \dots, 15$. Each non-root bag shares a six-variable separator with its parent and introduces ten fresh variables. If the parent is the root, child slot c uses parent positions $6c, \dots, 6c+5$ modulo 16. Otherwise write the parent bag in its stored order as six inherited variables followed by ten introduced variables. Child slot c takes inherited positions $3c, 3c+1, 3c+2$ modulo six and introduced positions $3c, 3c+1, 3c+2$ modulo ten. Appending ten globally fresh variables gives the child's stored order. This rule ensures that the bags containing any fixed variable form a connected subtree.

There are 1,216 binary-choice gadgets, with choice base $34{,}049 = 1216(31-3)+1$. Spoke weights and choice offsets are independent and uniform in $\{3, \dots, 31\}$, and the planted assignment consists of fair bits. In every bag, independently choose a clause size uniformly from $\{3, 4\}$, uniformly shuffle the 16 variables and take the selected prefix, give its variables fair literal values, and repair one uniformly selected literal to its planted value if necessary. Reject within-bag duplicate signed clauses until the bag has ten. For every bag β add the center-only group $\{z_i : x_i \in \beta\}$, and for every parent separator S add $\{z_i : x_i \in S\}$; forced center singletons make these groups redundant for feasibility.

The graph has 3,649 vertices, 3,648 edges, and 3,883 groups: 1,216 singleton centers, 1,216 choice groups, 121 bag groups, 120 separator groups, and 1,210 clause groups. A bottom-up dynamic

program enumerates the 2^{16} assignments to each bag, conditions each child table on the six separator bits, and charges a variable's choice cost only in the bag where it is introduced. Its root minimum is published as B.

C1.6.6 Deep shared-routing ancestor coverage. Start with the complete binary tree whose root r is at level zero and whose leaves are at level 11; it has 4,095 routing vertices and 4,094 routing edges. Number its vertices in breadth-first order, so the parent of $v > 0$ is $\lfloor (v-1)/2 \rfloor$. Attach two terminal leaves x_v^0, x_v^1 to every routing vertex v. Routing-edge weights lie in $\{3, \ldots, 31\}$; terminal-edge weights are $114{,}661 = 4095(31-3)+1$ plus an offset in that interval. The terminal pair at every owner is a group, forcing at least one terminal edge. Reaching such a leaf forces the unique root-to-owner route, so all routing edges occur in every feasible solution; the common base makes exactly one terminal per owner optimal. All routing weights and terminal offsets are sampled independently and uniformly, and every owner receives an independent fair planted bit.

For an owner v, list v followed by its nearest ancestors, stopping after ten vertices or at the root. For each of four coverage groups, uniformly shuffle this list, take its first $\min\{3, \mathrm{depth}(v)+1\}$ owners, and, if v is absent, replace the first selected owner by v. Independently sample one fair terminal value for each selected owner; if none agrees with the planted bits, choose one selected position uniformly and replace its value by the corresponding planted bit. The resulting terminals form the group; different generated groups are retained even when their member sets coincide.

The resulting graph has 12,285 vertices, 12,284 edges, and 20,475 groups. Every edge set accepted at the optimum budget contains all 4,094 routing edges and exactly one of the two terminal edges at each owner, for 4,095 terminal edges in total. A bottom-up dynamic program conditions each subtree on the values of its nine closest ancestors, checks its owner's four groups, and publishes the minimum routing-plus-terminal cost as B.

E TIER-2: INTERACTIVE PROOFS

Tier-2 contains interactive tasks in which Merlin must commit to a message before Arthur samples the fresh randomness used to check it. The tasks documented here use hidden graph relabelings, the Sum-Check protocol, the GKR reduction for layered arithmetic circuits, affine hashing of circuit images, Shamir-style arithmetization of quantified Boolean formulas, and a bind–challenge–open proof of Hamiltonicity. Each run is subject to a uniform 600-second wall-clock budget.

E.1 GRAPH NON-ISOMORPHISM

Graph Non-Isomorphism (GNI) asks whether two graphs have different structures even after their vertices are renamed. Interaction turns this decision problem into a source-identification game: Arthur secretly chooses one of two public non-isomorphic graphs, randomly relabels it, and asks Merlin which source was used. The task is a parallel repetition of the classical GNI protocol Goldreich et al. (1991).

A vertex-colored undirected simple graph is a triple

$$G = ([N], E, \chi), \qquad [N] = \{0, 1, \dots, N-1\},$$

where $E \subseteq \binom{[N]}{2}$ and $\chi : [N] \to \mathbb{Z}_{\geq 0}$. A color-preserving isomorphism from G to G' is a bijection $\varphi : [N] \to [N]$ such that

$$\{u, v\} \in E(G) \iff \{\varphi(u), \varphi(v)\} \in E(G'), \qquad \chi(u) = \chi'(\varphi(u)).$$

We write $G \cong_{\mathrm{col}} G'$ when such a bijection exists. The protocol is defined for two same-order public graphs G_0, G_1. Perfect completeness is evaluated when $G_0 \ncong_{\mathrm{col}} G_1$, whereas soundness is evaluated when $G_0 \cong_{\mathrm{col}} G_1$. All seven generated pairs are single-colored and non-isomorphic, and their non-isomorphism follows from the construction-specific invariants stated below.

Merlin first sends a fixed, content-independent start signal. Arthur then creates 24 independent challenge lanes. In lane j he samples

$$\beta_j \xleftarrow{\$} \{0, 1\}, \qquad \pi_j \xleftarrow{\$} S_N, \qquad H_j = \pi_j(G_{\beta_j}),$$

where π_j transports adjacency and colors. The bit β_j has no graph- theoretic meaning beyond identifying the chosen source. Arthur returns the 24 graphs H_j, after which Merlin submits one ordered vector $(\widehat{\beta}_0, \dots, \widehat{\beta}_{23})$, and Arthur accepts exactly when $\widehat{\beta}_j = \beta_j$ for every lane. Thus the protocol has two Merlin messages and one intervening private-coin challenge.

Lemma E.1 (Perfect completeness and soundness)**.** *If $G_0 \ncong_{\mathrm{col}} G_1$, an unbounded honest Merlin is accepted with probability* 1*. If the two sources in the soundness experiment are isomorphic, every Merlin is accepted with probability at most 2^{-24}.*

Proof. For non-isomorphic sources, the color-preserving isomorphism orbits of G_0 and G_1 are disjoint, so every challenge graph determines a unique source. If the sources are isomorphic, a uniformly relabeled copy has the same distribution for $\beta_j = 0$ and $\beta_j = 1$. Conditional on the entire challenge vector $(H_0, \dots, H_{23})$, the source vector $(\beta_0, \dots, \beta_{23})$ is therefore uniform on $\{0, 1\}^{24}$, giving the bound 2^{-24} even when Merlin processes all lanes jointly. □

Every case is first constructed in logical coordinates. Before publication, the two source graphs are independently relabeled by seed-derived uniform permutations, and their order is swapped with probability $1/2$. These transformations erase the generator coordinates without changing isomorphism type.

C2.1.1 Connected prism–Möbius baseline. An odd integer r is sampled uniformly from the odd values in $[701, 1001]$. The first source is the circular prism

$$P_r = C_r \,\square\, K_2,$$

where the Cartesian product $X \square Y$ has vertex set $V(X) \times V(Y)$ and joins (x, y) to (x', y') exactly when either $x = x'$ and $yy' \in E(Y)$, or $y = y'$ and $xx' \in E(X)$. The second source is the Möbius ladder on $\mathbb{Z}_{2r}$,

$$E(M_{2r}) = E(C_{2r}) \cup \big\{\{i, i + r\} : 0 \leq i < r\big\}.$$

Both sources are connected cubic graphs with $2r$ vertices and $3r$ edges. The prism contains an odd rim C_r and is not bipartite. Parity of the index gives a bipartition of M_{2r} because both a cycle edge and an antipodal chord change parity when r is odd.

(a) $P_5 = C_5 \square K_2$ (b) M_{10}



Figure 8: The two C2.1.1 constructions at the illustrative value $r = 5$; generated instances use an odd $r \in [701, 1001]$.

C2.1.2 Connected Shrikhande–rook amplification. The Shrikhande graph S has vertex set $\mathbb{Z}_4^2$, with x adjacent to y when

$$y - x \in \{\pm(1,0),\ \pm(0,1),\ \pm(1,1)\}.$$

The 4×4 rook graph $R_{4,4}$ has the board cells as vertices and joins two cells in a common row or column. Both graphs are strongly regular with parameters $\mathrm{srg}(16, 6, 2, 2)$ Brouwer & Haemers (2012), but $R_{4,4}$ contains row and column copies of K_4, whereas the largest clique in S has size three.

The generator samples q uniformly from the odd integers in $[89, 127]$ and publishes

$$S \,\square\, C_q \qquad \text{and} \qquad R_{4,4} \,\square\, C_q.$$

They are connected 8-regular graphs with $16q$ vertices and $64q$ edges. A clique in a Cartesian product lies in a single factor fiber; hence the rook product contains a K_4 and the Shrikhande product does not. For every vertex v, the two induced neighborhood graphs are

$$(S \square C_q)[N(v)] \cong C_6 \sqcup 2K_1, \qquad (R_{4,4} \square C_q)[N(v)] \cong 2K_3 \sqcup 2K_1,$$

where the two isolated vertices are the neighbors in the cycle direction.

$S \square C_q :\ G[N(v)] \cong C_6 \sqcup 2K_1$ $R_{4,4} \square C_q :\ G[N(v)] \cong 2K_3 \sqcup 2K_1$



Figure 9: The subgraph induced by the eight neighbors of a selected vertex in C2.1.2. The selected vertex and its incident edges are omitted.

C2.1.3 Locally matched group-table geometries. For a finite Abelian group H, form its addition table and let $L(H)$ be the Latin-square graph whose vertices are cells $(x, y) \in H^2$. Two distinct cells are adjacent when they have the same row, the same column, or the same symbol $x + y$. The sources use

$$H_0 = C_{16} \times C_2, \qquad H_1 = C_8 \times C_4.$$

Here $C_m = \mathbb{Z}/m\mathbb{Z}$ denotes the cyclic group, rather than a cycle graph. The construction is deterministic before the final random relabeling. Each graph has 1,024 vertices, degree $3(32 - 1) = 93$, and 47,616 edges; both have strongly regular parameters $\mathrm{srg}(1024, 93, 32, 6)$. The maximal 32-cliques recover the row, column, and symbol classes, up to a permutation of these three families. Permuting the three roles is a *parastrophe*; independently renaming the row, column, and symbol labels is an

isotopy. Thus a graph isomorphism would recover the two group tables up to parastrophe and isotopy. Parastrophes of a group table are isotopic to the group, while isotopic groups are isomorphic Albert (1943).

The group element-order distributions are

	1	2	4	8	16
$C_{16} \times C_2$	1	3	4	8	16
$C_8 \times C_4$	1	3	12	16	0

If the two Latin-square graphs were isomorphic, the preceding recovery would make their group tables isotopic and hence the groups isomorphic, contradicting the different element-order distributions. The two graphs are therefore non-isomorphic.

Common CFI construction for C2.1.4–C2.1.7. The last four cases use the Cai–Fürer–Immerman (CFI) construction Cai et al. (1992). Its starting graph Q is the incidence graph of the generalized quadrangle $GQ(2,2)$ Payne & Thas (2009). One bipartite class consists of the 15 unordered pairs from a six-element set and the other of the 15 partitions of that set into three pairs; a pair is adjacent to a partition precisely when it is one of its parts. Thus Q is connected, cubic, bipartite, and has 30 vertices, 45 edges, and girth eight.

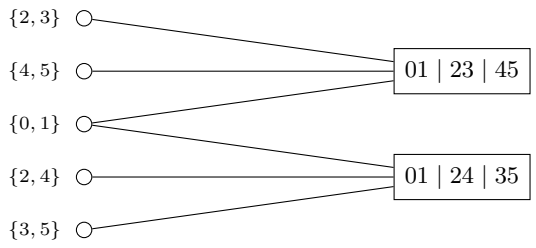

Figure 10: Two partition vertices of the $GQ(2,2)$ incidence graph. A rectangle is adjacent to the three pair vertices appearing in its partition; the full construction contains all 15 vertices of each type.

Index the vertices of Q by listing the 15 pairs and the 15 partitions in lexicographic order, and index its edges lexicographically. For a lift factor f, orient every edge from its smaller endpoint to its larger endpoint and assign it a voltage $z_{uv} \in \mathbb{Z}_f$, with $z_{vu} = -z_{uv}$. The cyclic lift B_f has

$$V(B_f) = V(Q) \times \mathbb{Z}_f, \qquad (u, a) \sim (v, a + z_{uv}).$$

The spanning tree is obtained by breadth-first search from vertex zero, visiting neighbors in increasing order. Tree edges receive voltage zero; one non-tree edge is selected uniformly and receives voltage one; every other non-tree edge receives an independent uniform element of $\mathbb{Z}_f$. All choices are drawn from the instance's seeded random stream. The voltage-one fundamental cycle makes the lift connected. Consequently B_f is a connected cubic graph with $30f$ vertices, $45f$ edges, and girth at least eight.

Each vertex of B_f is replaced by a ten-vertex gadget. Its three incident base edges, ordered by their edge indices, correspond to three *port pairs* $\{i{:}0, i{:}1\}$, $i \in \{1, 2, 3\}$; a port is an outer vertex through which the gadget connects to a neighboring gadget. Four middle vertices are indexed by the even-parity words $000, 011, 101, 110$, and word $a_1a_2a_3$ is adjacent to $i{:}a_i$ for every i. Across a base edge $e = uv$, a twist bit τ_e determines a two-edge matching as follows. If e has local incidence rank $i_u(e)$ at u and $i_v(e)$ at v, add exactly

$$\big\{\{(u, i_u(e), b), (v, i_v(e), b \oplus \tau_e)\} : b \in \{0, 1\}\big\}.$$

Thus "equal" and "opposite" refer only to the binary labels within the two endpoint-specific port pairs; the local incidence ranks need not agree.

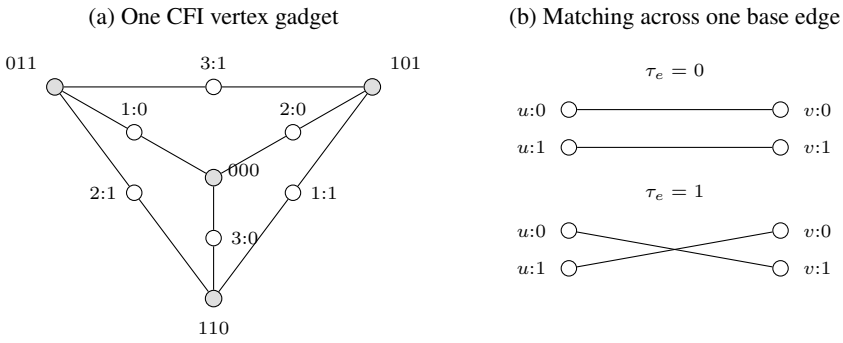

Figure 11: The CFI gadget and its straight and crossed port matchings. The three-bit label of a gray vertex specifies its neighbor in every port pair.

For $b \in \{0, 1\}$, sample the first $|E(B_f)| - 1$ twist bits independently and uniformly, and set the final bit so that

$$\bigoplus_{e \in E(B_f)} \tau_e^{(b)} = b.$$

This samples $\tau^{(b)}$ uniformly from the parity-b affine subspace. Let $R_f^{(b)}$ denote the resulting CFI graph over B_f; the two vectors $\tau^{(0)}$ and $\tau^{(1)}$ are sampled independently. No outer/middle colors are retained. Nevertheless, the gadget decomposition is intrinsic. Form the auxiliary graph on the same vertex set by joining two vertices exactly when they have a common neighbor in the CFI graph. The four middle vertices of each gadget are exactly the maximal K_4 sets that recover the gadgets in this auxiliary graph; their six neighbors in the original graph split into three complementary port pairs. Choose an arbitrary order of the three pairs and an arbitrary $0/1$ orientation within each pair. The four recovered middle words then have one common parity $p_v \in \mathbb{F}_2$. For a reconstructed base edge e, let $h_e \in \mathbb{F}_2$ be the parity of its two-edge matching in these local frames. The quantity

$$I(X) = \bigoplus_v p_v \ \oplus \bigoplus_e h_e$$

is independent of all frame choices: reversing one port pair flips exactly one p_v and one h_e, while permuting the three pairs preserves parity. In the generated frame, $p_v = 0$ and $h_e = \tau_e$, so $I(X) = \bigoplus_e \tau_e$. The opposite-parity CFI roots are therefore non-isomorphic. A root with lift factor f has $300f$ vertices, $450f$ edges, and degree three.

C2.1.4 Uncolored enlarged CFI parity. This case publishes $R_{12}^{(0)}$ and $R_{12}^{(1)}$ without a further graph transformation. Each source is connected, single-colored, and cubic, with 3,600 vertices and 5,400 edges. The unordered pair of intrinsic invariant values is $\{0, 1\}$.

C2.1.5 Fisher-transformed uncolored CFI parity. For $b \in \{0, 1\}$, first subdivide every edge of $R_{10}^{(b)}$ once and then take the line graph. Thus the two published graphs are obtained by applying

$$F(R) = L(S(R)).$$

The vertices of a line graph $L(X)$ are the edges of X, and two are adjacent when their corresponding edges share an endpoint. In $F(R)$, the three incidences at every cubic vertex of R form a triangle, and the two incidences of every original edge are joined by one triangle-external edge. Every output vertex lies in exactly one such triangle and exactly one external matching edge. These are exactly the triangles of $F(R)$, so they are intrinsically identifiable; contracting each triangle recovers R. Each published graph is connected, single-colored, cubic, and has 9,000 vertices and 13,500 edges.

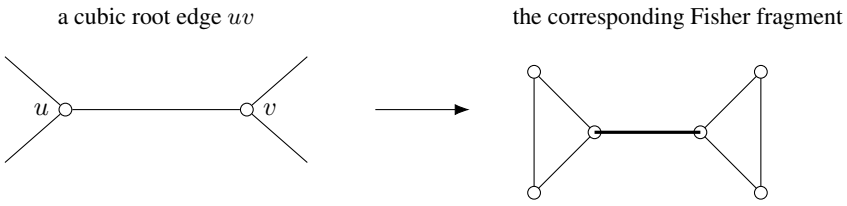

Figure 12: Local form of the Fisher transform in C2.1.5. Each root vertex becomes a triangle; each root edge becomes one edge between two triangles.

C2.1.6 Line graph of uncolored CFI parity. This case publishes $L(R_{16}^{(0)})$ and $L(R_{16}^{(1)})$. Each CFI root is triangle-free: the gadget is bipartite internally, and an inter-gadget edge cannot close a three-cycle. Hence the maximal K_3 subgraphs of $L(R)$ are exactly the three root edges incident with a common root vertex. Reconstructing these stars recovers R; equivalently, uniqueness follows from Whitney's line-graph theorem Whitney (1932), with neither root belonging to its $K_3/K_{1,3}$ exceptional pair. Each source is connected, single-colored, and 4-regular, with 7,200 vertices and 14,400 edges.

C2.1.7 Double line graph of uncolored CFI parity. This case publishes $L(L(R_{12}^{(0)}))$ and $L(L(R_{12}^{(1)}))$. Since $L(R)$ is 4-regular, the maximal K_4 subgraphs of $L(L(R))$ are exactly the four-edge stars of $L(R)$ and recover that graph up to isomorphism. Since the root R is cubic and triangle-free, the maximal K_3 subgraphs of the recovered $L(R)$ are exactly the three-edge stars of R and recover R. Thus two applications of line-graph inversion determine the opposite-parity roots up to isomorphism. Each source is connected, single-colored, and 6-regular, with 10,800 vertices and 32,400 edges.

E.2 BOOLEAN-HYPERCUBE SUM-CHECK

This task asks Merlin to compute a weighted sum over all Boolean assignments to a public factor model and then prove that sum by interaction. The model first specifies Boolean variables and local tables, each depending on only a few variables. Multiplying the tables gives a weight for every global assignment; the desired quantity is the sum of those weights. Directly enumerating the Boolean cube would require at least 2^{288} assignments in the generated cases. The Sum-Check protocol instead reduces the claimed sum to one public polynomial evaluation by fixing the variables one at a time Lund et al. (1992).

All arithmetic is over

$$\mathbb{F}_p, \qquad p = 2^{61} - 1,$$

where p is prime. The public instance contains variables $x_0, \dots, x_{m-1}$ and a nonempty family of factors. Factor a has an ordered scope $S_a = (s_{a,0}, \dots, s_{a,k_a-1})$ of distinct variable indices and a table $f_a : \{0,1\}^{k_a} \to \mathbb{F}_p$. Its multilinear extension is

$$\widetilde{f}_a(y) = \sum_{b \in \{0,1\}^{k_a}} f_a(b) \prod_{j=0}^{k_a-1} \big(b_j y_j + (1 - b_j)(1 - y_j)\big).$$

We refer to $\widetilde{f}_a$ as the multilinear extension (MLE) of f_a. Define

$$g(x) = \prod_a \widetilde{f}_a(x|_{S_a}), \qquad Z = \sum_{b \in \{0,1\}^m} g(b) \pmod p. \tag{1}$$

On Boolean inputs, $\widetilde{f}_a$ agrees with its table, so (1) is precisely the partition function of the factor model. In all seven cases every variable occurs in at most five factors; hence g has individual degree at most five.

Merlin first chooses an arbitrary permutation $\sigma = (\sigma_0, \dots, \sigma_{m-1})$ of the variables and claims Z. Write $z_i = x_{\sigma_i}$ and define

$$g_\sigma(z_0, \dots, z_{m-1}) = g(x_0, \dots, x_{m-1}), \qquad x_{\sigma_i} = z_i.$$

After challenges $r_0, \dots, r_{i-1}$ have been fixed, round i concerns the univariate polynomial

$$q_i(T) = \sum_{z_{i+1}, \dots, z_{m-1} \in \{0,1\}} g_\sigma(r_0, \dots, r_{i-1}, T, z_{i+1}, \dots, z_{m-1}). \tag{2}$$

Merlin submits the six coefficients of q_i in increasing-power order, including trailing zeros. Arthur checks

$$q_i(0) + q_i(1) = C_i,$$

where C_0 is the claimed sum and $C_i = q_{i-1}(r_{i-1})$ thereafter. Only after this message has been recorded does Arthur sample a fresh uniform $r_i \in \mathbb{F}_p$ and set $C_{i+1} = q_i(r_i)$. After m rounds, Arthur evaluates every public factor MLE at the assembled random point and accepts exactly when

$$q_{m-1}(r_{m-1}) = g_\sigma(r_0, \dots, r_{m-1}).$$

The claimed value is not compared with a stored answer; acceptance follows solely from these algebraic checks.

Lemma E.2 (Perfect completeness and soundness)**.** *An honest Merlin claiming the value in (1) is accepted with probability* 1*. For a false initial claim, the acceptance probability is at most*

$$\frac{5m}{p} \le \frac{2000}{2^{61} - 1} < 2^{-50}.$$

Proof. For an honest transcript, (2) is the exact remaining Boolean sum. Summing its two Boolean endpoints restores the preceding claim, and after the final round no variables remain, so the terminal value is $g(r_0, \dots, r_{m-1})$. For soundness, whenever the submitted polynomial differs from the true round polynomial, their nonzero difference has degree at most five and vanishes at the fresh challenge with probability at most $5/p$. If it does not vanish, a false claim persists to the next round and is exposed by the final public evaluation. A union bound over $m \le 400$ rounds gives the stated result. □

The generators first build a logical factor model and then use the seeded random stream to apply four value-preserving transformations: a uniform permutation of the variable names, an independent uniform permutation of each factor's axes with the table reordered accordingly, independent uniform gauge bits $h_v \in \{0,1\}$ applied consistently as $x_v \mapsto x_v \oplus h_v$, and a uniform permutation of the factor list. Each operation is a reparameterization of the Boolean cube, so it preserves Z. The descriptions below give the logical coordinates before this hiding step.

C2.2.1 Rank-one factors on a hidden 4-regular graph. On $m = 384$ variables, the generator takes the union of two edge-disjoint Hamilton cycles. The first is the cyclic order $(0, 1, \ldots, m-1)$; the second is obtained by repeatedly sampling a uniform vertex permutation until its cycle is simple and edge-disjoint from the first. The result is a simple 4-regular graph with 768 edges. Every edge $e = \{u, v\}$, with $u < v$, receives the binary table

$$f_e(x_u, x_v) = a_{e,u}(x_u)a_{e,v}(x_v), \qquad f_e(0,0)f_e(1,1) = f_e(1,0)f_e(0,1).$$

The four vector coordinates $a_{e,u}(0), a_{e,u}(1), a_{e,v}(0), a_{e,v}(1)$ are sampled independently and uniformly from $\{1, \ldots, 7\} \subset \mathbb{F}_p^*$. There are 768 binary factors and no other factors, so every variable occurs four times. The product consequently separates by variables,

$$g(x) = \prod_v A_v(x_v), \qquad A_v(T) = \prod_{e \ni v} a_{e,v}(T),$$

and $Z = \prod_v (A_v(0) + A_v(1))$. Axis permutations and Boolean gauges preserve the rank-one identity.

C2.2.2 Weighted signed-equivalence model. This case uses an independently generated instance of the same two-cycle construction on $m = 360$ variables, with 720 binary factors. Independent uniform bits s_v are drawn in logical vertex order. For every edge uv, the binary table has nonzero entries exactly on the two assignments satisfying

$$x_u \oplus x_v = s_u \oplus s_v,$$

with independent uniform weights from $\{1, \ldots, 7\}$ on the two allowed entries. A unary table whose two entries are sampled independently and uniformly from $\{1, \ldots, 7\}$ is attached to every variable. Thus the model has 360 unary and 720 binary factors, and every variable occurs five times. Because the two-cycle graph is connected, the common support of the binary tables consists of exactly two global assignments, $x = s$ and $x = \mathbf{1} \oplus s$.

C2.2.3 Cylindrical two-spin model of width 16. The logical interaction graph is the Cartesian product $C_{16} \square P_{25}$. Its Boolean spins are $x_{r,c}$ for $r \in \mathbb{Z}_{16}$ and $0 \le c < 25$; edges join (r, c) to $(r + 1 \bmod 16, c)$ and, when $c < 24$, to $(r, c + 1)$. Each unary table has two independent uniform entries in $\{1, 2, 3\}$, and each binary table has four such entries, with an edge's smaller variable index used as its first axis. There are 400 cycle-direction edges and $16(25 - 1) = 384$ longitudinal edges, giving 400 unary and 784 binary factors. Boundary spins occur in four factors and all other spins in five.

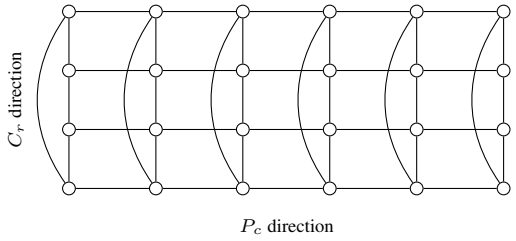

Figure 13: A small schematic of $C_r \square P_c$. Each displayed column is cyclic; the generated C2.2.3 and C2.2.4 instances use $(r, c) = (16, 25)$ and $(12, 33)$, respectively.

C2.2.4 Cylindrical two-spin model of width 12. Here the logical graph is $C_{12} \square P_{33}$. Its 396 spins again receive unary factors whose two entries are independent and uniform in $\{1, 2, 3\}$; its 780 edges

receive binary factors whose four entries are sampled in the same way. Coordinates and factor-axis order follow C2.2.3, with $r \in \mathbb{Z}_{12}$ and $0 \le c < 33$. The edge set consists of 396 cycle-direction edges and $12(33-1) = 384$ longitudinal edges. The factor counts are therefore 396 unary and 780 binary, with maximum variable occurrence five. Figure 13 shows the common product geometry.

C2.2.5 Cylindrical monomer–dimer model. Let $H = C_6 \square P_{30}$, with 180 vertices and 354 edges. There is one Boolean variable x_e per edge, where $x_e = 1$ means that e is selected. Each edge has unary weight $(1, w_e)$, where w_e is sampled independently and uniformly from $\{2, \dots, 8\}$ with edges ordered lexicographically by their endpoint pairs. For every vertex v, an occupancy factor on the incident edge variables takes value one exactly when at most one of them equals one, and zero otherwise:

$$\psi_v((x_e)_{e \ni v}) = \mathbf{1}\left[\sum_{e \ni v} x_e \le 1\right].$$

The scope axes of ψ_v list the incident edges in increasing order of their global lexicographic edge indices. Hence the nonzero Boolean assignments are precisely the matchings of H; an uncovered vertex is a monomer and a selected edge is a dimer Heilmann & Lieb (1972). The model has 354 unary edge factors, 12 arity-three occupancy factors at the two boundary cycles, and 168 arity-four occupancy factors in the interior. Every edge variable occurs in its unary factor and in the two endpoint occupancy factors.

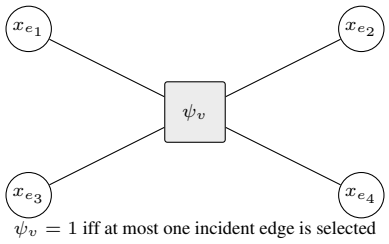

Figure 14: The arity-four occupancy factor at an interior vertex of the monomer–dimer graph in C2.2.5.

C2.2.6 Six-vertex model on a torus. The site graph is the toroidal grid $C_6 \square C_{24}$, with 144 sites and 288 edges. Index sites in row-major order; from each site, index its eastward edge and then its southward edge, with coordinates taken modulo the two side lengths. The four factor axes are its incident edge indices in increasing order. Each edge carries one Boolean variable. At each site, an arity-four factor has nonzero values exactly on the six configurations of Hamming weight two, with an independent uniform weight in $\{1, 2, 3\}$ for each such configuration. This local two-of-four constraint is the six-vertex, or ice, rule. Every edge also receives a unary factor $(1, w_e)$, where w_e is sampled independently and uniformly from $\{1, 2, 3\}$ and independently of all site weights. Thus there are 144 arity-four factors and 288 unary factors, and every variable occurs three times. The Boolean gauge described above can complement edge variables, so the published six allowed entries need not literally be the Hamming-weight-two entries even though they are a consistent relabeling of this rule.

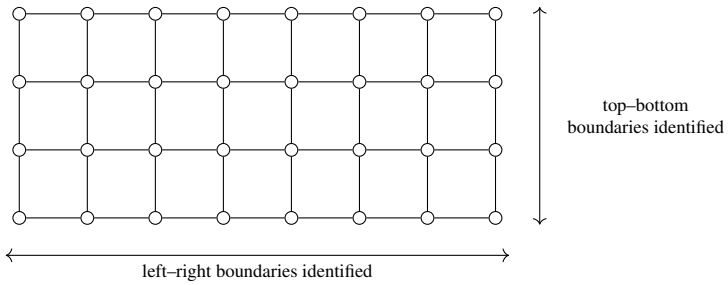

Figure 15: A fundamental rectangle of a toroidal grid. C2.2.6 uses six rows and 24 columns, with opposite boundaries identified coordinatewise.

C2.2.7 Memory-ten tail-biting enumerator. Let $n = 160$ and interpret all subscripts modulo n. The 320 variables are input bits $u_0, \ldots, u_{n-1}$ and output bits $v_0, \ldots, v_{n-1}$. For each time t, define the arity-four factor, in the displayed argument order, by

$$Q_t(v_t, u_t, u_{t-3}, u_{t-10}) = \mathbf{1}[v_t = u_t \oplus u_{t-3} \oplus u_{t-10}]; \tag{3}$$

exactly eight of its 16 table entries are one. The largest delay is ten, so this is a memory-ten encoder. Using all indices modulo n is the tail-biting convention: the ten delayed input positions wrap around cyclically. Each v_t has a unary factor $(1, \mu_t)$, where the μ_t are independent and uniform in $\{2, \ldots, 6\}$. Consecutive input bits have the rank-one factor

$$J_t(u_t, u_{t+1}) = \lambda_t^{u_t + u_{t+1}}, \qquad \lambda_t \xleftarrow{\$} \{2, \ldots, 6\},$$

where all λ_t are independent of one another and of the μ_t. The scopes (u_t, u_{t+1}), including (u_{n-1}, u_0), form the cyclic time-order graph; algebraically, J_t contributes one factor λ_t for each of its two incident inputs that equals one. The model has 160 factors of each arity one, two, and four. Every input bit occurs in $Q_t, Q_{t+3}, Q_{t+10}, J_{t-1}, J_t$, and every output bit in Q_t and its unary factor.

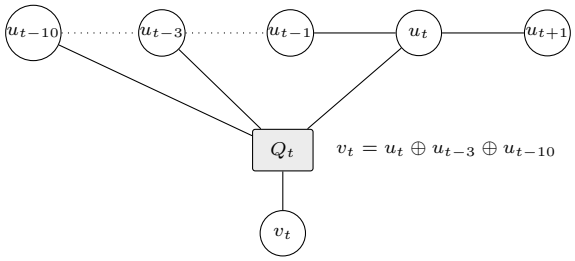

Figure 16: Local factor-incidence structure in C2.2.7. Horizontal solid edges denote adjacent-input factors; dotted segments abbreviate omitted positions of the 160-cycle.

E.3 GKR Layered Arithmetic-Circuit Evaluation

This task asks Merlin to evaluate a public arithmetic circuit and prove its scalar output. The circuit is organized into layers: each gate reads two values from the next layer, while the last layer contains public inputs. The Goldwasser–Kalai–Rothblum (GKR) protocol follows the computation backward, reducing one claimed layer evaluation to a claimed evaluation of the next layer until Arthur can check the public input directly Goldwasser et al. (2008). All circuit data are public; the interaction certifies consistent evaluation rather than knowledge of a hidden witness.

All arithmetic is over $\mathbb{F}_p$, where the prime $p = 2^{61} - 1$. Write $[N] = \{0, \dots, N-1\}$. Layers are numbered from the scalar output toward the inputs:

$$V_0, V_1, \dots, V_L, \qquad N_i = |V_i| = 2^{s_i}, \qquad N_0 = 1.$$

The table V_L contains the public inputs. For $i < L$ and gate position $g \in [N_i]$, the public circuit specifies field coefficients $a_i(g), b_i(g), c_i(g)$ and child positions $\lambda_i(g), \rho_i(g) \in [N_{i+1}]$, with semantics

$$V_i(g) = a_i(g)V_{i+1}(\lambda_i(g)) + b_i(g)V_{i+1}(\rho_i(g)) + c_i(g)V_{i+1}(\lambda_i(g))V_{i+1}(\rho_i(g)). \tag{4}$$

Equation (4) represents copy, addition, subtraction, scalar multiplication, and multiplication gates by appropriate coefficient choices. A semantic gate list is padded by appending positions until its length is the next power of two. Every ordinary padding position is the canonical zero gate $(a, b, c, \lambda, \rho) = (0, 0, 0, 0, 0)$; the explicitly specified expansion gates in C2.3.5–C2.3.7 are exceptions. Within every semantic micro-layer, gates and copy rails are appended in the order stated by the case construction, and only then is padding appended. The generator and serialized public gate table are the canonical specification of this low-level ordering and of all child indices. The descriptions below specify the semantic circuit and all nontrivial instance parameters; they are not intended as a second, byte-for-byte reimplementation of that serializer. Merlin initially claims $y = V_0(0)$.

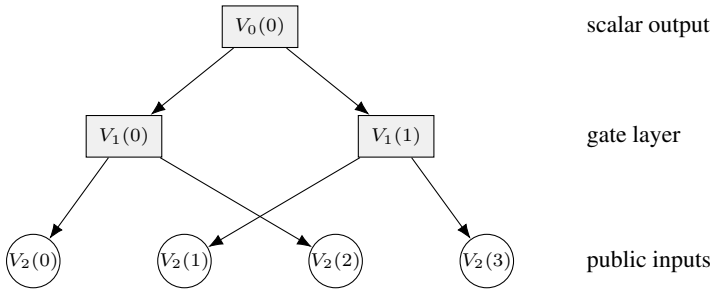

Figure 17: A strictly layered fan-in-two arithmetic circuit. Each rectangle applies (4) to two positions in the next layer.

Identify position $j \in [N_i]$ with $\mathrm{bits}_{s_i}(j)$, its s_i-bit binary vector in least-significant-bit-first order. For $z \in \mathbb{F}_p^s$ and $b \in \{0,1\}^s$, define

$$\mathrm{eq}_s(z, b) = \prod_{k=0}^{s-1} \big((1 - z_k)(1 - b_k) + z_k b_k\big).$$

The multilinear extension of a layer is

$$\widetilde{V}_i(z) = \sum_{g=0}^{N_i-1} \mathrm{eq}_{s_i}(z, \mathrm{bits}_{s_i}(g))V_i(g). \tag{5}$$

For $D \in \{A, B, M\}$, let $d_i(g)$ be, respectively, $a_i(g), b_i(g), c_i(g)$, and set

$$\begin{aligned}\widetilde{D}_i(r, u, v) = \sum_{g=0}^{N_i-1} d_i(g)\,\mathrm{eq}_{s_i}(r, \mathrm{bits}_{s_i}(g)) \\ \cdot \mathrm{eq}_s(u, \mathrm{bits}_s(\lambda_i(g)))\,\mathrm{eq}_s(v, \mathrm{bits}_s(\rho_i(g))),\end{aligned} \tag{6}$$

where $s = s_{i+1}$. Expanding (4) on the Boolean child positions gives

$$\widetilde{V}_i(r) = \sum_{u,v\in\{0,1\}^s} F_i(r,u,v), \tag{7}$$

with

$$F_i(r,u,v) = \widetilde{A}_i(r,u,v)\widetilde{V}_{i+1}(u) + \widetilde{B}_i(r,u,v)\widetilde{V}_{i+1}(v) + \widetilde{M}_i(r,u,v)\widetilde{V}_{i+1}(u)\widetilde{V}_{i+1}(v).$$

Every coordinate of F_i has degree at most two.

The protocol starts from the unique point $r_0 = () \in \mathbb{F}_p^0$ and $C_0 = y$. At the beginning of layer i, the current claim is $C_i = \widetilde{V}_i(r_i)$. Merlin and Arthur apply Sum-Check to (7), with claimed sum C_i, over the $2s$ coordinates $u_0, \ldots, u_{s-1}, v_0, \ldots, v_{s-1}$ in that order. In each round Merlin submits exactly three coefficients of the degree-at-most-two remaining-sum polynomial, in increasing-power order and including a zero quadratic coefficient when necessary. Arthur checks that the first polynomial's values at zero and one sum to C_i, and thereafter that they sum to the preceding polynomial evaluated at the previous challenge. Only then does he sample the next challenge independently and uniformly from $\mathbb{F}_p$. The challenges define $u^*, v^* \in \mathbb{F}_p^s$ and leave one claimed value H for F_i.

Merlin next supplies

$$U = \widetilde{V}_{i+1}(u^*), \qquad V = \widetilde{V}_{i+1}(v^*),$$

and all $s+1$ coefficients, in increasing-power order, of the line restriction

$$d(T) = \widetilde{V}_{i+1}\big(u^* + T(v^* - u^*)\big), \qquad \deg d \le s. \tag{8}$$

Arthur evaluates the wiring polynomials (6) at (r_i, u^*, v^*) from the public gate table and checks

$$H = \widetilde{A}_i(r_i,u^*,v^*)U + \widetilde{B}_i(r_i,u^*,v^*)V + \widetilde{M}_i(r_i,u^*,v^*)UV, \qquad d(0) = U, \qquad d(1) = V.$$

After these values are committed, he samples an independent uniform $t_i \in \mathbb{F}_p$ and sets

$$r_{i+1} = u^* + t_i(v^* - u^*), \qquad C_{i+1} = d(t_i).$$

After layer $L-1$, Arthur computes $\widetilde{V}_L(r_L)$ from the public input table and accepts exactly when it equals C_L. The transcript contains

$$1 + \sum_{i=0}^{L-1}(2s_{i+1} + 1)$$

Merlin messages: one output claim, $2s_{i+1}$ Sum-Check polynomials per layer, and one line-reduction message per layer.

Lemma E.3 (Perfect completeness and soundness)**.** *An honest Merlin claiming $V_0(0)$ is accepted with probability* 1*. For a false output claim, the generated instances satisfy*

$$\Pr[\text{accept}] \le \frac{5\sum_{i=0}^{L-1} s_{i+1}}{p} < 2^{-49}.$$

Proof. For an honest Merlin, (7) is the exact expansion of the gate semantics, every Sum-Check polynomial is the true remaining sum, and (8) is the actual restriction of the next-layer MLE. All checks therefore hold exactly. At a layer carrying a false claim, degree-two Sum-Check over $2s_{i+1}$ coordinates contributes at most $4s_{i+1}/p$ soundness error. If a false next-layer value passes the endpoint checks, the submitted line polynomial and the true restriction differ by a nonzero polynomial of degree at most s_{i+1}, which agrees at the fresh t_i with probability at most s_{i+1}/p. Otherwise the false claim reaches the final public input check. A union bound proves the formula. Every generated circuit uses at most 512 verifier challenges, so $\sum_i s_{i+1} < 256$, which gives the numerical bound. □

Each case is built in semantic coordinates and padded to power-of-two layer widths. The input layer and every non-output gate layer are then permuted by independent uniform permutations from the seeded random stream, and all child indices are rewritten consistently. These permutations preserve

the scalar output but remove the original semantic ordering. Before these permutations, a *logical position* is the zero-based index in the ordered semantic gate list after ordinary power-of-two padding. In an expanded layer, the active application gates occupy the prefix in their original order and the explicitly defined extra gates occupy the remaining indices. References to an "original logical prefix" in C2.3.5–C2.3.7 use this convention; the following layer refers to its images after permutation. For the numerical summaries below, L is the number of non-input layers, $W = \max_{0 \le i \le L} N_i$, $S = \sum_{i=0}^{L} N_i$, and $R = \sum_i (2s_{i+1} + 1)$ is the number of post-claim randomness barriers.

C2.3.1 Balanced inner product. The generator samples all coordinates of $a, b \in \mathbb{F}_p^{64}$ independently and uniformly. In semantic input order, positions $0, \ldots, 63$ store a and positions $64, \ldots, 127$ store b. One layer computes $a_j b_j$ at position j, and each of six balanced addition layers adds consecutive pairs of its child layer, reducing them to

$$y = \sum_{j=0}^{63} a_j b_j.$$

From input to output the widths are $128, 64, 32, 16, 8, 4, 2, 1$. Thus $(L, W, S, R) = (7, 128, 255, 63)$.

C2.3.2 Batched second-order affine recurrences. There are $B = 8$ independent batches and $T = 6$ states per batch. For each $b \in \{0, \ldots, 7\}$, the generator samples $\alpha_b, \beta_b, \gamma_b, u_{b,0}, u_{b,1}, \eta_b$ independently and uniformly from $\mathbb{F}_p$, stores these six rails consecutively for each batch, and computes

$$u_{b,t+2} = \alpha_b u_{b,t+1} + \beta_b u_{b,t} + \gamma_b, \qquad 0 \le t \le 3.$$

For each update, the first fan-in-two layer copies the six rails and appends $\alpha_b u_{b,t+1}$ and $\beta_b u_{b,t}$; the second copies $\alpha_b, \beta_b, \gamma_b, u_{b,t+1}, \eta_b$ and forms the sum of the products; the third adds γ_b and restores the six-rail order with state pair $(u_{b,t+1}, u_{b,t+2})$. After four updates, one layer computes the eight products $\eta_b u_{b,5}$, and three consecutive-pair addition layers produce

$$y = \sum_{b=0}^{7} \eta_b u_{b,5}.$$

The resulting profile is $(L, W, S, R) = (16, 64, 847, 184)$.

C2.3.3 Matrix triple product. The public inputs are three matrices $A, B, C \in \mathbb{F}_p^{8 \times 8}$, whose entries are sampled independently and uniformly and stored in matrix order A, B, C, each in row-major order. A 512-gate product table, ordered lexicographically by (i, j, k), forms $A_{ik} B_{kj}$. The 64 entries of C are copied after these products. Three balanced layers add consecutive k-pairs while continuing to copy C; this computes $(AB)_{ij}$. The 64 results are multiplied by C_{ji}, and six consecutive-pair addition layers compute

$$y = \operatorname{tr}(ABC) = \sum_{i,j,k=0}^{7} A_{ik} B_{kj} C_{ji}.$$

The 512 products together with 64 copied entries pad to width 1,024. The profile is $(L, W, S, R) = (11, 1024, 2303, 137)$.

C2.3.4 Walsh–Hadamard XOR convolution. The generator samples every coordinate of $a, b, d \in \mathbb{F}_p^{128}$ independently and uniformly and stores the three vectors consecutively. It defines

$$c_z = \sum_{x=0}^{127} a_x b_{x \oplus z}, \qquad y = \sum_{z=0}^{127} c_z d_z,$$

where $\oplus$ is bitwise exclusive-or on seven-bit indices. The circuit computes c using the fast Walsh–Hadamard transform. At butterfly stage $q \in \{0, \ldots, 6\}$, indices j with bit q equal to zero are paired with $j + 2^q$; the two output positions receive

$$(x, y) \longmapsto (x + y, x - y)$$

The seven stages are applied in parallel to a and b, while all entries of d are copied. The transformed vectors are multiplied coordinatewise; the same seven stages are then applied to that product, followed by multiplication by $128^{-1} \bmod p$. Finally, the result is multiplied coordinatewise by d and reduced through seven consecutive-pair addition layers. The profile is $(L, W, S, R) = (24, 512, 6655, 368)$.

Proof-relevant inactive expansion layers. C2.3.5–C2.3.7 each contain one layer of width 2^{18} or 2^{19}. A prefix of that layer carries the application computation, while its remaining gates are not referenced by the next semantic layer and therefore do not affect $V_0(0)$. They are nevertheless not removable from the GKR proof. A random MLE evaluation of the entire wide layer is a linear combination of all its positions; after line reduction, the next GKR claim therefore depends on the values of both the active and inactive positions. Per-layer permutation removes the contiguous-prefix layout from the published numbering.

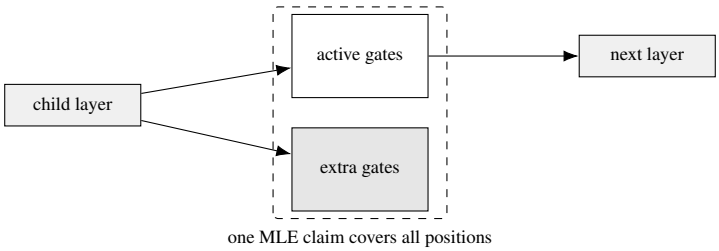

Figure 18: Logical role of an expanded layer before its positions are permuted. Extra gates do not feed the application output, but their values enter a random multilinear evaluation of the complete layer.

For the exact definitions below, $j \operatorname{shr} k$ denotes $\lfloor j/2^k \rfloor$, $\oplus_b$ denotes bitwise XOR on nonnegative integers, and all gate coefficients are reduced modulo p.

C2.3.5 Bitonic Boolean-key payload routing. The input consists of eight records, each with a Boolean key k_i and four independent uniform nonzero field-valued payloads. The keys are independent uniform bits, and records are stored in index order with the key before its four payloads. A six-stage Batcher bitonic sorting network Batcher (1968) routes the records into nondecreasing key order. For an ascending comparator on keys a, b, let

$$s = a(1-b) = a - ab, \qquad a' = a - s, \quad b' = b + s.$$

For a payload pair P, Q, the same swap bit gives

$$P' = P + s(Q - P), \qquad Q' = Q + s(P - Q). \tag{9}$$

A descending comparator uses $s = (1-a)b$. Each comparator stage is expanded into five fan-in-two layers: copy all record fields and compute ab; copy them and compute the direction-specific swap bit; copy them and s and compute both payload differences; multiply each difference by s; and write the updated keys and payloads. Formula (9) is applied independently to all four payload coordinates. The six comparator stages, listing (i, j) followed by $+$ for ascending and $-$ for descending, are

1	$(01)+, (23)-, (45)+, (67)-$
2	$(02)+, (13)+, (46)-, (57)-$
3	$(01)+, (23)+, (45)-, (67)-$
4	$(04)+, (15)+, (26)+, (37)+$
5	$(02)+, (13)+, (46)+, (57)+$
6	$(01)+, (23)+, (45)+, (67)+$

After sorting, 40 independent uniform nonzero field weights multiply the flattened records, and six consecutive-pair addition layers reduce the padded 64-position table to the scalar digest.

The third micro-layer of the first comparator stage (the first layer that contains payload differences) has 128 active gates and is extended to $D = 2^{19}$ positions. The preceding layer has width 64. For $128 \le j < D$, the extra gate reads

$$\ell_j = j \bmod 64, \qquad r_j = ((j \operatorname{shr} 6) \oplus_b (17j) \oplus_b 45) \bmod 64,$$

and has coefficients

$$a_j = \alpha + \texttt{0x9e3779b1}\, j,$$
$$b_j = \beta + \texttt{0x85ebca77}\, j,$$
$$c_j = \gamma + \texttt{0xc2b2ae3d}\, j,$$

where α, β, γ are sampled independently and uniformly from $\mathbb{F}_p^*$. Only the original 128 logical positions feed the next comparator layer. The profile is $(L, W, S, R) = (37, 524288, 527039, 499)$.

C2.3.6 Rule 110 periodic spacetime. Rule 110 is a radius-one binary cellular automaton. The generator samples a Boolean state $x^{(0)} \in \{0,1\}^{256}$ as independent uniform bits on a ring and performs four synchronous updates, with indices modulo 256:

$$x_j^{(t+1)} = R(x_{j-1}^{(t)}, x_j^{(t)}, x_{j+1}^{(t)}), \qquad R(\ell, c, r) = c + r - cr - \ell cr. \tag{10}$$

On neighborhoods $111, 110, 101, 100, 011, 010, 001, 000$, (10) gives $0, 1, 1, 0, 1, 1, 1, 0$, respectively. Each update is expanded into four binary layers. The first copies the 256 cells and appends all cr products. The second computes all $c + r$, copies cr, and computes $\ell(cr)$. The third forms $c+r-cr$ and copies ℓcr; the fourth subtracts these two values. After four updates, 256 independent uniform nonzero field weights multiply $x^{(4)}$, and eight consecutive-pair addition layers form the scalar digest.

The second micro-layer of the first update has 1,024 logical gate and rail positions and is expanded to $D = 2^{19}$ gates; its child layer has width 512. For $j \geq 1024$, define

$$\ell_j = (j \oplus_b (j \operatorname{shr} 9) \oplus_b \texttt{0x151}) \bmod 512, \quad r_j = (29j + (j \operatorname{shr} 4) + \texttt{0x6d}) \bmod 512,$$

with coefficients

$$(a_j, b_j, c_j) = (\alpha + \texttt{0x27d4eb2d}j, \beta + \texttt{0x165667b1}j, \gamma + \texttt{0xd3a2646c}j).$$

α, β, γ are sampled independently and uniformly from $\mathbb{F}_p^*$. Only the original 1,024 logical positions feed the next micro-layer. The profile is $(L, W, S, R) = (25, 524288, 533247, 419)$.

C2.3.7 Boolean repeated-squaring transitive closure. The input is a directed graph on $n = 16$ vertices. The diagonal of its adjacency matrix is set to one; every off-diagonal arc is otherwise included independently with probability $1/4$. The resulting row-major Boolean table is $R^{(0)}$. Four Boolean matrix squarings are then performed:

$$R_{ij}^{(t+1)} = \bigvee_{k=0}^{15} \left(R_{ik}^{(t)} \wedge R_{kj}^{(t)}\right), \qquad 0 \leq t < 4. \tag{11}$$

The arithmetic circuit represents AND by xy and binary OR by $x + y - xy$. Each squaring uses a 4,096-gate product layer in lexicographic (i, j, k) order, followed by four balanced OR layers that combine consecutive k-pairs for each fixed (i, j). Induction gives

$$R_{ij}^{(t)} = 1 \iff \text{there is an } i\text{-to-}j \text{ walk of length at most } 2^t.$$

The diagonal ones pad shorter walks, and every reachable pair has a simple path of length at most $15 < 2^4$. Thus $R^{(4)}$ is the transitive closure. Eight consecutive-pair addition layers compute $y = \sum_{i,j} R_{ij}^{(4)}$, which counts reachable ordered pairs as an ordinary integer because $0 \leq y \leq 256 < p$.

The first product layer is expanded from 4,096 to $D = 2^{18}$ positions; its child layer is the 256-entry relation table. For $j \geq 4096$, define

$$\ell_j = (j \oplus_b (j \operatorname{shr} 8) \oplus_b (j \operatorname{shr} 16) \oplus_b \texttt{0xa7}) \bmod 256,$$
$$r_j = (37j + (j \operatorname{shr} 5) + \texttt{0x53}) \bmod 256,$$

with coefficients

$$(a_j, b_j, c_j) = (\alpha + \texttt{0x7feb352d}j, \beta + \texttt{0x846ca68b}j, \gamma + \texttt{0x9e3779b9}j).$$

α, β, γ are sampled independently and uniformly from $\mathbb{F}_p^*$. Only the original 4,096 logical product positions, or their images under the subsequent layer permutation, feed the first OR-reduction layer. The profile is $(L, W, S, R) = (28, 262144, 290303, 512)$.

E.4 Boolean-Circuit Image-Size Lower Bound

This task gives a public Boolean circuit and asks Merlin to demonstrate that the circuit has many distinct outputs. The set of possible outputs is the *image* of the function computed by the circuit; if many inputs collide, the image may be much smaller than the domain. Merlin does not report the image size directly. Instead, Arthur chooses random affine constraints on the output, and Merlin supplies circuit inputs whose outputs satisfy sufficiently many of them. A large image is likely to intersect most of the random affine buckets, whereas a small image is unlikely to do so. This is a finite-field instantiation of the hashing technique used in public-coin set-size lower-bound protocols Goldwasser & Sipser (1986).

The public circuit uses Boolean constants and the gates NOT, XOR, and AND and computes

$$F : \{0,1\}^m \longrightarrow \{0,1\}^n.$$

Its gates are given in topological order, so Arthur can evaluate $F(x)$ for any submitted input. Define

$$S = \operatorname{Im} F = \{F(x) : x \in \{0,1\}^m\}, \qquad T = 2^t,$$

where $t \geq 0$ is part of the instance. The promise is

$$|S| \geq 16T \quad (\mathsf{YES}), \qquad \text{or} \qquad |S| \leq T \quad (\mathsf{NO}). \tag{12}$$

All generated instances are YES instances. A *preimage* of an output $z \in S$ is any input x satisfying $F(x) = z$; no canonical preimage is required.

All hashing arithmetic is over $\mathbb{F}_2$. Put $k = t + 2$. For each lane $j \in \{0, \ldots, 127\}$, Arthur independently samples

$$A_j \xleftarrow{\$} \mathbb{F}_2^{k \times n}, \qquad b_j \xleftarrow{\$} \mathbb{F}_2^k.$$

The corresponding affine bucket is

$$B_j = \{z \in \mathbb{F}_2^n : A_j z = b_j\}. \tag{13}$$

Uniform affine hashing is pairwise independent Carter & Wegman (1979): for distinct z, z', membership of z and z' in a fixed random bucket is independent.

The three-step interaction contains two Merlin messages. Merlin first sends a fixed, content-independent start signal. Only after it has been recorded does Arthur sample and return all 128 pairs (A_j, b_j). Merlin then returns one entry per lane: either an input $x_j \in \{0,1\}^m$ or a null entry. For every non-null entry, Arthur evaluates the public circuit and checks

$$A_j F(x_j) = b_j.$$

A null entry fails; a non-null lane succeeds exactly when this equality holds, and Arthur accepts exactly when at least 64 lanes succeed. Thus a purported output is insufficient: every counted lane must contain an actual circuit preimage. The statistical statement below abstracts away this operational limit. In the generated instances $m \leq 12$, so exhaustive evaluation of at most 2^{12} inputs suffices to find a preimage for every answerable bucket.

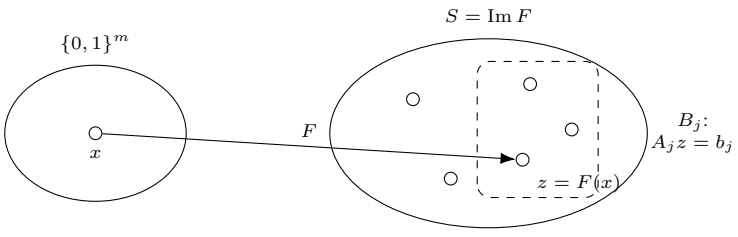

Figure 19: One lane of the image-size protocol. A valid response gives an input x whose circuit output lies in Arthur's random affine bucket B_j.

Lemma E.4 (Statistical completeness and soundness)**.** *On a* YES *instance, an unbounded honest Merlin is rejected with probability less than* 10^{-10}*. On a* NO *instance, every Merlin is accepted with probability less than* 2^{-23}*.*

Proof. For one lane, let

$$X = |S \cap B_j|, \qquad \lambda = \frac{|S|}{2^k}.$$

Pairwise independence gives $\mathbb{E}[X] = \lambda$ and $\mathbb{E}[X^2] \le \lambda^2 + \lambda$. The Paley–Zygmund inequality at threshold zero therefore yields

$$\Pr[X > 0] \ge \frac{\lambda}{1+\lambda}.$$

For a YES instance, $2^k = 4T$ and $\lambda \ge 4$, so a lane is answerable with probability at least $4/5$. For a NO instance, the union bound gives $\Pr[X > 0] \le |S|/2^k \le 1/4$. The 128 lane indicators are independent. Hoeffding's inequality consequently gives

$$\Pr_{\mathsf{YES}}[\text{fewer than 64 successes}] \le \exp\!\big(-2 \cdot 128(0.8 - 0.5)^2\big) < 10^{-10},$$
$$\Pr_{\mathsf{NO}}[\text{at least 64 successes}] \le \exp\!\big(-2 \cdot 128(0.5 - 0.25)^2\big) < 2^{-23}.$$

A Merlin cannot make an empty bucket successful, because Arthur independently evaluates $F(x_j)$ and (13) for every counted response. □

For every case, the construction has an exact image size $s \ge 16$, as established below, and the generator sets

$$t = \lfloor \log_2 s \rfloor - 4. \tag{14}$$

Thus $16 \cdot 2^t \le s < 32 \cdot 2^t$, so the instance satisfies the YES side of (12). The logical construction assigns input roles by a uniform permutation from the seeded random stream, then applies an independent uniform output-coordinate permutation and independent uniform output-complement bits. Writing π for the linear map induced by the coordinate permutation and $c \in \mathbb{F}_2^n$ for the complement mask, the latter operation has the form $z \mapsto \pi(z) \oplus c$ and is a bijection of $\mathbb{F}_2^n$, so it preserves the image size. The following descriptions use the logical coordinates before this hiding transformation. The canonical compiler numbers the input wires $0, \dots, m-1$ and then appends each requested gate immediately, so every gate reads only earlier wires. Constants zero and one are each emitted on first use and reused thereafter. Iterated XORs and conjunctions are left-associated; the empty XOR is zero and the empty conjunction is one. A requested OR $a \vee b$ is emitted as three successive gates $u = a \oplus b$, $v = a \wedge b$, and $u \oplus v$. The logical output list is permuted only after all of its wires have been constructed, and the NOT gates that implement output complementation are then appended. Together with each case's stated loop order, these conventions determine the published topological gate table.

C2.4.1 Systematic subcube image. The circuit has $m = 10$ inputs and $n = 12$ outputs. Eight randomly selected inputs are copied to eight logical output coordinates: specifically, a uniform permutation of $[10]$ is sampled and its first eight distinct entries are $(i_1, \dots, i_8)$ in output order. The other four output coordinates are zero, and the remaining two inputs are unused. Before the final affine hiding, the map is

$$(x_1, \dots, x_{10}) \longmapsto (x_{i_1}, \dots, x_{i_8}, 0, 0, 0, 0).$$

The eight active bits vary independently, so $|\operatorname{Im} F| = 2^8 = 256$. Equation (14) gives $t = 4$, and each challenge has $k = 6$ hash equations.

C2.4.2 Hidden affine image. This case has $m = 12$ and $n = 14$. Eight shuffled input coordinates are active. The first eight logical outputs copy them individually, while each of the six remaining outputs is determined as follows: independently include every active input with probability $1/2$; if fewer than two are included, replace the list by two independently sampled active coordinates, allowing repetition. The output is the left-associated XOR of that list. After the output permutation and shift, the circuit computes

$$F(x) = Lx \oplus c, \qquad L \in \mathbb{F}_2^{14 \times 12}, \qquad \operatorname{rank} L = 8.$$

Before the output permutation, the eight systematic rows form an identity submatrix; row permutation preserves rank irrespective of the additional rows. Hence the image is an affine subspace of dimension eight and has size 256; again $t = 4$ and $k = 6$.

C2.4.3 Hamming ball via truncation. Here $m = n = 12$. The generator chooses a hidden ordering of the input coordinates by a uniform permutation σ and scans them in that order. If $z_{\sigma(q)}$ denotes the retained bit at scan position q, then

$$z_{\sigma(q)} = x_{\sigma(q)} \wedge \mathbf{1}\left[\sum_{r<q} z_{\sigma(r)} < 3\right].$$

The threshold predicate is maintained by three Boolean rails recording whether at least one, two, or three set bits have appeared; they are updated after each input. Before a scan, let A_h mean that at least h earlier input bits were one, for $h = 1, 2, 3$, with all three rails initially zero. For the next scanned bit x, first emit $z = x \wedge \neg A_3$; retain the old rails while emitting, in the order $h = 3, 2, 1$,

$$A_1' = A_1 \vee x, \qquad A_h' = A_h \vee (A_{h-1} \wedge x) \quad (h = 2, 3).$$

The canonical OR expansion above determines the individual gates. Thus only the first three set bits survive. After an output permutation and shift, the image is an affine copy of the radius-three Hamming ball

$$B_{12}(0, 3) = \{z \in \mathbb{F}_2^{12} : \mathrm{wt}(z) \le 3\}.$$

Every circuit output has weight at most three before hiding, while every word of weight at most three is unchanged by truncation when used as the input. Consequently

$$|\operatorname{Im} F| = \sum_{i=0}^{3} \binom{12}{i} = 1 + 12 + 66 + 220 = 299.$$

The threshold parameters are $t = 4$ and $k = 6$.

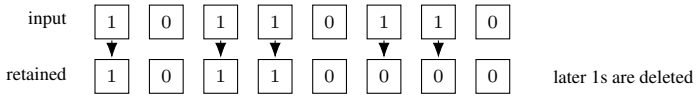

Figure 20: An illustrative scan for C2.4.3. The first three 1s in the hidden coordinate order are retained; the generated circuit has 12 coordinates.

C2.4.4 Separable nonlinear block encoding. A uniform permutation of the 12 inputs is sampled, and consecutive pairs in that order form six blocks (u_i, v_i), $1 \le i \le 6$. Each block is encoded by the injective nonlinear map

$$\gamma(u_i, v_i) = (u_i, v_i, u_i v_i).$$

Here $u_i v_i$ is multiplication in $\mathbb{F}_2$, implemented by an AND gate. The six three-bit codewords are concatenated with six zero coordinates to give 24 outputs, which are then permuted and shifted. Each block has four distinct images and the blocks vary independently, so

$$|\operatorname{Im} F| = 4^6 = 2^{12} = 4096.$$

Here $t = 8$ and $k = 10$. The product coordinate $u_i v_i$ makes the map non-affine, while the two systematic block coordinates preserve injectivity.

C2.4.5 Rank-at-most-one matrices over $\mathbb{F}_2$. A uniform permutation of the nine inputs is sampled; its first four entries, in order, form $u \in \mathbb{F}_2^4$, and its last five form $v \in \mathbb{F}_2^5$. The 20 logical outputs are the row-major entries of the outer-product matrix

$$M = uv^{\mathsf{T}}, \qquad M_{ij} = u_i v_j.$$

All pairs with $u = 0$ or $v = 0$ give the zero matrix. Every nonzero binary rank-one matrix determines a unique nonzero pair (u, v), since the only nonzero scalar in $\mathbb{F}_2$ is one. Therefore

$$|\operatorname{Im} F| = 1 + (2^4 - 1)(2^5 - 1) = 466.$$

The output entries are finally permuted and complemented; $t = 4$ and $k = 6$.

C2.4.6 Grid independent-set image. Let $Q = P_3 \square P_4$ be the 3×4 rectangular grid. One shuffled input bit y_v is assigned to every grid vertex by a uniform input permutation, and the vertices are processed in a second independent uniform permutation. Thus $m = n = 12$. When vertex v is reached, the circuit sets

$$z_v = y_v \wedge \bigwedge_{\substack{u \in N_Q(v) \\ u \text{ processed earlier}}} \neg z_u. \tag{15}$$

where $N_Q(v)$ is the set of grid neighbors and the conjunction is one when v has no earlier neighbor. The selected vertices $\{v : z_v = 1\}$ are always independent. Conversely, for any independent set I, choosing $y = \mathbf{1}_I$ and inducting over the processing order gives $z = \mathbf{1}_I$. The image before its final coordinate permutation and shift is therefore exactly the family of independent sets of Q. For the canonical netlist, grid vertices have row-major indices. At each scanned vertex, earlier neighbors are considered in the fixed order up, down, left, right; their already computed outputs are individually negated in that order and then conjoined with y_v from left to right.

Its cardinality is obtained by a column transfer. Let

$$\mathcal{M} = \{a \in \{0,1\}^3 : \text{no two consecutive coordinates of } a \text{ are one}\}$$

be the vertically independent column masks. With $D_1(a) = 1$ for every $a \in \mathcal{M}$, define, for $c = 1, 2, 3$,

$$D_{c+1}(b) = \sum_{\substack{a \in \mathcal{M} \\ \mathrm{supp}(a) \cap \mathrm{supp}(b) = \varnothing}} D_c(a).$$

Then $\sum_{b \in \mathcal{M}} D_4(b) = 227$. Hence $|\operatorname{Im} F| = 227$, $t = 3$, and $k = 5$.

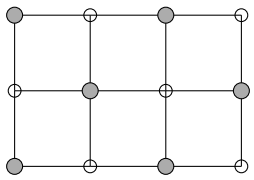

Figure 21: One independent set of the 3×4 grid in C2.4.6. No two shaded vertices share an edge; every such set occurs as a circuit output.

E.5 SHAMIR-STYLE TQBF INTERACTIVE PROOF

A true quantified Boolean formula (TQBF) is a Boolean circuit preceded by universal and existential quantifiers. A universal variable represents a choice for which both Boolean values must succeed, whereas an existential variable represents a response for which at least one value must succeed. This task asks Merlin to certify the truth of such a formula. The prover must supply the polynomial messages below; merely supplying an existential Boolean strategy is not accepted. Following Shamir's arithmetization of TQBF Shamir (1992), Merlin must maintain a sequence of low-degree polynomial claims, each fixed before Arthur samples the random point used to check it.

The public formula is

$$\Phi = Q_0 x_0\, Q_1 x_1 \cdots Q_{n-1} x_{n-1} : C(x_0, \ldots, x_{n-1}), \qquad Q_i \in \{\forall, \exists\}. \tag{16}$$

The circuit is acyclic and uses Boolean constants and the gates NOT, AND, OR, XOR, and ITE. Here $\mathrm{ITE}(c, a, b)$ returns a when $c = 0$ and b when $c = 1$. All protocol arithmetic is over the finite field

$$\mathbb{F}_p, \qquad p = 2^{61} - 1,$$

using the gate polynomials

$$\begin{array}{lll} \neg a = 1 - a, & a \wedge b = ab, & a \vee b = a + b - ab, \\ a \oplus b = a + b - 2ab, & \mathrm{ITE}(c, a, b) = (1 - c)a + cb. & \end{array} \tag{17}$$

These expressions agree with the Boolean gates on $\{0, 1\}$, but are also defined at Arthur's non-Boolean field challenges.

Let $\widehat{C} = P_n$ be the arithmetized circuit polynomial. For a polynomial f and a variable X_j, write $f_0 = f|_{X_j=0}$ and $f_1 = f|_{X_j=1}$, and define

$$\mathcal{A}_j(f) = f_0 f_1, \qquad \mathcal{E}_j(f) = f_0 + f_1 - f_0 f_1, \qquad \mathcal{R}_j(f) = (1 - X_j) f_0 + X_j f_1. \tag{18}$$

The first two operators arithmetize universal conjunction and existential disjunction. The third is the unique degree-one interpolation in X_j that preserves the two Boolean restrictions; it is called *multilinearization in* X_j. Eliminating variables from the inside out, for $i = n, n-1, \ldots, 1$ set

$$G_{i-1} = \begin{cases} \mathcal{A}_{i-1}(P_i), & Q_{i-1} = \forall, \\ \mathcal{E}_{i-1}(P_i), & Q_{i-1} = \exists, \end{cases} \qquad P_{i-1} = \mathcal{R}_0 \mathcal{R}_1 \cdots \mathcal{R}_{i-2}(G_{i-1}), \tag{19}$$

where the product of reduction operators is empty when $i = 1$. The operators are applied from right to left, so $\mathcal{R}_0$ is the outermost remaining operator and is checked first. On Boolean outer variables this recurrence is exactly quantified evaluation, so the formula is true precisely when the constant P_0 equals one. Every generated instance is promised to be true.

Merlin begins by claiming $P_0 = 1$. Arthur then traverses (19) from the outside toward the circuit. At stage i, the public round order is

$$\begin{array}{c|l} i = 1 & Q_0 X_0 \\ i = 2 & \mathcal{R}_0,\ Q_1 X_1 \\ i = 3 & \mathcal{R}_0,\ \mathcal{R}_1,\ Q_2 X_2 \\ \vdots & \vdots \\ i = n & \mathcal{R}_0, \ldots, \mathcal{R}_{n-2},\ Q_{n-1} X_{n-1}. \end{array} \tag{20}$$

Thus there are $R = n(n+1)/2$ polynomial rounds. At each stage, the true current multivariate polynomial is obtained by starting from G_{i-1}, retaining the reduction operators not yet checked in (20), and substituting every coordinate sampled in earlier rounds. The current claim v is its value after the remaining displayed operators are applied. If the next round concerns X_j, the honest continuation $h^*(T)$ is the restriction of that polynomial with $X_j = T$ and all earlier challenges fixed. Merlin submits exactly $d_q + 1$ coefficients of a univariate $h(T)$ in increasing-power order, including trailing zeros, where d_q is the announced degree bound. Arthur computes $h_0 = h(0)$ and $h_1 = h(1)$ and checks exactly one anchor equation:

$$\begin{array}{rcll} v & = & (1 - a_j)h_0 + a_j h_1, & \text{reduction round}, \\ v & = & h_0 h_1, & Q_j = \forall, \\ v & = & h_0 + h_1 - h_0 h_1, & Q_j = \exists. \end{array} \tag{21}$$

The verifier stores a field assignment vector $a = (a_0, \ldots, a_{n-1})$, initially all zero. At any round, a_j denotes the most recently sampled challenge assigned to X_j; before the first round that concerns X_j, its initial value is immaterial because the quantifier anchor does not use it. Each successful reduction or quantifier round for X_j refreshes this coordinate with the new challenge. Only after this equation holds does Arthur sample an independent uniform $r \in \mathbb{F}_p$, replace a_j by r, and replace the claim by $h(r)$. For all stages below the final circuit stage, reduction and quantifier rounds have degree bounds two and one, respectively. At the final stage, let Δ_j be the syntactic individual degree of the circuit output in X_j. Input X_j has degree vector e_j; constants have degree zero; NOT copies its input vector; AND, OR, and XOR add their two vectors. If the individual-degree vectors of the condition, zero branch, and one branch of an ITE are d_c, d_0, d_1, respectively, its syntactic vector is

$$d_{\mathrm{ITE}} = \max\{d_0,\ d_c + d_0,\ d_c + d_1\},$$

where addition and the maximum are coordinatewise. This is the envelope of the unreduced expression $(1 - c)a + cb$. The final-stage reduction bound for X_j is $2\Delta_j$, while the final quantifier bound is Δ_{n-1}. After the last challenge, Arthur directly evaluates the arithmetized public circuit at the accumulated field point and compares it with the final claim. A malformed message or failed equation terminates the one-shot interaction, whose total wall-clock budget is 600 seconds.

Lemma E.5 (Perfect completeness and statistical soundness)**.** *An honest Merlin is accepted with probability one on every generated instance. If Φ is false, the probability that any Merlin makes Arthur accept the initial claim one is at most*

$$\frac{D}{p}, \qquad D = \sum_{q=0}^{R-1} d_q, \tag{22}$$

where d_q is the public degree bound in round q. For the six generated profiles, the values of $(n, R, \max_q d_q, D)$ are

	C2.5.1	C2.5.2	C2.5.3	C2.5.4	C2.5.5	C2.5.6
n	18	24	24	44	44	44
R	171	300	300	990	990	990
$\max_q d_q$	2	2	2	6	10	10
D	324	576	576	2008	2060	2060

and hence the acceptance probability is less than 2^{-49}.

Proof. For perfect completeness, Merlin submits the actual univariate restriction of the appropriate polynomial in (19). Equations (18)–(21) then hold identically, and the last restriction evaluates to the public circuit polynomial.

For soundness, maintain the claim defined by the corresponding true polynomial at Arthur's accumulated point. Whenever Merlin passes an anchor while the submitted continuation differs from the true continuation, their difference is a nonzero univariate polynomial of degree at most d_q. It vanishes at the fresh challenge with probability at most d_q/p. Unless this happens, the false claim persists to a later round and is eventually contradicted by the direct circuit evaluation. A union bound over all rounds proves (22). □

The first three cases are compiled from finite-state branching programs. For a state set S, transition functions δ_i^0, δ_i^1, and terminal accepting set A, the generator constructs the ITE circuit backward from

$$F_{n,s} = \mathbf{1}[s \in A], \qquad F_{i,s} = \mathrm{ITE}\big(x_i, F_{i+1,\delta_i^0(s)}, F_{i+1,\delta_i^1(s)}\big), \tag{23}$$

and publishes F_{0,s_0}. Seed-derived double negations or conjunctions with one are appended as semantic padding. Specifically, 16 independent bits from the case-separated seeded stream choose, at each step, either $z \mapsto \neg\neg z$ or $z \mapsto z \wedge 1$. Constants and all state-layer ITE gates are emitted as distinct DAG nodes. This padding changes the circuit representation but not its Boolean or field polynomial.

C2.5.1 Width-four alternating response game. There are nine consecutive pairs $\forall u_i \exists e_i$, hence $n = 18$. The four states are *ready*, *remember 0*, *remember 1*, and an absorbing *reject* state; the initial state is ready. At a universal layer, ready moves to the selected remember state and every other state moves to reject. At an existential layer, remember 0 moves to ready on input zero and to reject on input one, while remember 1 does the reverse; ready and reject move to reject. Thus the universal choice u_i selects the corresponding remember state. The existential choice returns to ready exactly when $e_i = u_i$; the other choice enters reject. Only ready is terminally accepting, so $e_i = u_i$ for every pair is a winning strategy. The published circuit has 106 gates, 171 polynomial rounds, and maximum round degree two.

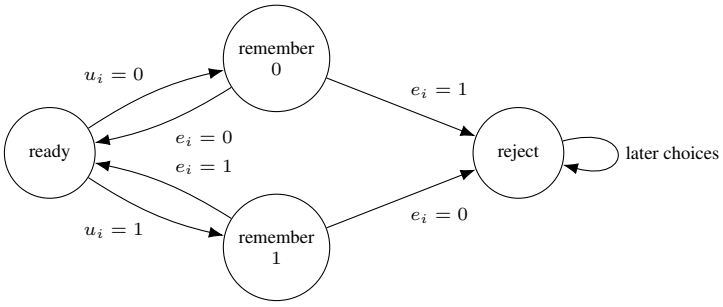

Figure 22: One universal–existential pair in C2.5.1. A matching response restores the ready state; a mismatch is irreversible.

C2.5.2 Memory-five recurrence response game. This case has twelve pairs $\forall u_i \exists e_i$ and $n = 24$. A state label $s \in \{0, \dots, 63\}$ encodes a five-bit register $m = s \bmod 32$ and a bit $b = \lfloor s/32 \rfloor$; there is also an absorbing sink $\perp$, giving 65 states. At the beginning of a universal layer the reachable labels have $b = 0$, initially $s = 0$. Reading u_i changes the label to $m + 32u_i$, thereby retaining both the old register and the pending universal bit. At the following existential layer, the unique non-sink response is

$$e_i = u_i \oplus \mathrm{parity}(m), \qquad m \leftarrow ((m \ll 1) \mid u_i) \bmod 32, \tag{24}$$

where $\mathrm{parity}(m)$ is the XOR of the five register bits; the register update occurs only after e_i has been checked. Any other response enters the sink, while all labels $0, \dots, 31$ are terminally accepting. The generated ITE circuit has 1,594 gates and 300 polynomial rounds; every round has degree at most two.

C2.5.3 Rank-five affine-syndrome game. The prefix consists of twelve universal bits followed by twelve existential bits. The running state, called the *syndrome*, is a vector $\sigma \in \mathbb{F}_2^5$ initialized to zero. The generator includes the five standard basis columns, uniformly permutes all 31 nonzero vectors of $\mathbb{F}_2^5$, and appends the first seven of that order to obtain $a_0, \dots, a_{11}$. When the current bit z_i equals one, the state updates as $\sigma \leftarrow \sigma \oplus a_i$; a zero leaves it unchanged. The existential block uses the same multiset in an independent uniform permutation $a_{\pi(0)}, \dots, a_{\pi(11)}$. Therefore, for every universal assignment x, choosing $y_j = x_{\pi(j)}$ adds the same syndrome a second time and returns it to zero, the sole accepting state. The public circuit has 802 gates, 300 polynomial rounds, and maximum round degree two.

The last three cases share a nonlinear relation on 21 universal bits x and 21 existential bits y. Independent uniform coordinate permutations divide both vectors into two matching blocks. Within a block of size k, write $a_i = x_{\pi_{\mathrm{in}}(i)}$ and $b_i = y_{\pi_{\mathrm{out}}(i)}$ for the permuted input and output coordinates. A single-tap block is defined by

$$\begin{aligned} T_0(a) &= \neg a_0, \\ T_1(a) &= \neg a_1 \oplus a_0, \\ T_i(a) &= \neg a_i \oplus (a_{i-1} a_{i-2}), \quad 2 \le i < k. \end{aligned} \tag{25}$$

A double-tap block additionally XORs $a_{i-3}a_{i-4}$ into T_i for every $i \ge 4$. In either form, $T_i(a) = \neg a_i \oplus g_i(a_0, \dots, a_{i-1})$; the inputs can therefore be recovered uniquely in order from $T(a)$. Each block map and their direct product are bijections on the Boolean cube.

Let $F(x, y)$ be the conjunction of the 21 coordinate equalities $b_i = T_i(a)$. Each equality is implemented as $\neg(b_i \oplus T_i(a))$. The indicators are uniformly permuted and combined by a balanced tree: consecutive pairs are conjoined, and an unpaired final entry is carried unchanged to the next level. Two final variables u, e give the public quantified wrapper

$$W(x, y, u, e) = \mathrm{ITE}\big(e, \mathrm{ITE}(u, F(x, y), 1), 0\big), \tag{26}$$

with prefix $\forall x\, \exists y\, \forall u\, \exists e$. Eliminating e returns $\mathrm{ITE}(u, F, 1)$ exactly, and eliminating u returns $F \cdot 1 = F$ exactly. Since every x has the unique response $y = T(x)$, the formula is true. Moreover, after the 21 universal bits are fixed, the 2^{21} assignments leave pairwise distinct residual predicates $\mathbf{1}[y = T(x)]$.

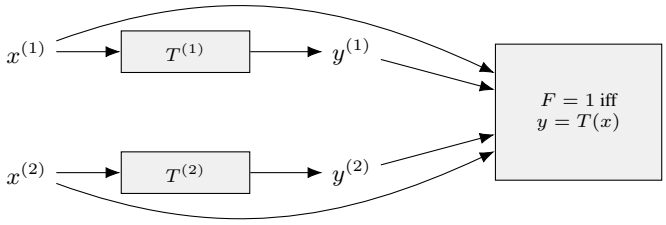

Figure 23: The two disjoint reversible components underlying C2.5.4–C2.5.6. The public coordinate permutations hide the displayed block order but do not change the relation.

C2.5.4 Hidden blocked reversible map. The two block sizes are 11 and 10, and both use the single-tap rule (25). The common coordinate-equality, aggregation, and wrapper conventions above are then applied. The resulting 44-variable circuit has 195 gates and 990 polynomial rounds. Its largest announced round degree is six.

C2.5.5 Double-tap blocked reversible map. The block sizes are 12 and 9. Both use the double-tap rule, so coordinates $i \geq 4$ contain the two quadratic terms $a_{i-1}a_{i-2}$ and $a_{i-3}a_{i-4}$. All other coordinate-equality, aggregation, wrapper, and padding conventions are those of C2.5.4. The public circuit has 234 gates and 990 polynomial rounds, with maximum round degree ten.

C2.5.6 Identity-cloaked double-tap reversible map. This case uses the same 12-and-9 block sizes and double-tap definition as C2.5.5, with independently generated coordinate orders. Before aggregation, each equality indicator z is wrapped once, using an independent uniform choice among the polynomial identities

$$z \mapsto \neg\neg z, \qquad z \mapsto z \wedge 1, \qquad z \mapsto z \vee 0, \qquad z \mapsto \mathrm{ITE}(c, z, z),$$

where the last template uses an independent uniform constant $c \in \{0, 1\}$. Every AND in the conjunction tree is replaced by $\mathrm{ITE}(a, 0, b) = ab$. These identities hold for all field inputs, not merely Boolean assignments. The public syntactic degree schedule uses the unsimplified gate-level recurrence stated above; for these constant-controlled or equal-branch templates it has the same maximum bounds reported below. The published circuit has 277 gates, 990 polynomial rounds, and maximum round degree ten.

E.6 HAMILTONICITY BIND–CHALLENGE–OPEN

The Hamiltonicity problem asks whether an undirected graph contains a cycle that visits every vertex exactly once. In this task the public graph is promised to be Hamiltonian, and Merlin must prove that it contains such a cycle without sending the cycle before Arthur chooses his challenge. Each lane of the protocol first binds Merlin to a relabeled graph. Arthur then asks Merlin to reveal either the relabeling or a Hamilton cycle in the committed graph. Running 24 parallel lanes with independent challenge bits gives a constant-round proof with two messages from Merlin and soundness error at most 2^{-24} on a non-Hamiltonian input. This is the standard bind–challenge–open pattern underlying classical interactive proofs for graph properties Goldreich et al. (1991); the present task uses the committed graphs as explicit public objects and makes no cryptographic hiding or zero-knowledge claim.

The generated instances satisfy the Hamiltonicity promise; the soundness statement below applies more generally when the same protocol is run on an arbitrary non-Hamiltonian input. Formally, the input is a simple undirected graph $G = ([n], E)$ with $n \geq 3$. A Hamilton cycle is a permutation

$$C = (v_0, v_1, \ldots, v_{n-1})$$

of $[n]$ such that $\{v_i, v_{i+1}\} \in E$ for every i, with indices taken modulo n. For a permutation $\pi \in S_n$, write $\pi(G)$ for the graph with edge set $\{\{\pi(u), \pi(v)\} : \{u, v\} \in E\}$.

The interaction is a three-message public-coin protocol with two prover messages, summarized in Figure 24. In the first message, "commit" means that Merlin sends complete encodings of all 24 graphs and Arthur records this immutable vector before sampling any challenge bit; it does not denote a cryptographic commitment.

1. Merlin atomically commits to 24 simple undirected graphs $H_0, \ldots, H_{23}$, each with vertex set $[n]$.
2. After all commitments have been recorded, Arthur samples independent uniform bits $c_0, \ldots, c_{23} \in \{0, 1\}$.
3. For every lane j, Merlin supplies one opening. If $c_j = 0$, the opening is a permutation π_j and Arthur verifies $H_j = \pi_j(G)$. If $c_j = 1$, the opening is a Hamilton cycle of H_j and Arthur checks that its vertices form a permutation of $[n]$ and that every consecutive pair is an edge.

Arthur accepts only if all 24 lanes pass. Every committed graph must have a canonical simple-graph encoding on $[n]$; a self-loop, repeated edge, out-of-range endpoint, malformed message, or failed check terminates the run with rejection. A 600-second wall-clock timer starts when Arthur loads the protocol runtime and includes both prover messages, verification, and the terminal response; expiration causes rejection.

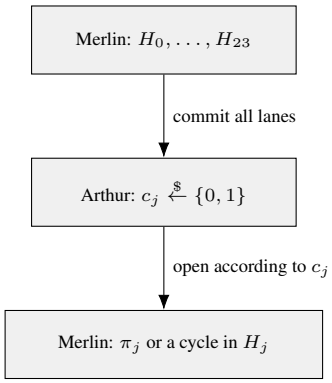

Figure 24: The order of messages in the Hamiltonicity protocol. The challenge bits are sampled only after the complete vector of committed graphs is fixed.

Lemma E.6 (Completeness and soundness)**.** *If G is Hamiltonian and Merlin knows a Hamilton cycle of G, the protocol has perfect completeness. If G is non-Hamiltonian, every prover is accepted with probability at most 2^{-24} over Arthur's challenge bits.*

Proof. For completeness, Merlin independently chooses permutations π_j, commits to $H_j = \pi_j(G)$, and answers a zero challenge with π_j and a one challenge with the relabeled known cycle $\pi_j(C)$. Both verification conditions then hold.

For soundness, condition on the prover's internal randomness and its complete first message before Arthur samples the challenges. If a particular H_j admits a valid zero-opening, then $H_j \cong G$ and is therefore non-Hamiltonian. It cannot also admit a valid one-opening. Thus at most one of the two values of c_j can be answered successfully in each lane. The 24 bits are independent and uniform, so the probability that all lanes receive answerable challenges is at most $(1/2)^{24}$. □

Every test-point generator first constructs a semantically labeled graph G_0 together with an explicit Hamilton cycle C_0 and checks the witness. All random choices are drawn from a domain-separated deterministic stream derived from the instance seed: bounded integers use rejection sampling, and permutations use Fisher–Yates shuffling. The generator finally samples a uniform permutation ρ of $[n]$ and publishes the graph whose edges are $\{\{\rho(u), \rho(v)\} : \{u, v\} \in E(G_0)\}$. This public relabeled graph is the sole instance supplied to Merlin and Arthur. Thus "semantic labels" below refer to the internal labels before this final relabeling; neither those labels nor the planted cycle is supplied to the prover or verifier.

The last five cases use the same reduction from a satisfiable CNF formula to an undirected Hamiltonian graph. Variables, clauses, and literals within a clause retain their generation order. If variable x_i has k_i occurrences, create its *occurrence row* $u_{i,0}, \ldots, u_{i,k_i}$. If its tth occurrence is in clause q_m, add both arcs between $u_{i,t}$ and $u_{i,t+1}$. A positive occurrence adds the directed detour

$$u_{i,t} \longrightarrow q_m \longrightarrow u_{i,t+1},$$

whereas a negative occurrence adds $u_{i,t+1} \to q_m \to u_{i,t}$. From each endpoint of row i add an arc to each endpoint of row $i + 1$. A source s has arcs to both endpoints of row zero, both endpoints of the last row have arcs to a sink t, and the arc $t \to s$ closes the traversal. A satisfying assignment traverses row i from left to right when x_i is true and from right to left otherwise. For each clause, its first satisfied literal in generation order is selected, and the traversal uses the corresponding detour to visit that clause vertex exactly once.

Finally, each vertex v of this directed graph is replaced by the undirected three-vertex chain

$$v_{\mathrm{in}} - v_{\mathrm{mid}} - v_{\mathrm{out}},$$

and every directed arc $u \to v$ is replaced by the undirected edge $\{u_{\mathrm{out}}, v_{\mathrm{in}}\}$. Expanding every vertex of the directed witness in the order $v_{\mathrm{in}}, v_{\mathrm{mid}}, v_{\mathrm{out}}$ gives the planted undirected Hamilton cycle. Conversely, the middle vertex has degree two, so any Hamilton cycle passes through every triple consecutively. If the CNF has V variables, M clauses, and L literal occurrences, the intermediate directed graph has

$$D = L + V + M + 2 \quad \text{vertices and} \quad A = 4L + 4(V - 1) + 5 \quad \text{arcs};$$

the undirected graph therefore has $3D$ vertices and $2D + A$ edges. Figure 25 shows the two local ingredients of the construction.

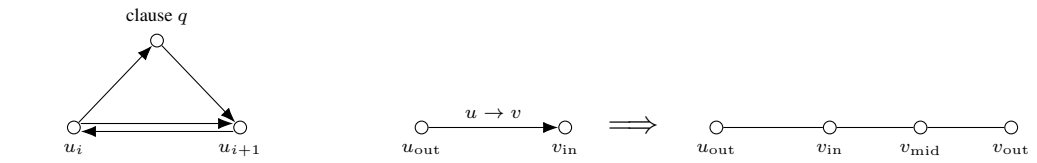

one position of a positive literal — the undirected forced triple for v

Figure 25: Local pieces of the common CNF construction. Left: a clause vertex can be inserted while traversing an occurrence in its satisfying direction. Right: replacing each directed vertex by a degree-two three-vertex chain preserves the directed order inside an undirected Hamilton cycle.

C2.6.1 Scaled randomly relabeled wheel. Before relabeling, the graph is the 1000-vertex wheel obtained from a cycle C_{999} by adding one universal hub. The hub has label zero, and the rim vertices $1, \ldots, 999$ occur in that cyclic order. Thus $n = 1000$, $|E| = 1998$, and $C_0 = (0, 1, \ldots, 999)$ is a Hamilton cycle.

C2.6.2 Scaled balanced complete bipartite graph. The semantic graph is $K_{128,128}$ with partite sets $A = \{0, \dots, 127\}$ and $B = \{128, \dots, 255\}$. Its edges are all pairs $\{i, 128 + j\}$ for $0 \le i, j < 128$. It has $n = 256$ and $|E| = 16{,}384$, and $C_0 = (0, 128, 1, 129, \dots, 127, 255)$ is a Hamilton cycle.

C2.6.3 Quiet-planted satisfiability lift. First sample 64 independent uniform Boolean values as the planted assignment. For each candidate clause, sample an ordered triple of distinct variable indices uniformly without replacement. Independently choose one of the four truth patterns

$$(1,1,1), \qquad (1,0,0), \qquad (0,1,0), \qquad (0,0,1)$$

uniformly, and set each literal's sign so that its value under the planted assignment is the corresponding bit. Clauses are identified canonically by sorting their signed literals by variable index; a duplicate is discarded and resampled until 272 distinct clauses have been retained. Thus every literal position has marginal truth probability $1/2$; this is the precise sense in which the planting has no one-position sign bias. Here $V = 64$, $M = 272$, and $L = 816$, so the common construction gives $D = 1{,}154$ directed vertices and an undirected graph with 3,462 vertices and 5,829 edges.

C2.6.4 Row- and column-permuted affine-parity lift. Start with the 80×80 binary cyclic matrix A whose row r has support

$$\{r, r+1, r+2\} \pmod{80}.$$

Its kernel is trivial: $z_r + z_{r+1} + z_{r+2} = 0$ for every r implies $z_r = z_{r+3}$, and $\gcd(3, 80) = 1$ then makes every coordinate equal, whence the equations force that common value to zero. Sample uniform planted values $z \in \mathbb{F}_2^{80}$. Next sample a uniform column permutation τ and then an independent uniform row permutation σ, and let equation i contain the three variables indexed by $\tau(\sigma(i)), \tau(\sigma(i)+1), \tau(\sigma(i)+2)$ modulo 80, written in increasing variable order. Set its right-hand side to the parity of these three coordinates of z. The permuted matrix remains full rank, so z is the unique solution.

For each equation, enumerate the eight local Boolean assignments in binary order. For each of the four assignments having the wrong parity, append the unique three-literal clause that is false on exactly that assignment. This gives $M = 320$ clauses and $L = 960$ literal occurrences. The common construction therefore has $D = 1{,}362$ directed vertices and produces an undirected graph with 4,086 vertices and 6,885 edges.

C2.6.5 Weak-signal planted satisfiability lift. Sample a uniform planted assignment on 40 variables. Each candidate clause uses an ordered uniform sample of three distinct variables. With probability $7/8$, choose a uniformly random two-element subset of its three literal positions to be true under the planted assignment; with probability $1/8$, choose a uniformly random singleton. Literal signs are set accordingly. After sorting signed literals by variable index, discard a duplicate clause and resample; stop after retaining 320 distinct clauses. Each literal position therefore has marginal truth probability $(7/8)(2/3) + (1/8)(1/3) = 5/8$; "weak-signal" refers only to this per-position bias. With $V = 40$, $M = 320$, and $L = 960$, the common construction has $D = 1{,}322$ directed vertices and yields an undirected graph with 3,966 vertices and 6,645 edges.

C2.6.6 Anchored equality/inequality ring lift. Sample a uniform planted assignment on variables $x_0, \dots, x_{159}$ and an independent uniform permutation σ of their indices. Regard $x_{\sigma(0)}, \dots, x_{\sigma(159)}$ as a cyclic order, including the pair from position 159 back to position zero. For neighboring variables x, y with equal planted values, append the pair of clauses

$$(\neg x \vee y) \wedge (x \vee \neg y)$$

enforces $x = y$; for unequal planted values,

$$(x \vee y) \wedge (\neg x \vee \neg y)$$

enforces $x \neq y$. Process the 160 adjacent pairs in cyclic order, giving 320 binary clauses, and then append the unit literal $x_{\sigma(0)}$ or $\neg x_{\sigma(0)}$ according to its planted value. The ring relations and this anchor determine the assignment uniquely. Here $V = 160$, $M = 321$, and $L = 641$, so the common construction forms $D = 1{,}124$ directed vertices and an undirected graph with 3,372 vertices and 5,453 edges.

C2.6.7 Chained-auxiliary affine Hamilton lift. Let A be the 23×23 binary cyclic matrix whose row r has support $\{r, r+1, r+2, r+3, r+4\} \pmod{23}$. This matrix is nonsingular: subtracting two consecutive homogeneous equations gives $z_r = z_{r+5}$; since $\gcd(5, 23) = 1$, all coordinates are equal, and a weight-five equation then forces their common value to zero. Independently sample uniform column and row permutations τ and σ, in that order. Equation i uses the ordered tuple

$$\big(\tau(\sigma(i)), \tau(\sigma(i)+1), \ldots, \tau(\sigma(i)+4)\big) \pmod{23}.$$

Next sample a uniform assignment to the 23 original variables and evaluate these rows on it to obtain the right-hand sides.

To encode one equation

$$x_a \oplus x_b \oplus x_c \oplus x_d \oplus x_e = r,$$

the generator introduces three fresh auxiliary variables, used only by that equation, and the chain

$$y_1 = x_a \oplus x_b, \qquad y_2 = y_1 \oplus x_c, \qquad y_3 = y_2 \oplus x_d, \qquad y_3 \oplus x_e = r.$$

For each ternary relation, enumerate the eight assignments to its three variables and append the four three-literal clauses that individually exclude the assignments violating the XOR equality. Encode the final binary equality or inequality analogously with the two clauses excluding its two incorrect assignments. Thus every equation contributes 14 clauses and 40 literal occurrences. Across all 23 equations this introduces 69 auxiliary variables, numbered consecutively in groups of three after the 23 original variables as the equations are processed. Hence $V = 92$, $M = 322$, and $L = 920$. The common construction has $D = 1{,}336$ directed vertices and yields an undirected graph with 4,008 vertices and 6,721 edges.

F TIER-3: REAL-WORLD TASKS

Tier-3 evaluates the production of standard, independently checkable evidence artifacts from three established verification ecosystems. Merlin submits a Lean proof, a Dafny program, or a DRAT proof log; Arthur invokes the corresponding pinned native checker on the exact digest-bound public instance. All three tasks are deterministic and one-shot. The names Arthur and Merlin therefore describe the separation between expensive evidence construction and comparatively direct verification, rather than an interactive Arthur–Merlin protocol in the complexity-theoretic sense. Every run has one 600-second wall-clock budget, including local computation, artifact upload, and Arthur's terminal check. Each task accepts exactly one raw artifact, not an archive: the Lean source is limited to 262,144 bytes, the Dafny source to 1,048,576 bytes, and the DRAT proof to 16,777,216 bytes.

F.1 MACHINE-CHECKED MATHEMATICS

Machine-Checked Mathematics asks Merlin to turn a finite mathematical certificate into a proof term accepted by Lean. The public instance contains a common prelude, a case-specific module `Challenge.lean`, their SHA-256 digests, and a structured copy of the instance data. The authoritative module defines transparent predicates `Challenge.valid : List Nat -> Prop` and the closed proposition `Challenge.MathematicalClaim : Prop`; the latter records instance-level well-formedness independently of the witness. The target is

$$\texttt{Challenge.Target} := \exists z : \texttt{List Nat},\ \texttt{Challenge.valid}(z) \wedge \texttt{Challenge.MathematicalClaim}.$$

Merlin submits one UTF-8 Lean source file whose only import is `Challenge` and which exports `AMBenchSolution.proof : Challenge.Target`. Arthur checks the source envelope and public hashes, compiles the public modules and submission with Lean 4.19.0, checks the declaration at the exact target type, and rejects any reported axiom dependency. After compiling the participant module, an Arthur-owned wrapper checks `example : Challenge.Target := AMBenchSolution.proof` and executes `#print axioms AMBenchSolution.proof`; acceptance requires Lean's report that this declaration does not depend on any axioms. Constructs that can bypass the intended kernel judgment, including `sorry`, additional axioms, unsafe or native evaluation, custom elaborators, host I/O, and additional imports, are forbidden. Lean's elaborator may construct the term, but acceptance rests on kernel type checking of the final proof de Moura & Ullrich (2021). The list z is embedded as the existential witness in that proof term; no separate certificate file is submitted.

The public Lean source is the canonical certificate specification. The descriptions below state the same relations mathematically. A little-endian radix-B word with digits $d_0, \ldots, d_{k-1}$ denotes $\sum_{j=0}^{k-1} d_j B^j$; a final partial word contains only its remaining digits. Matrices are serialized in row-major order, finite-field elements use their standard representatives in $[0, p)$, and a packed permutation lists $\pi(0), \pi(1), \ldots$ in that order. Bit i occupies bit $i \bmod w$ of word $\lfloor i/w \rfloor$. Conditions involving the witness form `valid`; closed identities involving only published constants form `MathematicalClaim`. The phrase "Lean checks" may refer to either part, whereas a stated generator invariant is not an additional acceptance condition unless explicitly identified as such. Random choices use a deterministic case-seeded SHA-256 stream; uniform and conditioned samples are taken over the stated finite sets. The generator constructs and verifies a private reference solution, which is not disclosed to Merlin.

Lemma F.1. *For every case below, Arthur accepts exactly when the submitted source obeys the source policy and the Lean 4.19.0 kernel derives an axiom-free term of the published type* `Challenge.Target`.

Proof. The Arthur-owned modules fix the transparent target and certificate predicate. The submitted declaration is checked at that exact type, the axiom audit excludes additional assumptions, and the public digests bind the judgment to the published instance. □

C3.1.1 Dense binary linear certificate. Set $n = 80$. Over $\mathbb{F}_2$, independently generate a unit lower-triangular matrix L and a unit upper-triangular matrix U, with every off-diagonal entry an

independent uniform bit. Form $A = LU$ and apply independent uniform row and column permutations, replacing A by $P_{\mathrm{row}} A P_{\mathrm{col}}$. Draw x by rejection from uniform bit vectors until $26 \le |x| \le 53$, define $S_i = \{j : A_{ij} = 1\}$, and publish these row supports together with $b = Ax$. A certificate is a list $z \in \{0,1\}^{80}$, and Lean checks

$$\sum_{j \in S_i} z_j \equiv b_i \pmod 2 \qquad (0 \le i < 80).$$

Both triangular factors are nonsingular, so the permutations preserve invertibility and the accepted vector is unique.

C3.1.2 Shuffled CRT reconstruction certificate. Set the search floor $F = 10^6$, window width $W = 200{,}000$, and $\Delta = \max\{2, \lfloor W/12 \rfloor\}$. Sample the initial cursor uniformly from $\{F, \dots, F + W - 1\}$. If m_i is the least prime not below the current cursor, update the cursor to $m_i + 1 + D_i$, where D_i is uniform on $\{0, \dots, \Delta - 1\}$; the cursor is not required to remain in the initial window. Repeat until twelve distinct primes have been obtained. Let $M = \prod_i m_i$ and sample $x \in [\lfloor M/3 \rfloor, \lfloor 2M/3 \rfloor]$ uniformly. The pairs (m_i, r_i), where $r_i = x \bmod m_i$, are uniformly shuffled and reindexed as $i = 0, \dots, 11$ before publication; M is also public. In this order, Merlin supplies

$$z = [x, q_0, \dots, q_{11}], \qquad q_i = (x - r_i)/m_i.$$

Lean checks $0 < x < M$, the list lengths, $M = \prod_i m_i$, and every identity $x = r_i + q_i m_i$. Primality, residue bounds, and pairwise coprimality are generator invariants rather than conjuncts of either target predicate. Under these stated generator invariants, the Chinese remainder theorem makes the accepted value unique in $[0, M)$; the Lean certificate itself establishes the published divisibility identities, not primality or coprimality.

C3.1.3 Hidden line-graph root certificate. For a graph X, its line graph $L(X)$ has one vertex per edge of X, with two vertices adjacent precisely when the corresponding edges meet. Construct a connected cubic bipartite graph R on two sets of 32 vertices as the union of three perfect matchings with cyclic shifts 0, 1, and a seed-selected $s \in \{2, \dots, 31\}$, sampled uniformly. Matching t joins left vertex i to right vertex $i + t \bmod 32$. Let $H = L(R)$ and publish a uniformly relabeled copy of $G = L(H)$. Thus H has 96 vertices and 192 edges, while G has 192 vertices, 576 edges, and degree six.

For each public vertex v of G, the certificate assigns a candidate root edge $\{a_v, b_v\}$ with $0 \le a_v < b_v < 96$. Encode $c_v = 96a_v + b_v$ and pack each consecutive group of eight codes as $w_j = \sum_{t=0}^{7} c_{8j+t}(96^2)^t$, producing 24 natural numbers. Lean checks all bounds, that every recovered root vertex occurs exactly four times, and that the two recovered pairs associated with the endpoints of every edge of G intersect. The 96 four-cliques formed by the stars of the four-regular graph H give a reference reconstruction. Since $96\binom{4}{2} = 576 = |E(G)|$, the checked local incidences account for every edge; pairwise distinctness and the disjointness of pairs assigned to nonadjacent vertices need not be separate predicates. Indeed, the recovered four-regular multigraph contributes exactly 576 endpoint-sharing incidences counted with multiplicity, while the 576 distinct public edges must all occur among them. A repeated recovered pair, a pair sharing both endpoints, or an additional intersection on a public nonedge would reduce the number of available distinct incidences below 576. Hence the checked containment and count imply that two public vertices are adjacent exactly when their recovered pairs intersect. This is the incidence form of line-graph inversion Whitney (1932).

C3.1.4 Anonymous affine-plane decoding certificate. Generate $AG(2, 19)$, containing 361 points and 380 lines of 19 points each, and independently relabel the points, the lines, and the order within each line. After shuffling, move one fixed horizontal reference line to the first serialized position; this identifies one otherwise arbitrary line but exposes neither an origin nor a coordinate parametrization. Its parallel class is, of course, recoverable from the published incidence relation as the set of lines disjoint from it. In hidden coordinates choose

$$f(X, Y) = \sum_{i+j \le 8} c_{ij} X^i Y^j$$

of total degree exactly eight. The coefficients are serialized by increasing Y-exponent $j = 0, \dots, 8$ and, for fixed j, increasing X-exponent $i = 0, \dots, 8 - j$. Choose two horizontal fibres uniformly

without replacement. Corrupt all 19 readings on those fibres; on each other fibre, choose two X-coordinates uniformly without replacement. Every selected reading receives an independent uniform error from $\mathbb{F}_{19}^*$. Thus the published value at public point P is $y_P = f(P) + e_P$, serialized by public point index, and the word contains exactly $2 \cdot 19 + 17 \cdot 2 = 72$ errors.

The certificate contains a coordinate code $x + 19y \in [0, 361)$ for every public point and an inverse table mapping each coordinate code back to its public point index, each packed 19 digits per base-361 word; it then contains the 45 triangularly ordered coefficients c_{ij} and the 361 error bits packed 19 per binary word. These four portions contain 19, 19, 45, and 19 natural numbers. Lean checks that the coordinate tables are inverse permutations, every published block becomes a complete affine line, the polynomial has exact total degree eight, and the weight-72 indicator marks exactly the disagreements. The evaluation code has distance $19(19-8) = 209$; since $2 \cdot 72 < 209$, the accepted evaluation word is unique within the stated radius MacWilliams & Sloane (1977).

C3.1.5 Anonymous modular column equivalence. Work over $\mathbb{F}_{1009}$. Select 80 points uniformly without replacement from $\mathbb{P}^1(\mathbb{F}_{1009})$ and map them by the quadratic Veronese embedding

$$(u : v) \longmapsto (v^2 : uv : u^2) \in \mathbb{P}^2(\mathbb{F}_{1009}).$$

For the right-hand configuration, apply pointwise a seed-derived element of $\mathrm{PGL}_2(\mathbb{F}_{1009})$ obtained by starting at I_2 and applying twelve elementary row operations. Each operation independently and uniformly chooses one of: swap two distinct uniform rows; add a uniform nonzero multiple of one row to another; or multiply one row by a uniform nonzero scalar. On each side, independently construct a 3×3 transformation from I_3 by eighteen operations with the same rule, apply independent uniform nonzero column scalings, and uniformly permute the columns. Publish the two full-row-rank matrices $L, R \in \mathbb{F}_{1009}^{3\times 80}$, omitting all canonical parameters and hiding maps.

Merlin supplies $A, A^{-1} \in \mathbb{F}_{1009}^{3\times 3}$, nonzero scales $s_0, \ldots, s_{79}$, a column permutation π, and its inverse. Each permutation is packed ten base-80 digits per word, so the complete certificate has $9 + 9 + 80 + 8 + 8 = 114$ natural numbers. Lean checks both matrix-inverse identities, all bounds, the permutation inverses, and

$$s_j(AL_{\bullet j})_r = R_{r,\pi(j)} \pmod{1009} \quad (0 \le j < 80,\ 0 \le r < 3).$$

An accepted certificate is therefore an exact monomial equivalence of the two anonymous projective column configurations.

C3.1.6 Composite cube-root certificate. Sample k uniformly from $[2^{127}, 2^{128})$. Starting from $k^3 + 17k + 29$ and $k^3 + 997k^2 + 19k + 43$, respectively, advance to the least integer not below the starting value and congruent to $5 \bmod 6$, then test candidates at increments of six until one passes the strong probable-prime screen for bases

$$2, 3, 5, 7, 11, 13, 17, 19, 23, 29, 31, 37, 41, 43, 47, 53, 59, 61, 67, 71, 73, 79, 83, 89;$$

Call the results p and q, and set $n = pq$. Let $W = \lceil \mathrm{bitlen}(n)/8 \rceil$. Encode p and q as their minimal big-endian byte strings, each preceded by its two-byte big-endian length. Append SHA-256 digests of a fixed domain separator, these two encoded factors, and four-byte big-endian counters $0, 1, \ldots$ until the material has at least $W + 16$ bytes. If H is the big-endian integer represented by the complete concatenation and $L = \lfloor n/3 \rfloor$, set

$$m = L + \big(H \bmod (n - L)\big).$$

Publish n, exponent 3, and $c = m^3 \bmod n$. The screen controls only the generated profile and is not trusted by the acceptance relation.

The certificate is $[p, q, m]$. Lean checks

$$1 < p < n, \quad 1 < q < n, \quad pq = n, \quad m < n, \quad m^3 \equiv c \pmod{n}.$$

Acceptance therefore certifies a nontrivial factorization and an exact modular cube root, irrespective of whether the factors are prime.

C3.1.7 Anonymous modular subset certificate. Let $h(\ell, i)$ be the big-endian integer represented by SHA-256 of a fixed family domain separator, label ℓ, and four-byte big-endian index i. Starting with $S_{-1} = 0$, set

$$s_i = S_{i-1} + 1 + \big(h(\texttt{increment}, i) \bmod 1024\big), \qquad S_i = S_{i-1} + s_i.$$

Thus $s_i > \sum_{j<i} s_j$. Set $M = S_{255} + 1 + (h(\texttt{modulus-gap}, 0) \bmod 2^{20})$. Direct evaluation with the generator's fixed domain separator gives $2^{265} \le M < 2^{266}$; this bit-length profile is not asserted as a consequence of superincreasingness alone. Starting from $2 + \big(h(\texttt{multiplier}, 0) \bmod (M-3)\big)$, scan cyclically through $\{2, \ldots, M-1\}$ and take the first value a with $\gcd(a, M) = 1$. The case seed selects a uniform permutation of the 256 residues $as_i \bmod M$ and a uniformly sampled 128-subset of their public positions. Publish the permuted weights b_i, M, and $t = \sum_i b_i x_i \bmod M$.

The first eight certificate words encode all 256 selection bits in 32-bit blocks; the next sixteen entries are

$$c_k = \sum_{i=16k}^{16k+15} b_i x_i \bmod M \qquad (0 \le k < 16).$$

Lean checks all bounds, recomputes every c_k, and requires their sum modulo M to equal t. The chunk residues split the exact dot-product check into sixteen bounded reductions; they do not add independent witness information. Hamming weight 128 is a generation property, not an acceptance condition. Superincreasingness makes hidden integer subset sums distinct and smaller than M, while multiplication by a is a bijection; hence the public modular relation has a unique bit-vector solution.

C3.1.8 Anonymous binary syndrome certificate. Use the primitive narrow-sense binary BCH code of length $2^9 - 1 = 511$ and designed distance 57 over $\mathbb{F}_{2^9} = \mathbb{F}_2[X]/(X^9 + X^4 + 1)$. Let α be the residue class of X, with polynomial-basis coefficients stored from low to high bit. For coordinate i, concatenate the 9-bit representations of

$$\alpha^i, \alpha^{3i}, \ldots, \alpha^{55i}$$

to form its canonical 252-bit column. The 28 odd syndromes suffice because binary Frobenius gives $S_{2j} = S_j^2$. For operation index $r = 0, \ldots, 3023$, let

$$H_\ell(r) = \mathrm{int}_{\mathrm{be}}\big(\mathrm{SHA256}(D \parallel \ell \parallel \mathrm{be}_8(r))\big),$$

where D is a fixed case-specific ASCII domain separator, defined by the released generator and followed by one zero byte, and $\mathrm{be}_k(r)$ is the k-byte big-endian encoding of r. The label satisfies $\ell \in \{\texttt{row-left}, \texttt{row-right}, \texttt{row-kind}\}$. Set $i_r = H_{\texttt{row-left}}(r) \bmod 252$. Reduce $H_{\texttt{row-right}}(r)$ modulo 251 and increment the result when it is at least i_r, thereby obtaining the distinct source row j_r. Swap rows i_r, j_r exactly when $H_{\texttt{row-kind}}(r) \equiv 0 \pmod 8$; otherwise XOR row j_r into row i_r. Apply these operations in increasing r. The fixed column permutation sorts coordinate i by $\mathrm{SHA256}(D \parallel \texttt{column-order} \parallel \mathrm{be}_4(i))$, breaking ties by i. The case-seeded generator stream then selects a uniform 28-subset of canonical coordinates. Publish the transformed columns in this public order and the transformed XOR syndrome. Every column and the syndrome are stored as eight little-endian 32-bit words, with the unused top four bits zero.

Merlin's first sixteen words encode the 511 error bits, with 31 active bits in the last word and its unused top bit required to be zero; sixteen further entries give the corresponding population counts (popcounts). Lean checks these bounds and counts, total weight 28, and all 252 parity equations. The count entries support word-by-word checking and carry no independent witness information. Two accepted vectors would differ by a nonzero codeword of weight at most 56, contradicting the BCH distance bound, so the accepted error vector is unique MacWilliams & Sloane (1977).

F.2 Dafny-Verified Programs

Dafny-Verified Programs asks Merlin to implement a small software component. Preconditions delimit legal calls; postconditions use side-effect-free specification functions and predicates to characterize the required outputs. The public instance contains a module `Challenge`, which declares the data types and an abstract `Candidate` trait with its contracts, and a module `ArthurHarness`,

which executes deterministic case-seeded examples. Merlin submits one UTF-8 file defining exactly one module `Solution`, importing only `Challenge`, and providing a concrete class `Candidate` that extends the public trait and implements every abstract method.

Arthur first rejects any source that violates the policy below. It then concatenates the three modules, invokes Dafny 4.11.0 with its bundled Z3 backend to verify all proof obligations, compiles the same verified program to Java, and runs the fixed harness. Acceptance requires policy compliance, zero verification errors and exactly one case-specific success marker. The harness constructs the submission through the public trait type, so the inherited contract remains an obligation of every concrete override. Assumptions, axioms, external implementations, verification-altering attributes, wildcard termination, additional includes, I/O, and a participant-defined main method are forbidden. The accepted artifact is checked by the standard Dafny verification pipeline Leino (2010).

Arthur verifies `Combined.dfy` with a 120-second verification limit, two verifier cores, warnings treated as errors, and Dafny's determinism enforcement enabled. Arthur then invokes the Java backend on the unchanged file with verification disabled, because that same source has already passed the preceding verifier call, and gives the execution subprocess a separate 120-second limit; warnings are again treated as errors. The evaluator-provided Java runtime executes only the generated harness; Dafny and its bundled Z3 discharge the proof obligations.

The API and its quantified specification are fixed for each case. A deterministic SHA-256 counter stream only changes the concrete values embedded in `ArthurHarness`; these examples bind executable behavior but do not replace verification of the universal contracts. In particular, changing the case seed changes the runtime replay but not the method signature, contract, or universal proof obligation. Integers sampled from a stated interval are independent and uniform unless a later conditioning rule is given.

Lemma F.2. *If Arthur accepts a Dafny submission, every implemented method satisfies the public inherited contract under Dafny's verification semantics, and the verified Java program produces the required outputs on the digest-bound harness instance.*

Proof. The public trait fixes the method signatures and contracts used at every call site. Dafny verifies the concrete overrides against those inherited obligations before compilation. Arthur then executes the same merged source and accepts only the unique expected marker, while the source policy excludes constructs that would replace a proof obligation by an assumption or external implementation. □

C3.2.1 Stable partition preservation. For an integer sequence a, let $N(a)$ be its negative entries in original order and $P(a)$ its nonnegative entries in original order. The required method returns exactly

$$\mathrm{StablePartition}(a) = N(a) \parallel P(a),$$

where $\parallel$ denotes sequence concatenation. The public module defines N and P recursively on the head and tail of the sequence. They are ordinary public Dafny functions and may be called by the submitted implementation; the acceptance relation does not prescribe a particular implementation strategy. Equality to this specification fixes both membership and relative order. The harness independently samples twelve integers from $[-20, 20]$ and compares the executable output with the two stable subsequences. Verification must establish the equality for every finite input sequence; equality of multisets alone is insufficient.

C3.2.2 Boundary-safe lower-bound search. For a nondecreasing sequence a and key k, the method returns an index $r \in [0, |a|]$ satisfying

$$\forall i\,(0 \le i < r \implies a_i < k), \qquad \forall i\,(r \le i < |a| \implies k \le a_i).$$

These two quantified conditions also cover the boundary answers 0 and $|a|$. The harness samples eighteen integers from $[-30, 30]$, sorts them, samples k from $[-25, 25]$, and compares the result with the first index whose entry is at least k, or 18 if no such entry exists.

C3.2.3 Capacity-constrained reservation update. Let $C \ge 0$, let u satisfy $0 \le u_i \le C$ for every $0 \le i < |u|$, and let $d \ge 0$. The returned Boolean $accepted$ must satisfy

$$accepted \quad \iff \quad \forall i\,(0 \le i < |u| \implies u_i + d \le C).$$

If accepted, the returned sequence has entries $u_i + d$; otherwise it is exactly the original sequence. Hence no partial update is permitted. The harness samples $C \in [12, 24]$, ten entries independently from $[0, C - 3]$, and $d \in [1, 5]$, then computes both expected outputs from the displayed relation.

C3.2.4 Precedence-constrained earliest schedule. For any equal-length sequences d and p, the legal-input predicate requires $d_i > 0$ and either $p_i = -1$ or $0 \le p_i < i$ for every index i. The output has $|s| = |d|$ and is the unique sequence

$$s_i = \begin{cases} 0, & p_i = -1, \\ s_{p_i} + d_{p_i}, & 0 \le p_i < i. \end{cases}$$

for all $0 \le i < |d|$. For the harness, sample fourteen durations $d_0, \ldots, d_{13}$ independently from $[1, 9]$. Set $p_0 = -1$; for each $i = 1, \ldots, 13$, set $p_i = -1$ with probability $1/4$ and otherwise sample p_i uniformly from $\{0, \ldots, i - 1\}$. The strict index condition makes the predecessor relation acyclic in the published order; the contract is therefore earliest-start propagation on a parent forest.

C3.2.5 Dependency-order validation. The public specification defines a recursive $\mathrm{Position}(\pi, v)$ and requires the input order π to be a duplicate-free permutation of $\{0, \ldots, n - 1\}$; every edge endpoint must also lie in this range. The method returns true exactly when

$$\mathrm{Position}(\pi, u) < \mathrm{Position}(\pi, v) \qquad \text{for every published edge } (u, v).$$

For the harness, set $n = 10$ and $\pi = (0, 1, \ldots, 9)$. For each $v = 1, \ldots, 9$, add one edge (u, v) with u uniform in $\{0, \ldots, v-1\}$. When $v > 2$, independently with probability $1/2$, draw another source u' uniformly from the same set and append (u', v); the two edges may coincide. The resulting example is topologically ordered, while the fixed runtime harness therefore exercises the true branch. The verified method must nevertheless return the correct Boolean for every well-formed order and edge sequence, including sequences with backward edges, for which the result is false.

C3.2.6 Audited priority-firewall batch evaluation. This case uses an abstract first-match rule table: a packet is already encoded as a Boolean vector recording which rules match it. For an arbitrary action sequence and a packet matrix whose rows all have the same width as that sequence, the contract applies the ordered first-match rule to every row and audits the resulting decisions. In the harness there are sixteen ordered rules, each action being independently true with probability $1/2$, and eleven packets represented by sixteen-bit match rows. Before conditioning, each match bit is independently true with probability $1/7$; the first row is then forced to all false, and each later all-false row is repaired by setting one uniform position true. For packet p, the decision is $(-1, \mathrm{false})$ when no rule matches and otherwise records the least matching index j and action a_j. In addition to all eleven decisions, the method returns a sixteen-entry audit vector

$$h_j = |\{p : 0 \le p < |\mathit{decisions}|, \text{ decision } p \text{ uses rule } j\}|.$$

The public recursive function `CountPrefix` defines these counts from the decision sequence, coupling the functional result and its audit log.

C3.2.7 Reference-counted handle-table preservation. A state consists of an $m \times r$ Boolean matrix R and counts c_j. It is valid exactly when every row has width r and

$$c_j = |\{i : R_{ij} = \mathrm{true}\}| \qquad (0 \le j < r).$$

Calls require $0 \le i < m$ and $0 \le j < r$. Acquiring an unheld pair (i, j) changes only R_{ij} to true; acquiring an already held pair is rejected without changing the state. Releasing a held pair changes only R_{ij} to false, whereas releasing an unheld pair is rejected unchanged. Every accepted update must re-establish the complete count invariant. The harness uses $m = 8, r = 10$ and samples each matrix entry true with probability $1/4$. It then selects an acquire cell uniformly from all mr cells, forces that cell false, and computes the initial counts from the resulting matrix. After the acquire, it releases the first true cell in row-major order. Expected matrices and column counts are recomputed after each exact update.

C3.2.8 Free-list memory-pool preservation. A pool state is (C, f, O), where $C \geq 0$, f is a duplicate-free sequence of free block IDs and O is the set of owned IDs. Every ID lies in $[0, C)$ and

$$b \in O \quad \Longleftrightarrow \quad b \notin f \qquad (0 \leq b < C).$$

Allocation returns an acceptance flag, a block integer, and a next state. If f is empty it rejects and preserves the state; the block result is unconstrained by the public contract, and Arthur makes no rejected-branch comparison involving that field. Otherwise it accepts, returns f_0, removes that entry, and adds the block to O. Release is legal only under the precondition $b \in O$; it removes b from O and prepends it to f. The harness fixes $C = 6$, $f = [0, 1, 2]$, and $O = \{3, 4, 5\}$, allocates block zero, and then releases a uniformly selected block from $\{3, 4, 5\}$. Both operations must preserve the quantified partition invariant, not merely return the harness values.

F.3 DRAT-Certified Bounded Hardware Safety

This task asks Merlin to certify that a sequential Boolean circuit cannot reach its designated bad output within a public time horizon. The circuit is published as a standard sequential ASCII AIGER file: its combinational network uses literals, two-input AND gates, and complemented edges, while latches carry state between frames Biere (2007). It has exactly one ordinary AIGER output, named `bad`, and no other output or property section. For horizon H, the public bounded-model-checking formula is

$$F_H = \mathrm{Init}(s_0) \wedge \bigwedge_{t=0}^{H-1} \mathrm{Trans}(s_t, i_t, s_{t+1}) \wedge \bigvee_{t=0}^{H} \mathrm{Bad}(s_t, i_t).$$

Thus the unrolling contains $H + 1$ independently unconstrained input vectors $i_0, \ldots, i_H$; the final vector is used only if the bad output depends combinationally on an input. All eight circuits are safe, so F_H is unsatisfiable. Merlin submits one standard ASCII or binary DRAT proof. Arthur writes the digest-bound public DIMACS and the submitted proof into a fresh directory and accepts only when a pinned `drat-trim` executable at commit `2e3b2dc0ecf938addbd779d42877b6ed69d9a985` derives the empty clause. The SAT solver used to discover a proof is not part of the trusted boundary Wetzler et al. (2014).

The submitted proof is a nonempty, uncompressed byte string of at most 16,777,216 bytes. Arthur imposes no separate line-count or proof-step limit and does not pre-parse the artifact as text: the same raw bytes are passed to `drat-trim`, which recognizes standard ASCII and binary DRAT and supports ordinary deletion records. In the fresh directory Arthur runs `drat-trim bound.cnf proof.drat -w` with a 180-second subprocess timeout. The terminal check accepts exactly when the process exits with code zero and its combined output contains `s VERIFIED`. This checker call runs inside the task-wide envelope of two CPU cores, 2,048 MiB of memory, and 2,048 MiB of disk.

The DIMACS file is produced by one fixed compiler. If M is the greatest AIG variable index, write $x_{t,v}$ for DIMACS variable $tM + v$ and map an AIGER literal ℓ by

$$L_t(0) = \bot, \qquad L_t(1) = \top, \qquad L_t(2v) = x_{t,v}, \qquad L_t(2v+1) = \neg x_{t,v}.$$

Every latch has a specified initial value in $\{0, 1\}$. For every AIGER AND whose output and input literals are z, a, b, respectively, and every frame $0 \leq t \leq H$, the compiler adds

$$(\neg L_t(z) \vee L_t(a)), \qquad (\neg L_t(z) \vee L_t(b)), \qquad (L_t(z) \vee \neg L_t(a) \vee \neg L_t(b)).$$

For every latch equation $q' = e$ and $t < H$, it adds the two clauses for $L_{t+1}(q) \leftrightarrow L_t(e)$; frame zero receives one unit clause per initial latch. Finally, one clause contains $L_t(bad)$ for every frame. During emission, a clause containing $\top$ or a complementary literal pair is omitted, $\bot$ and repeated literals are deleted, and no other simplification or variable reindexing is performed. Hence the DIMACS header declares $(H + 1)M$ variables, including unused frame copies.

The public instance binds both the AIGER and DIMACS bytes by SHA-256 and publishes the exact variable and clause counts. To sample a parameter below B, the generator hashes a fixed domain separator, the case seed, and an eight-byte big-endian counter. A 256-bit digest is accepted only below the largest multiple of B smaller than 2^{256}, and its residue modulo B is returned; otherwise the counter advances and sampling repeats.

Lemma F.3 (Bounded-safety meaning of an accepted proof)**.** *Assuming the correctness of the AIGER parser and fixed compiler, the SHA-256 bindings, and the pinned DRAT checker, an accepted artifact proves that the published AIGER circuit has no initialized trace of length at most H whose bad output is true.*

Proof. The literal map preserves constants and complementation. A topological induction over the AND gates in each frame shows that their three Tseitin clauses reproduce the combinational AIG semantics, and the two latch clauses reproduce each next-state equation. Induction over frames then gives a correspondence between satisfying assignments of F_H and initialized AIG traces reaching bad by frame H. An accepted DRAT derivation proves the digest-bound DIMACS formula unsatisfiable, excluding every such trace. □

C3.3.1 FIFO occupancy safety. Sample the FIFO depth D uniformly from $\{4, 5\}$ and the horizon H from $\{20, 21, 22, 23\}$. Latches $o_0, \ldots, o_{D-1}$ initially equal zero and encode occupancy k as the unary prefix $1^k 0^{D-k}$. With public inputs $p = push$ and $r = pop$, define

$$P = p \wedge \neg r \wedge \neg o_{D-1}, \qquad R = r \wedge \neg p \wedge o_0.$$

If P holds, set $o'_0 = 1$ and $o'_j = o_{j-1}$ for $j > 0$; if R holds, set $o'_j = o_{j+1}$ for $j < D - 1$ and $o'_{D-1} = 0$; otherwise hold every latch. The simultaneous request $p = r = 1$ therefore leaves the abstract occupancy unchanged. The bad output is

$$\bigvee_{j=1}^{D-1} (o_j \wedge \neg o_{j-1}).$$

Both shifts preserve the prefix form, so the initialized circuit never raises bad.

C3.3.2 FIFO underflow safety. Use the same unary FIFO transition with independent parameters D and H sampled uniformly from $\{10, 11, 12\}$ and $\{28, 29, 30, 31, 32\}$, respectively. The controller's firing signal and bad output are

$$pop_fire = pop \wedge o_0, \qquad bad = pop_fire \wedge \neg o_0.$$

Here pop_fire is the controller guard, rather than the pop-only state-update enable R; a simultaneous push and pop may therefore raise the guard while leaving the occupancy unchanged. The guard includes o_0, so the bad expression is identically false.

C3.3.3 Round-robin mutual exclusion. Sample N and H uniformly from $\{6, 7\}$ and $\{20, 21, 22\}$, respectively. The token latches are initialized to $(1, 0, \ldots, 0)$. With public requests r_j and an unconstrained input $a = advance$, set

$$t'_j = \begin{cases} t_{(j-1) \bmod N}, & a = 1, \\ t_j, & a = 0, \end{cases} \qquad g_j = r_j \wedge t_j.$$

The bad output is $\bigvee_{j<k}(g_j \wedge g_k)$. Rotation and hold both preserve the one-hot token invariant, hence at most one grant can be true in every frame.

C3.3.4 Round-robin bounded fairness. Sample N and H uniformly from $\{7, 8\}$ and $\{22, 23, 24\}$, respectively, and use the same one-hot token, requests, grants, and nondeterministic advance input as in C3.3.3. Introduce N zero-initialized wait latches and define

$$c = r_0 \wedge a \wedge \neg g_0, \qquad w'_0 = c, \qquad w'_j = c \wedge w_{j-1}\ (1 \le j < N), \qquad bad = c \wedge w_{N-1}.$$

The wait vector records consecutive clock frames in which c has remained true, so bad would require $N + 1$ such frames. In fact, no run of N consecutive c-frames exists: each one advances the one-hot token, which must visit client zero within N advances and then makes g_0 true. This monitor concerns consecutive active clock frames; it does not impose progress across idle frames or assert an unbounded fairness condition.

C3.3.5 Credit-router conservation. Sample capacity C and horizon H uniformly from $\{6, 7\}$ and $\{22, 23, 24\}$, respectively. Two unary vectors $c_0, \ldots, c_{C-1}$ and $f_0, \ldots, f_{C-1}$ represent available credits and in-flight flits: with k flits in flight, they have forms $c = 1^{C-k}0^k$ and $f = 1^k 0^{C-k}$. Initially $c_j = 1$ and $f_j = 0$. Define

$$S = send \wedge c_0, \qquad R = credit_return \wedge f_0, \qquad S_o = S \wedge \neg R, \quad R_o = R \wedge \neg S.$$

On S_o, set $c'_j = c_{j+1}$ for $j < C-1$, $c'_{C-1} = 0$, $f'_0 = 1$, and $f'_j = f_{j-1}$ for $j > 0$. On R_o, set $c'_0 = 1$, $c'_j = c_{j-1}$ for $j > 0$, $f'_j = f_{j+1}$ for $j < C-1$, and $f'_{C-1} = 0$; otherwise hold both vectors. In particular, when both S and R are true, the two events cancel and the state is held. The bad output is

$$\bigvee_{j=0}^{C-1} \big(c_j \oplus \neg f_{C-1-j}\big).$$

The complementary mirror relation $c_j = \neg f_{C-1-j}$ holds initially and is preserved by every branch, expressing exact credit conservation.

C3.3.6 Credit-router forwarding safety. Sample C and H uniformly from $\{12, 13, 14\}$ and $\{36, 37, 38, 39, 40\}$, respectively. Construct two disjoint latch families implementing the credit/flight tracker from C3.3.5, named actual and shadow, with identical initial values and driven by the same *send* and *credit-return* inputs. Let

$$\begin{aligned} \mathit{actual_forward} &= \mathit{send} \wedge c_0^{\mathrm{actual}}, \\ \mathit{shadow_forward} &= \mathit{send} \wedge c_0^{\mathrm{shadow}}, \\ \mathit{bad} &= \mathit{shadow_forward} \wedge \neg \mathit{actual_forward} = \mathit{shadow_forward} \wedge \neg c_0^{\mathrm{actual}}. \end{aligned}$$

Thus bad is the one-directional mismatch in which the shadow tracker permits forwarding but the actual tracker does not. The two latch families obey identical deterministic recurrences, so equality of corresponding latches is inductive and excludes this mismatch.

C3.3.7 Pipeline flush-stall safety. Sample the number of stages S and horizon H uniformly from $\{9, 10, 11\}$ and $\{30, 31, 32, 33, 34\}$, respectively. The circuit has valid latches v_j, a pending-flush latch p, and an S-bit progress register w_j, all initialized to zero, with inputs *issue*, *stall*, and *flush*. Write

$$a = p \vee \mathit{flush}, \qquad d = a \wedge \neg \mathit{stall}, \qquad q = w_{S-1}.$$

The pending latch uses set-dominant priority,

$$p' = \begin{cases} 1, & \mathit{flush}, \\ 0, & \neg \mathit{flush} \wedge q, \\ p, & \text{otherwise}. \end{cases}$$

The valid latches obey

$$v'_j = \begin{cases} v_j, & \mathit{stall}, \\ \mathit{issue} \wedge \neg a, & \neg \mathit{stall} \wedge j = 0, \\ v_{j-1}, & \neg \mathit{stall} \wedge j > 0. \end{cases}$$

Thus no new valid entry is inserted while a flush is active. The progress recurrence uses $\sigma_0 = 1$ and $\sigma_j = w_{j-1}$ for $1 \le j < S$, and is

$$w'_j = \begin{cases} [j = 0], & \mathit{flush} \wedge \neg \mathit{stall}, \\ 0, & \mathit{flush} \wedge \mathit{stall}, \\ \sigma_j, & \neg \mathit{flush} \wedge d, \\ w_j, & \neg \mathit{flush} \wedge \neg d \wedge p, \\ 0, & \text{otherwise}, \end{cases}$$

where $[j = 0]$ denotes the Boolean indicator of $j = 0$. The bad output is $q \wedge \bigvee_j v_j$. Whenever q is true, the active flush has accumulated S nonstalling shifts since the progress register was reset; no valid entry was inserted during those shifts, so the pipeline is empty.

C3.3.8 Pipeline writeback consistency. Sample S and H uniformly from $\{14, 15, 16\}$ and $\{44, 45, 46, 47, 48\}$, respectively. Three zero-initialized length-S pipelines store valid bits v_j, one-bit tags t_j, and independently represented one-bit shadow tags $\widehat{t}_j$. The control priority is: flush first, stall second, and shift otherwise. A flush sets all three next-state vectors to zero, a stall holds them, and a shift sets

$$v'_0 = \mathit{issue}, \qquad t'_0 = \widehat{t}'_0 = \mathit{input_tag}, \qquad v'_j = v_{j-1}, \quad t'_j = t_{j-1}, \quad \widehat{t}'_j = \widehat{t}_{j-1} \quad (1 \le j < S).$$

The bad output is $v_{S-1} \wedge (t_{S-1} \oplus \widehat{t}_{S-1})$. Corresponding tag and shadow latches are equal initially and receive equal updates in every control branch, so an enabled writeback cannot contain mismatched tags.

G TOOL USE AND PROBLEM COMPLEXITY

G.1 AUXILIARY POLYNOMIAL-TIME TASKS

The auxiliary Tier-0 contains 18 cases: the six Max-Flow / Min-Cut cases from C1.1, six 2-SAT cases, and six bipartite minimum vertex-cover cases. The latter two tasks correspond to restricted forms of the satisfiability and set-cover problems in Tier-1. They use a single deterministic certificate submission. We give their task-level definitions below; no additional case-specific construction is introduced here.

G.1.1 MAX-FLOW / MIN-CUT

The public input is a capacitated directed multigraph $G = (V, E)$, nonnegative integer capacities $(c_e)_{e\in E}$ and distinct terminals s, t. Parallel edge occurrences have distinct identifiers. Merlin submits a flow $(f_e)_{e\in E}$, its claimed value F, and a source-side cut $S \subseteq V$. Arthur checks $s \in S$, $t \notin S$, capacity constraints $0 \le f_e \le c_e$, conservation at every nonterminal vertex, and

$$\sum_{e:u_e=s} f_e - \sum_{e:v_e=s} f_e = F = \sum_{e:v_e=t} f_e - \sum_{e:u_e=t} f_e = \sum_{e:u_e\in S,\, v_e\notin S} c_e.$$

Feasibility gives a lower bound and the cut gives the same upper bound, so acceptance certifies both a maximum flow and a minimum cut. The task and six cases are the same as C1.1.

G.1.2 2-SAT

The public instance is a Boolean formula in 2-CNF,

$$\varphi(x_1, \dots, x_n) = \bigwedge_{j=1}^{m} C_j, \qquad C_j = \ell_{j,1} \vee \ell_{j,2}, \qquad \ell_{j,k} \in \{x_i, \neg x_i : i \in [n]\}.$$

Every clause contains exactly two literal entries. The task is a decision problem rather than a weighted optimization problem: all clauses are hard and there are no soft-clause weights.

Let $D_\varphi = (V_\varphi, A_\varphi)$ denote the implication graph, where $V_\varphi = \{x_i, \neg x_i : i \in [n]\}$ and each clause $\ell_{j,1} \vee \ell_{j,2}$ contributes the two arcs $\overline{\ell_{j,1}} \longrightarrow \ell_{j,2}, \overline{\ell_{j,2}} \longrightarrow \ell_{j,1}$. Here $\overline{\ell}$ denotes the complementary literal. Write $\mathsf{Path}_{D_\varphi}(u, v)$ for the set of directed paths from u to v in this graph.

Merlin submits one of two tagged certificates. A SAT certificate contains a complete Boolean assignment $a \in \{0,1\}^n$. An UNSAT certificate contains an index $i \in [n]$ and two explicit implication paths P^+ and P^-. Arthur accepts exactly when

$$\big[\pi = (\mathsf{SAT}, a) \ \wedge\ a \in \{0,1\}^n \ \wedge\ \bigwedge_{j=1}^{m} C_j(a) = 1\big]$$
$$\vee\ \big[\pi = (\mathsf{UNSAT}, i, P^+, P^-) \ \wedge\ i \in [n] \ \wedge\ P^+ \in \mathsf{Path}_{D_\varphi}(x_i, \neg x_i) \ \wedge\ P^- \in \mathsf{Path}_{D_\varphi}(\neg x_i, x_i)\big].$$

For a SAT certificate, the verifier evaluates every public clause directly. For an UNSAT certificate, it checks the endpoints of both paths and verifies that every consecutive pair of literals is an implication induced by a public clause. The two paths place x_i and $\neg x_i$ in the same strongly connected component and therefore certify unsatisfiability. Conversely, every unsatisfiable 2-CNF formula has such a complementary pair.

The current generator supplies both kinds of instances: four of the six case profiles are satisfiable and two are unsatisfiable. A certificate can be constructed in polynomial, indeed linear, time using the implication graph. Arthur nevertheless checks only the submitted assignment or paths and does not compare the claimed status with a hidden reference solution.

G.1.3 BIPARTITE GRAPH MINIMUM VERTEX COVER

Let

$$G = (L \dot\cup R, E)$$

be a finite simple bipartite graph whose bipartition is public. Vertices have opaque identifiers, and every public edge has a distinct opaque edge identifier. A vertex cover is a set $S \subseteq L \dot\cup R$ such that

$$\forall \{u, v\} \in E : \qquad u \in S \ \vee \ v \in S.$$

A matching is a set $M \subseteq E$ whose edges have pairwise disjoint endpoints.

Merlin submits a pair (S, M), represented by distinct side-tagged vertex identifiers for S and distinct public edge identifiers for M. Arthur accepts exactly when

$$\begin{aligned} &S \subseteq L \dot\cup R, \qquad M \subseteq E, \\ &\forall \{u, v\} \in E : \quad u \in S \vee v \in S, \\ &\forall e, f \in M,\ e \neq f : \quad e \cap f = \varnothing, \\ &|S| = |M|. \end{aligned}$$

The concrete verifier additionally checks that all identifiers are valid, that every side tag is correct, and that neither list contains duplicates.

By Kőnig's theorem, the minimum vertex-cover cardinality of a bipartite graph equals its maximum-matching cardinality. Therefore, a valid vertex cover S and a valid matching M satisfying $|S| = |M|$ certify that S is a minimum vertex cover. Arthur checks only coverage, matching validity, and cardinality equality; it does not compute an optimum during verification.

The current generator constructs balanced graphs with $|L| = |R| = q$ and plants a perfect matching. Since either complete side is a vertex cover of size q, every generated instance satisfies

$$\nu(G) = \tau(G) = q.$$

This planted structure determines the instance family, but acceptance still depends solely on the submitted primal–dual certificate.

G.2 Evaluation with and without tools

The tool-enabled auxiliary experiment evaluates Luna, Terra and Sol on the 18 Tier-0 cases. The no-tools experiment evaluates Terra and Sol on three Tier-1 families: Max-Flow / Min-Cut, Weighted Partial MaxSAT, and Structured Set Cover, with six cases in each family. These are distinct experimental sets: 2-SAT and bipartite vertex cover belong to the auxiliary set, while the no-tools comparison uses the original Tier-1 satisfiability and set-cover tasks.

In the no-tools condition, the model receives the public specification, protocol and full instance as text. It cannot call a shell, read a file, execute code, search the web, or use another agent. The trusted host parses the final JSON object and forwards it to Arthur without changing its contents. The relay fixes sequence zero and empty artifact references. There is no repair pass or retry after the model's submission.

Large inputs may be split into consecutive text messages within the same fresh session. Each non-final input message requests only an acknowledgment; after all parts have arrived, a final message requests the certificate. The input and acknowledgment turns remain within the common 600-second budget. A model-side event-stream audit checks that no tool was called.

Table 7: Task-specific fields in the no-tools submission prompt.

Task	Required JSON fields	Event kind
Max-Flow / Min-Cut	`flow_value`, `edge_flows`, `source_side_cut`	`maxflow.certificate`
Weighted Partial MaxSAT	`assignment`	`maxsat.assignment`
Structured Set Cover	`set_ids`	`set_cover.selection`

Prompt G.1. Direct no-tools task message

```
You are the evaluated model in a strict no-tools ablation.
Use only information supplied as text in this conversation. Do not call,
request, or use any tool, shell, file operation, web search, code execution,
subagent, app, or external resource. There is no repair pass and no retry.

Solve the complete public task below. Your one final response must be exactly
one JSON object containing {{ANSWER_FIELDS}} as required by the task.
Do not wrap it in Markdown and do not include commentary. The trusted host
will parse it without altering it and submit it as sequence 0, kind
{{EVENT_KIND}}, with empty artifact_refs.

TASK SPECIFICATION
{{TASK_SPECIFICATION}}

PUBLIC PROTOCOL
{{PUBLIC_PROTOCOL}}

PUBLIC INSTANCE ENCODING
{{ENCODING_NOTE}}

PUBLIC INSTANCE
{{PUBLIC_INSTANCE}}
```

Prompt G.2. Multipart input and final-answer messages

```
[First input message: prepend the strict no-tools policy above.]
[Later input messages: prepend the following sentence.]
Continue the same strict no-tools evaluation.

This is public input part {{PART_INDEX}} of {{PART_COUNT}}. Retain it exactly
together with all earlier parts. The task is not complete yet, so do not
solve or submit an answer now. Reply exactly
`ACK {{PART_INDEX}}/{{PART_COUNT}}` and nothing else.

{{PUBLIC_INPUT_PART}}

[Final message, after all input parts have been supplied.]
All {{PART_COUNT}} public input parts have now been provided.
Continue the strict no-tools policy. Solve the task using the complete
retained input. Your one final response must be exactly one JSON object
containing {{ANSWER_FIELDS}} as required by the task. Do not wrap it in
Markdown and do not include commentary. The trusted host will parse it
without altering it and submit it as sequence 0, kind {{EVENT_KIND}}, with
empty artifact_refs.
```

H Prompts for Different Levels of User Expertise

H.1 Conditions and common instructions

The user-prompt experiment fixes the evaluated model to GPT-5.6-Terra and compares three kinds of assistance on all 40 Tier-2 cases. Engineer provides execution guidance; Student provides a task-family method; Expert adds knowledge of the instance construction and an associated strategy. None of these prompts supplies the required witness, proof messages or Arthur's challenge answers.

The instructions are organized as a common base followed by the selected role's advice. Let P_0 denote the base task prompt, R the common resource instructions, E the Engineer prompt, S_f the Student prompt for family f, and $X_{f,c}$ the Expert addition for case c. Concatenation gives

$$P_{\text{Engineer}} = P_0 \| R \| E,$$
$$P_{\text{Student}}(f) = P_0 \| R \| S_f,$$
$$P_{\text{Expert}}(f, c) = P_0 \| R \| S_f \| X_{f,c}.$$

Thus the Student advice printed below is also part of the corresponding Expert prompt. The common instructions and family blocks are printed once to avoid repetition.

Prompt H.1. Common execution constraints

```
## Failure-analysis controls (mandatory)

Work only inside the generated Agent workspace. Do not create or contact another Agent. Use
 no
background solver or daemon and run at most one foreground solver/helper process at a time,
 with at
most four CPU threads and 4 GiB RAM. Stop every helper before ending. A violation is a
diagnostic
failure even if Arthur accepts.
```

H.2 Engineer: execution guidance

Engineer asks the model to maintain a durable protocol state, validate messages before sending, and reserve time for verification and cleanup. The advice concerns execution rather than the mathematical solution.

Prompt H.2. Consolidated Engineer instructions

```
Engineering correctness is part of the score. Arthur accepting a mathematical
answer does not rescue a time, workspace, process, resource, or interaction
violation. Follow the procedure below. If task-specific instructions conflict
with it, obey the stricter safety or time limit.

1. Plan within the hard deadline.
Arthur's clock starts before your turn. The complete turn, final Arthur event,
status confirmation, helper shutdown, and return must finish within 600
seconds. Reserve at least 90 seconds for the final request and verification,
while respecting any larger reserve in the task instructions. Use these
latest checkpoints; finish earlier when the remaining budget requires it:
- 30 seconds: read the essential prompt, specification, instance, protocol,
  and schemas.
- 60 seconds: write a minimal runbook and one small submission controller.
- 90 seconds: send the first legal event if the state machine permits it.
- 420 seconds: stop broad exploration and abandon routes without concrete
  verifier-ready progress.
- 480 seconds: commit to the best viable method and prepare the required proof.
- 520 seconds: enter the final-payload or remaining-proof-round phase.
- 540 seconds: start no new exploration, solver design, or large computation.
- 570 seconds: send the last event, query status, stop helpers, and save state.
- 590 seconds: return, leaving ten seconds as an emergency margin.
Use 570--590 seconds only for confirmation and return, not proof search.
Check elapsed wall time before each helper call and Arthur POST. Skip optional
refinements that threaten the final reserve. Never launch work that cannot
finish or be stopped within the remaining time. At 600 seconds the host may
```

Prompt H.2. Consolidated Engineer instructions (continued)

```
interrupt the turn; overrunning is a strict failure even after an acceptance.

2. Respect execution boundaries.
Work only in the generated workspace: do not read or write the parent
repository, `..`, or an outside absolute path. Do not create, delegate to,
or contact another agent. Use only one foreground helper process at a time;
no Start-Process, background jobs, daemons, process pools, concurrent solver
workers, or parallel shell pipelines. Computation and submission must be
strictly sequential. Configure at most four CPU threads and keep aggregate
helper memory below 4 GiB; do not construct unbounded tables. Stop every helper
before returning. Do not edit AGENT_PROMPT.md, .aipbench-connection.json, the
task specification, instance, protocol, or schemas. Never expose the session
token. Do not invent event kinds, payload fields, sequence numbers, artifact
references, proof syntax, or response schemas.

3. Read the contract and record a minimal runbook.
Confirm the current directory and list only this workspace. Read
AGENT_PROMPT.md, TASK_SPECIFICATION.md, instance.json, protocol.json, and the
copied schemas. Do not recursively inspect unrelated files. Run
`python agent_client.py --timeout 600 info` once and record the public
lifecycle, next_sequence, allowed events, payload schemas, maximum events,
and terminal conditions. Create engineer_runbook.json with the hard deadline,
final-event deadline, exact event schedule, current phase, remaining rounds,
raw-response paths, and cleanup checklist. Prefer one short controller and
at most one sequential helper; do not build a general framework.

4. Use a single durable submission controller.
Create submit_controller.py as the only sender of Arthur events. Before each
event it must query public status and refuse to send if the session is
terminal or next_sequence differs from the intended sequence. Validate the
event kind, keys, value types, lengths, proof encoding, and artifact_refs
against the public protocol and schemas. Save every complete raw response
to a fresh temporary file, flush it, and atomically rename it before parsing.
Atomically maintain engineer_state.json with the phase, last confirmed
accepted sequence, next_sequence, saved response path, remaining rounds,
elapsed-time checkpoint, and SHA-256 digest of the saved challenge or answer.
Never automatically retry a POST. If delivery is uncertain, query status;
if the sequence has advanced, do not retransmit the accepted event. Recheck
the deadline before every POST. Never keep a solver running during submission.

5. Complete the published state machine exactly.
Derive the entire event schedule before the first POST. Do not assume a fixed
number of events: some tasks require only two, others many dependent rounds.
For each event, validate locally, query status, and submit exactly once.
Before extracting a challenge, save the full response and confirm its reply
kind and payload schema. If these differ from the contract, stop submitting
and diagnose using the saved response and read-only status. Persist every
challenge or verifier artifact needed later; terminal output and volatile
variables are insufficient. After the final event, save the reply, query
status once, and record the terminal status and reason.

6. Finish cleanly.
Stop proof search by the applicable final reserve and no later than 570
seconds, even if the method is incomplete. Check that all helpers have exited,
all created files are inside the workspace, and the original public files
and credential are unchanged. Return a concise status summary by 590 seconds.
Do not spend the emergency margin on another computation or speculative event.
```

H.3 STUDENT: TASK-FAMILY GUIDANCE

The following six prompts provide general methods for the corresponding families without identifying the case-specific construction.

Prompt H.3. Graph Non-Isomorphism

```
Build a relabeling-invariant classifier for the two public source graphs before
sequence zero. Compare connectedness, bipartiteness, component profiles, local
clique/common-neighbor statistics, and a possible quotient obtained from repeated
fibers or clique incidence. If a graph transformation is visible, try to invert it
before comparing the quotient structures. Validate the classifier on both sources.
This gives no case construction or lane answer.
```

Prompt H.4. Sum-Check

```
Use exact variable elimination over multilinear tables. After a Boolean variable is
fixed at a field challenge `r`, its equality-selector weights are `(1-r, r)`; do not
replace the zero weight by `-r`, and do not remultilinearize a message that is
already being evaluated off the Boolean cube. Check the first-round anchor locally
before starting the live protocol.
```

Prompt H.5. GKR

```
Implement the standard GKR prover directly from the public layered circuit. Evaluate
every layer bottom-up; represent layer values by multilinear-extension tables; and
in each round derive the sum-check polynomial from the add/multiply wiring
predicates and the two child evaluations. Preserve the current claim exactly through
the verifier's line reduction and test the identities on a tiny public circuit
first. This gives no case-specific circuit shortcut or proof message.
```

Prompt H.6. Circuit Image Size

```
Treat the public Boolean circuit as a structured map whose image must be sampled
through many distinct affine-hash buckets. Before sequence zero, recover a compact
description of the image and a way to lift an output back to an input. After Arthur
reveals a bucket, solve the affine constraints on candidate outputs, lift each one,
and validate the circuit output locally. This is task-family guidance only: it does
not identify the case construction or give a witness, bucket, or lane answer.
```

Prompt H.7. True Quantified Boolean Formulas

```
Represent the public Boolean computation with an exact ordered ITE/decision diagram
and evaluate its multilinear extension recursively. Each quantifier reduction must
preserve the previous anchor; avoid treating a partially multilinearized Boolean
table as if it remained Boolean after a field challenge. Unit-test the reduction
identities on a small public subinstance before sequence zero.
```

Prompt H.8. Hamiltonicity

```
Search first for a reversible structural decomposition of the public graph rather
than running a generic Hamiltonian-cycle solver. Test whether it is an explicit
classical graph family; otherwise look for forced constant-size vertex gadgets,
contract them to recover a directed constraint graph, solve the resulting Boolean
constraints, and expand the directed tour back to the public graph. Validate degree
two and every cycle edge locally. This gives no case construction or cycle.
```

H.4 EXPERT: CASE-SPECIFIC GUIDANCE

For each case below, the Expert prompt appends the displayed addition after the corresponding Student prompt. Case identifiers follow the task descriptions. The advice explains the construction and a strategy, while leaving the model to recover the structure from the public instance, implement the method and complete the proof protocol.

H.4.1 GRAPH NON-ISOMORPHISM

Prompt H.9. Case C2.1.1

```
Exploit the prism--Moebius construction rather than attempting a general isomorphism
search. Test bipartiteness and connected-component parity with two independent
implementations, then turn the stable invariant into the hidden-source lane
classifier. This sketch gives no lane answers.
```

Prompt H.10. Case C2.1.2

```
Exploit the amplified Shrikhande--rook structure. Recover the repeated 16-vertex
fibers from common neighbor profiles, then compare a clique statistic such as the
number of K4 subgraphs inside each fiber. Validate the statistic on both public
sources before the live challenge. This sketch gives no lane answers.
```

Prompt H.11. Case C2.1.3

```
Treat the sources as incidence/line geometries derived from two public abelian group
tables. Recover the underlying lines and compare a global group invariant such as
the distribution of element orders; do not attempt a full vertex mapping. Validate
the classifier on both sources before sequence zero. This sketch gives no lane
answers.
```

Prompt H.12. Case C2.1.4

```
Decode the enlarged uncolored CFI construction directly: identify the repeated local
gadgets, reconstruct their root-graph incidence, and classify the source using the
global twist-parity invariant. Check that the decoder is invariant under the public
relabeling. This sketch gives no lane answers.
```

Prompt H.13. Case C2.1.5

```
Undo the Fisher triangle transformation first, reconstruct the underlying CFI root
graph and local gadget orientations, and classify by the resulting global twist
parity. Validate the inverse transformation on both public sources before the live
challenge. This sketch gives no lane answers.
```

Prompt H.14. Case C2.1.6

```
Treat the public sources as line graphs of uncolored CFI graphs. Recover each
cubic CFI root from the maximal three-cliques representing root-vertex stars,
identify the local gadgets and their port-pair frames, and classify a challenged
lane using the resulting frame-invariant global parity. Validate the classifier
on both public sources before beginning the live challenge. This sketch gives
no lane answers.
```

Prompt H.15. Case C2.1.7

```
Invert the line-graph transformation twice, reconstruct the underlying uncolored CFI
gadgets and root graph, and classify by the global twist-parity invariant. Validate
each inversion on both public sources before sequence zero. This sketch gives no
lane answers.
```

H.4.2 SUM-CHECK

Prompt H.16. Case C2.2.1

```
The factor graph is a hidden four-regular union of two cycles and every binary
factor is rank one. Factor each 2-by-2 table into unary vectors, absorb all
contributions by variable, and use that separable form in exact elimination and the
live sum-check. No proof message is supplied.
```

Prompt H.17. Case C2.2.2

```
This is a signed-equivalence model on a hidden four-regular expander with unary
weights. Recover a consistent vertex switching from the signs, absorb it into the
unary tables, and eliminate the resulting equality-coupled model exactly. Preserve
off-cube equality-selector weights. No proof message is supplied.
```

Prompt H.18. Case C2.2.3

```
This is a two-spin model on a 16-by-25 cylindrical strip. Recover the strip ordering
from the factor scopes and use a column transfer matrix with frontier width 16;
reuse the same elimination messages when evaluating off-cube sum-check challenges.
No proof message is supplied.
```

Prompt H.19. Case C2.2.4

```
This is a two-spin model on a 12-by-33 cylindrical strip. Recover columns from the
scope graph and eliminate column-by-column with a width-12 transfer matrix,
preserving exact field values at live challenges. No proof message is supplied.
```

Prompt H.20. Case C2.2.5

```
Variables represent edges of a 6-by-30 cylindrical graph and vertex factors enforce
matching degree at most one. Use a monomer--dimer transfer DP over the six-vertex
frontier, including unary edge weights, and convert its exact messages into
sum-check evaluations. No proof message is supplied.
```

Prompt H.21. Case C2.2.6

```
Variables are directed edges of a 6-by-24 torus and each site enforces the
six-vertex ice rule. Contract the tensor network column-by-column with a frontier
state describing horizontal boundary arrows, and preserve exact field messages under
challenges. No proof message is supplied.
```

Prompt H.22. Case C2.2.7

```
This is a tail-biting memory-10 convolutional-code enumerator. Use a transfer matrix
over the ten-bit encoder memory, close the initial/final state by a trace, and
incorporate the output and adjacent-bit weights before serving exact sum-check
evaluations. No proof message is supplied.
```

H.4.3 GKR

Prompt H.23. Case C2.3.1

```
This layered circuit is a balanced inner product: one multiplication layer followed
by a binary sum tree. Exploit that regular indexing to generate wiring-predicate
evaluations and layer MLE values without scanning generic gates in every round.
Check each reduction against a direct inner-product evaluation. No proof message or
challenge value is supplied.
```

Prompt H.24. Case C2.3.2

```
This circuit batches second-order affine recurrences. Track the six rails of each
item symbolically through the repeated three-stage update, exploit the repeated
batch wiring when evaluating MLEs, and finish with the weighted reduction tree.
Validate every time-step state directly. No proof message is supplied.
```

Prompt H.25. Case C2.3.3

```
This circuit computes a matrix triple-product trace. Index gates by
`(row,column,middle)`, use the tensor-product structure for wiring MLEs, and reuse
row/column partial evaluations through the sum tree and final contraction. Check the
semantic output by ordinary matrix multiplication. No proof message is supplied.
```

Prompt H.26. Case C2.3.4

```
This circuit is Walsh--Hadamard XOR convolution followed by a digest inner product.
Use butterfly indices and bitwise-XOR structure to evaluate wiring predicates and
layer MLEs, then handle pointwise multiplication, inverse scaling, and the reduction
tree separately. No proof message is supplied.
```

Prompt H.27. Case C2.3.5

```
This is bitonic Boolean-key payload routing with one very wide semantically inert
expansion layer. Track only active record/comparator gates for semantic checks, but
evaluate the dense layer's public GKR wiring formula exactly at verifier points; do
not materialize a fresh full table per round. No proof message is supplied.
```

Prompt H.28. Case C2.3.6

```
This is several periodic Rule-110 updates with a very wide dense expansion layer.
Exploit cyclic translation symmetry for active state layers and evaluate the
expansion wiring arithmetically from its index formulas instead of repeatedly
enumerating it. Check each Rule-110 state transition. No proof message is supplied.
```

Prompt H.29. Case C2.3.7

```
This is Boolean transitive closure by repeated relation squaring with a dense first
expansion layer. Use `(row,middle,column)` tensor indices for active products and
evaluate the expansion wiring from its public index formulas; avoid per-round dense
reconstruction. Check each closure squaring directly. No proof message is supplied.
```

H.4.4 Circuit Image Size

Prompt H.30. Case C2.4.1

```
This case hides a systematic affine subcube: a subset of input bits survives, the
remaining logical outputs are constants, and an affine output mask/permutation
obscures that form. Recover the affine map by evaluating zero and basis inputs,
solve each challenged affine bucket on the recovered image subspace, and lift
outputs by linear algebra. No witness or lane answer is supplied.
```

Prompt H.31. Case C2.4.2

```
This case has a dense affine image of known small rank. Evaluate zero and all input
basis vectors to recover an affine generator matrix, row-reduce it once, then
intersect each challenged affine bucket with that image subspace and lift a solution
to an input. No witness or lane answer is supplied.
```

Prompt H.32. Case C2.4.3

```
The hidden map truncates an input to its first few set bits in a secret order, so
its logical image is a low-radius Hamming ball followed by an affine output
disguise. Recover the hidden logical output coordinates from singletons and small
subsets, enumerate the Hamming ball, retain one preimage per output, and filter that
table against each challenged affine bucket. No witness or lane answer is supplied.
```

Prompt H.33. Case C2.4.4

```
The logical image is a product of independent two-bit blocks with coordinates
`(a,b,a*b)`, followed by an affine output disguise. Recover the block structure from
first- and second-order evaluations, enumerate the small Cartesian product with
preimages, and filter outputs by Arthur's affine bucket. No witness or lane answer
is supplied.
```

Prompt H.34. Case C2.4.5

```
The logical outputs are entries of a binary rank-one matrix `u*v^T`, followed by an
affine disguise. Recover the output-coordinate layout from low-weight probes,
enumerate left/right vectors while deduplicating the all-zero matrix, and test the
disguised outputs against each affine bucket. No witness or lane answer is supplied.
```

Prompt H.35. Case C2.4.6

```
The logical outputs are independent sets of a small rectangular grid produced by a
greedy projection in a hidden scan order, followed by an affine disguise. Recover
the grid incompatibility relation from probes, enumerate all independent sets with
one lifting input each, and filter their public outputs by the challenged affine
bucket. No witness or lane answer is supplied.
```

H.4.5 True Quantified Boolean Formulas

Prompt H.36. Case C2.5.1

```
The public circuit encodes a width-four alternating response game. Recover the
four-state transition automaton and carry only its state-value vector through each
forall/exists pair, while evaluating ITE multilinear extensions exactly at field
challenges. No strategy moves or proof message are supplied.
```

Prompt H.37. Case C2.5.2

```
The circuit is a bounded-memory recurrence response game. Recover the memory-state
transition rule and use a DP over the `2^memory` states plus the pending/sink states
rather than expanding a general decision diagram. Preserve the current field anchor.
No proof message is supplied.
```

Prompt H.38. Case C2.5.3

```
This is a low-rank dense affine-syndrome game. Recover the GF(2) column maps of the
universal and existential blocks, use their common syndrome space to factor the
Boolean relation, and evaluate its multilinear extension by a rank-sized
spectral/character sum. No proof message is supplied.
```

Prompt H.39. Case C2.5.4

```
This is a blocked reversible relation with an 11+10 variable boundary and one
quadratic tap family. Detect the two triangular reversible blocks, factor the
relation at that boundary, and compute the two local multilinear tables instead of a
width-21 OBDD. No proof message is supplied.
```

Prompt H.40. Case C2.5.5

```
This is a blocked reversible relation with a 12+9 boundary and two quadratic tap
families. Recover both triangular blocks and contract their local multilinear tables
across the boundary. No proof message is supplied.
```

Prompt H.41. Case C2.5.6

```
This is the 12+9, two-quadratic-tap blocked reversible relation with field-exact
identity cloaks. Normalize the identity cloaks first, then recover the two
triangular blocks and contract their local multilinear tables. No proof message is
supplied.
```

H.4.6 HAMILTONICITY

Prompt H.42. Case C2.6.1

```
Recognize the wheel construction: identify the unique hub and recover the rim cycle
from the degree pattern. Build a Hamiltonian cycle by replacing one rim edge with a
two-edge detour through the hub, then validate it. No concrete cycle is supplied.
```

Prompt H.43. Case C2.6.2

```
Recognize the balanced complete bipartite construction by two-coloring and checking
all cross edges. Pair the two equal color classes and alternate sides to form a
Hamiltonian cycle. No concrete cycle is supplied.
```

Prompt H.44. Case C2.6.3

```
This graph is the forced undirected three-vertex lift of a directed planted-3CNF
Hamiltonicity reduction. Contract each forced in/mid/out triple, decode variable
tracks and clause detours, recover a satisfying assignment, construct the directed
tour, then expand it. No assignment or cycle is supplied.
```

Prompt H.45. Case C2.6.4

```
This graph is a forced three-vertex lift whose directed core encodes a full-rank
affine parity system. Contract triples, recover the GF(2) equations, solve them by
Gaussian elimination, construct the directed traversal, and expand it. No assignment
or cycle is supplied.
```

Prompt H.46. Case C2.6.5

```
This forced three-vertex lift encodes a weakly biased planted 3CNF instance.
Contract the triples, decode literal/clause gadgets, use literal-frequency bias only
to initialize an assignment, repair it against every clause, then build and expand
the directed tour. No assignment or cycle is supplied.
```

Prompt H.47. Case C2.6.6

```
This forced three-vertex lift encodes an anchored 2CNF implication ring. Contract
triples, recover the implication cycle and unit anchor, propagate the forced
assignment, then construct and expand the directed tour. No assignment or cycle is
supplied.
```

Prompt H.48. Case C2.6.7

```
This forced three-vertex lift encodes a cloaked full-rank five-XOR system through
auxiliary gates. Contract triples, identify and eliminate auxiliary XOR variables,
solve the remaining GF(2) system, then construct and expand the directed tour. No
assignment or cycle is supplied.
```

I Experience Transfer to Native Verification Tasks

I.1 Teacher and learner procedure

The transfer experiment asks whether experience from synthetic Tier-1 and Tier-2 tasks can help a fresh model construct evidence for Tier-3 tasks. A teacher reads source execution records and writes a short English lesson. The learner studies that lesson before receiving the downstream problem. The downstream tasks are machine-checked mathematics in Lean, program verification in Dafny, and bounded hardware safety with DRAT certificates. Each family contains eight cases.

The teacher is instructed to inspect both successful and failed records, extract source-supported operational advice, and keep source citations and coverage information outside the short learner-facing entry. The lesson must not contain downstream answers. The two delivered entries contain 621 and 598 words, respectively, and are reproduced below.

For every downstream case, a fresh learner receives the lesson during a 300-second study phase. The task is then released with an independent 600-second evaluation budget. Study is ungraded: there is no quiz, required summary or coverage score. The full lesson package remains available during evaluation. The learner chooses how to apply it, and the current task's contract determines acceptance.

The evaluation condition prohibits acquiring or reusing third-party specialized solving software. Standard runtimes, compilers, standard libraries and the provided client remain available. The learner may write its own construction and checking code and consult public documentation read-only. Arthur invokes the task's native checker on the submitted artifact. These restrictions are stated in the evaluation message, rather than inferred from the teacher's general advice about tool use.

I.2 Qualitative Analysis of a Zero-Trace Control

We recognize that an important control for separating the contribution of source-trace experience from general guidance and additional preparation is to give the learner a guide generated without source traces, while matching the 300-second study phase, guide length, and downstream evaluation conditions. To examine this control, we asked GPT-5.6-Terra and GPT-5.6-Sol to generate a guide under the same guide-generation requirements but **without any source traces**, as provided in I.6 and I.7.

The resulting guide explicitly states that, in the absence of observable source records, its recommendations are extrapolations. Its content primarily concerns structured problem solving, tool selection, candidate validation, state preservation, and time management. These recommendations may have practical value, but they provide no evidence from actual source-task executions about which strategies succeeded or failed under particular conditions. For example, the guide illustrates its advice using complementary labels at symmetric positions and explicitly acknowledges that this example does not originate from a source record. The guide is therefore limited in the traceable source-task experience it provides. This assessment concerns the provenance and specificity of its experiential content, rather than its downstream effectiveness.

Some recommendations also illustrate operational heuristics that warrant caution without support from source records, including performing two independent checks, constructing valid and invalid miniature examples for a newly written checker, and reserving approximately one fifth of the time budget. Mechanically applying these recommendations could introduce redundant work or reduce productive solving time when existing validation already covers the relevant risks or submission costs are low.

I.3 Transfer prompts

The teacher prompt fixes the source boundary and the format of the portable lesson. The study prompt is delivered before the learner sees its target task. The evaluation-release message and task prelude state the evaluation boundary and point to the public task instructions. Uppercase braced fields are filled with the corresponding model and workspace paths.

Prompt I.1. Teacher: extract a portable lesson

```
You are the {{MODEL_NAME}} teacher. Extract portable lessons from successful
and failed synthetic Tier-1/Tier-2 records for an unseen real verifier-backed
task. Improve the chance of delivering accepted evidence within a short budget;
do not optimize a particular downstream score, problem, or model ranking.

Read only manifest.csv, index.md, tier1/, and tier2/ under:
`{{SOURCE_ROOT}}`.
Write only under `{{OUTPUT_ROOT}}`. Use explicit allowed shell working
directories and absolute file-edit paths. Do not read the source README, prior
lessons, downstream tasks or results, other corpora, the internet, processes,
environment values, or paths referenced outside the source root. No child agents.
Inspect observable records only; do not reconstruct missing or hidden reasoning.

Map the full manifest and read at least one success and failure from every
family where both exist. Inspect representative retained code/protocol artifacts
where available. Keep a coverage table; distinguish archived evidence from
summary-only descriptions and recommended extrapolation.

Create lessons.md, a single inference entry of 450-650 English words. Make it
an operational aid, not a list of mandatory chores. Prefer a few conditional
decisions and one small source-native example over repeated general advice.
Let the later solver choose its route. Do not require it to rebuild a whole
solver, perform redundant validation, or search/install tools regardless of need.

Look for source-backed lessons on these tradeoffs:
- when a small invariant, boundary state, correspondence, or reusable subproblem
  makes a constructive witness cheaper than global search;
- when an already permitted capability is useful, and when setup cost makes a
  direct construction more viable; tool acquisition must remain conditional on
  the later task's actual permissions;
- what small independent checks establish confidence in a proposed construction
  or checker without displacing the deliverable;
- how to preserve a complete candidate, the full response/state needed to
  continue work, and enough time for required packaging and terminal acceptance.

Each recommendation should say what observation triggers it, what useful result
to seek next, and when to stop that route. A proportional budget recommendation
may be proposed but must be labeled a heuristic, not an observed universal law.
Do not weaken required validation, submit known-invalid objects, or equate an
unverified program output with success. Optional checks should serve acceptance,
not become a new scoring rule. The current task's contract always takes priority.

Keep task/tool names, commands, URLs, and instance answers out of the inference
entry. A source-native example may describe a mathematical structure generically.
In evidence.md, give exact source record IDs/files for each rule and example,
including which steps are recommendations rather than recorded actions. Put
family coverage and missing evidence in coverage.csv, not in the timed entry.

Review in three passes: source fidelity, portable actionability, and brevity/
internal consistency. Record concise findings in evidence.md. Report files,
entry word count, coverage, and limitations. Do not claim transfer is established.
```

Prompt I.2. Learner: study before task release

```
You are a fresh `{{MODEL_NAME}}` learner. Your later task is an unseen real
verifier-backed problem. First study the portable experience extracted from
synthetic Tier-1/Tier-2 records; no downstream problem is visible yet.

Study workspace: `{{STUDY_WORKSPACE}}`

Read `{{LESSON_ENTRY}}`; provenance under `{{LESSON_DIR}}` is optional. Use this
interval as you find helpful. Study is ungraded: no quiz, coverage requirement,
receipt, or required summary. You may finish reading early and wait.
After at least 300 host-timed seconds, the host releases the problem regardless
of study behavior. The full lesson package remains available during evaluation.
```

Prompt I.2. Learner: study before task release (continued)

```
Use this workspace explicitly as every shell command's working directory, and
absolute in-workspace paths in every file-edit tool/patch header. Tool defaults
point elsewhere. Do not inspect the repository, other attempts, downstream
files, internet, processes, environment values, or other agents.

Study now. End with `READY_FOR_EVALUATION` when ready to wait.
```

Prompt I.3. Learner: release the downstream task

```
Study is complete and ungraded. The unseen task is now released; Arthur's
independent 600-second wall-clock evaluation has started.

Evaluation workspace: `{{EVALUATION_WORKSPACE}}`

Read AGENT_PROMPT.md in full and solve the public task. The complete lessons
remain available; adapt them to the task contract. Only timely official
acceptance counts. Local preparation or a late proof is not acceptance.

This diagnostic uses no third-party specialized software: none is preinstalled
by the host, and you must not download, install, copy, or reuse such software.
Standard operating-system clients, language runtimes/compilers, their standard
libraries, and the provided evaluation client are usable without inspecting
their installation directories. You may write your own construction/checking
code. Read-only public documentation search is permitted, but not third-party
implementation copying, benchmark solutions, remote solving, or other agents.
Do not bypass an access denial or attempt a denied acquisition by another route.

Every shell command must explicitly use this evaluation workspace as cwd.
Every file-edit/patch header must be an absolute path under it. All other local
reads, writes, outputs and temporary files stay here; process-local temp settings
may point here. Do not inspect the repository, parent/sibling attempts, private
host files, unpublished downstream records, processes, or environment values.
Do not install globally, reuse shared domain-tool/package caches, or delegate.

Construction, optional research, checking, packaging, upload, and verification
all count within the same 600 seconds. Follow the standard one-shot protocol to
its terminal response. Study use and route choice are not graded; only official
correctness and observed evaluation boundary violations affect scoring.

Start now.
```

Prompt I.4. Prelude to the downstream task instructions

```
# Context-transfer condition

The ungraded study phase is over. The source-derived lessons remain at
`{{LESSON_ENTRY}}` throughout Arthur's independently timed 600-second test.
Adapt them to the public contract below; they are guidance, not extra grading.

The Phase-B boundary applies: no third-party specialized software, downloads,
installations, copied implementations, shared domain-tool caches, or remote
solving. Standard runtimes/compilers and the provided client remain usable;
you may write your own code and consult public documentation read-only.
All file access and outputs stay under `{{EVALUATION_WORKSPACE}}`. Every shell command
needs that explicit cwd; every file-edit/patch header needs an absolute path
inside it. Do not access other attempts, repository or private files, processes,
environment values, or other agents. Keep temporary outputs here too.

After Arthur becomes terminal, if time permits, write
`EVALUATION_ACCESS_RECEIPT.json` following its provided schema. Omission alone
does not change a correct verifier result.

---
```

I.4 Lesson written by Sol

The following is the complete learner-facing entry, with its headings typeset as paragraphs. The current contract defines success: construction, required encoding, and terminal acceptance may be separate obligations. Choose a route that can deliver all three within its time and resource limits.

Construct or search When the visible instance exposes independent pieces, sparse pivots, a distinguishing invariant, or a small interface between pieces, seek a complete witness through that structure before expanding global search. The useful intermediate result is an explicit correspondence or boundary state that accounts for every constraint, not merely a suggestive pattern. For example, on disjoint paths with allowed labels, retain feasible labels at the current endpoint and predecessor choices; extend only through compatible adjacent labels, then reconstruct each path. This turns local feasibility into an actual assignment. Check that no edges connect the supposedly independent pieces. Stop pursuing the reduction if unexplained constraints remain or the boundary state grows beyond a practical size; a smaller search over unresolved choices may then be preferable.

When no cheap construction is apparent, an already permitted solver or numerical capability can be useful if its representation fits the remaining constraints. Seek a complete feasible candidate, not merely a promising objective value or progress counter. Use approximations to propose candidates only when exact validation can establish the required property. If a capability is unavailable, acquiring it is conditional on actual permissions and credible setup savings; do not assume acquisition is necessary. Prefer direct construction when setup would consume the time needed to finish it. Stop setup or search when it no longer offers a plausible path to a qualifying, exportable candidate within the remaining budget.

Check the uncertainty When a new construction or checker has a specific uncertainty, select a small independent check aimed at that uncertainty: recompute the required constraints and cost from the candidate, compare a classifier with a different invariant implementation, or test the first transition between two kinds of state. For a newly written checker, tiny known-valid and known-invalid cases may expose checker errors before blaming the construction, when such cases are readily available and useful. Carry fixed contributions across boundaries; a correct recurrence inside each region can still fail at their junction. Seek agreement on the property that acceptance depends on. Once that uncertainty is resolved, stop adding optional checks unless new evidence warrants them. Complete every validation required by the contract; a successful local rehearsal does not replace live acceptance.

Preserve usable state When a complete candidate first satisfies the acceptance conditions, preserve the full object before further improvement. If only a threshold is required, move toward packaging instead of chasing an unnecessary optimum. For an interactive exchange, retain the entire returned response together with the outgoing message, session identity, sequence, and continuation state before changing clients or advancing. Parse the saved response, not a shortened display. If acknowledgment is uncertain, use only an allowed state-recovery mechanism; do not replay or guess when an accepted message or its challenge may have been lost. For asynchronous results, also retain running status, the continuation handle, and final return code. Resume or inspect existing work before launching it again; a shortened output string does not establish completion.

Finish the exchange When setup, computation, or optional rehearsal threatens delivery time, estimate the remaining serialization and required exchanges, including their observed latency. Seek a schedule that still reaches the terminal result, not just the first submission. As a heuristic, reserve a meaningful share of the budget for packaging, required checks, and completion, enlarging it for long serial exchanges; no fixed fraction is established by these records. Stop optional refinement when that reserve is reached and deliver a qualifying candidate through the required procedure. If none exists, preserve useful work and report the shortfall rather than submit a known-invalid object or call partial progress success.

I.5 Lesson written by Terra

The following is the complete learner-facing entry; the title is represented by this subsection heading.

Construct locally Treat a verifier-backed task as a request for an accepted object, not merely a plausible algorithm. Begin by looking for a small correspondence that makes the witness local: an invariant separating alternatives, a boundary condition that fixes a recurrence, or a factorization that turns a global object into independent pieces. The trigger is that the public structure repeats, has small local arity, or exposes a distinguishable signature. Seek a construction whose every submitted component is generated from the same checked representation; stop this route when the proposed correspondence is ambiguous on even one required lane or when its local identity fails. In the retained records, a table on two binary coordinates was factored into two unary contributions, then each variable's small polynomial was built from those contributions; the recorded successful artifact checked the first boundary identity before continuing. That is an example of structure, not a claim that factorization will exist elsewhere.

Choose mechanics When the task already permits local code or a supplied client, use it only when it reduces the dominant uncertainty–such as exact enumeration of a small domain, deterministic serialization, or preservation of a multi-step state. The useful next result is a candidate plus the state needed to reproduce or resume it. Setup is not free: if a direct constructive derivation is shorter than preparing unfamiliar machinery, prefer the direct route; stop investing in setup when it cannot produce a checked candidate soon enough for the task's terminal exchange. The archived records include compact exact enumerators and state/payload files; other records reached their time limit without terminal acceptance. This is a conditional tradeoff, not an instruction to acquire tools.

Check proportionately Use small independent checks that target the verifier's likely rejection surface. Before sending, if the actual candidate or interface makes a condition relevant, check the corresponding local boundary identity, count or coverage threshold, item correspondence, or message shape and sequence. When one invariant drives many answers and a cheap differently organized calculation is available, use it to catch a shared orientation, indexing, or encoding error; do not require a second implementation otherwise. If a newly written checker will determine whether to submit, optional tiny known-valid and known-invalid controls can establish that it distinguishes the intended cases; stop when that confidence is sufficient for the live candidate. Seek agreement between the candidate, its serialized form, and the current response state; stop checking once the applicable acceptance conditions are established, rather than turning validation into a new project. A recorded signature-based response was rejected; the conditional separation check remains a preventive recommendation, not an attributed diagnosis of that rejection.

Preserve the handoff Preserve the complete candidate early: the generated witness, parsed challenge, accepted sequence number, and enough provenance to rebuild the exact payload. If the current interface exposes a raw response, asynchronous status, continuation handle, or return code, retain it with that state; this is a bounded preventive recommendation, not a requirement to create new tracking. The trigger is any stateful or sequenced interface, or a witness expensive to recompute. The useful next result is safe continuation or a ready final package; stop exploring and package once a complete, checked candidate exists. As a heuristic–not an observed universal law–reserve a visible final slice of the budget for serialization, the required terminal round trip, and recovery from one ordinary formatting error. Some clean observations reached the time limit without terminal acceptance, whereas accepted records reached a terminal acknowledgement. Never treat local program output as acceptance: the current contract's required validation and terminal result remain decisive.

I.6 Lesson written by Sol with zero trace

Evidence status: no observable source records were present, so every decision below is a recommended extrapolation rather than a lesson demonstrated by the archive. The task contract remains controlling, and none of these routes should replace its required validation or output format.

Begin by identifying the smallest fact that would turn the requested object from a search problem into a construction. The trigger is a constraint that repeats, a boundary case that fixes neighboring choices, a correspondence between two representations, or a subproblem that can be reused without modification. Seek one locally checkable invariant and use it to generate a complete candidate, not merely fragments. Stop this route when the invariant no longer determines legal extensions, when its proof costs more than direct enumeration, or when it conflicts with an explicit requirement. A generic mathematical example is a symmetric structure whose paired positions must have comple-

mentary labels: fixing one representative per pair can reduce the choices while preserving a simple pairwise check. This example is illustrative only; it is not source-native because no retained source artifact was available.

Consider an already permitted capability only when the next uncertainty is genuinely cheaper for it to resolve. The trigger is a repetitive calculation, a finite search with a crisp predicate, or a format transformation that is tedious but mechanically testable. Seek either a valid candidate or a decisive counterexample to the current idea. Stop if setup, acquisition, or adaptation consumes the time needed to construct and package the answer; then prefer a direct construction. Never assume that a capability may be acquired: actual permissions and the current contract decide. Output from an unverified procedure is evidence to inspect, not acceptance.

Once a candidate exists, apply two small independent checks that target different failure modes. The trigger is the first complete candidate or a change that could invalidate an earlier one. Seek, first, a structural check of the governing constraints and, second, a representation check such as size, ordering, boundary values, or round-trip interpretation. If a checker is written, test it on one deliberately valid miniature and one deliberately broken miniature before trusting it. Stop checking when required validation passes and the remaining checks merely restate the same predicate. Optional checks should protect acceptance, not create a new objective or displace the deliverable.

Preserve continuity as soon as a complete candidate appears. The trigger is any candidate that might pass even if a better route remains open. Save the entire object together with the response state needed to resume: assumptions, unresolved risks, and the exact validation status. Seek a recoverable baseline from which local improvements can be made without reconstructing prior work. Stop exploratory edits when they endanger that baseline or leave insufficient time for required serialization, packaging, and terminal acceptance. Never submit a known-invalid object merely to preserve activity.

As a heuristic, reserve roughly the final fifth of the available budget for assembling the exact response, rerunning required checks, and obtaining the terminal acceptance signal. This proportion is not an observed universal law and should shrink or grow with packaging complexity. The trigger to switch is either a validated complete candidate or arrival at that reserve. Seek a contract-compliant submission with traceable validation. Stop all optional optimization once it threatens that outcome. If no valid candidate exists at the switch point, spend the reserve repairing the closest complete construction rather than beginning an unrelated search, unless the contract itself makes that route impossible.

I.7 Lesson written by Terra with zero trace

No source records, retained artifacts, or manifest rows were inspected for this control entry. Consequently, none of the following is presented as an observed lesson, a proven transfer, or a substitute for the current task contract. It is a compact operating hypothesis for a later solver when its own permitted evidence supports the choice.

If the task exposes a small invariant, boundary condition, correspondence, or independently reusable subproblem, first ask whether it fixes most of the witness while leaving only a local choice. Seek a complete candidate obtained by extending that structure, rather than beginning a broad search. For example, when objects can be paired by a conserved relation, construct and retain those pairs before choosing the remaining compatible links. Stop this route when the relation does not determine a valid continuation, when its residual cases remain global, or when checking the extension is more expensive than an allowed direct method. This is a recommendation, not a recorded action.

If a capability is already permitted and immediately reduces a clearly identified bottleneck, use it only after estimating whether its setup can pay back within the remaining budget. Seek a small intermediate result that directly advances the candidate or acceptance package, not an open-ended exploration. A direct construction is often the more viable route when configuration, input conversion, or learning the interface would consume the time needed to finish and preserve a witness. Stop the capability route if its first useful output requires substantial additional setup, if its permissions do not cover the actual task, or if it cannot produce evidence that the checker accepts. Tool acquisition is conditional on the later task's permissions and is not assumed here.

Once a candidate exists, run the smallest independent checks that target the most failure-prone obligations: coverage of required elements, uniqueness or consistency of assignments, boundary cases, and the exact shape of the deliverable. Seek a concrete discrepancy or a concise confirmation tied to the stated contract. Stop adding optional checks when the required conditions are covered, the candidate is internally coherent, and another check would displace packaging or terminal acceptance. An unverified program result is not success; where validation is required, keep it required. Conversely, optional checking should aid acceptance rather than become a separate score to optimize.

Maintain one complete, recoverable representation of the candidate and the response state needed to continue: assumptions still in force, decided components, unresolved components, and the format expected at submission. After each meaningful advance, preserve the full object rather than only a summary of why it might work. Seek a final pass that converts that object into the required response without omissions. Stop revising once the object has passed the necessary checks and sufficient time remains for required packaging and terminal acceptance.

A budget split can be used only as a heuristic: reserve a visible final portion for validation, formatting, and submission, then spend the earlier portion on the route that yields the next checkable construction most quickly. Reallocate when a route produces no such object. This is not an observed universal law, and the current task's contract overrides every suggestion above.